Establishment and Characterization of a Human 3-D Fat Model

Adipogenesis of hASC in a Spheroid Model

3-D Cocultures of Adipocytes and Endothelial Cells

Dissertation

zur Erlangung des Doktorgrades der Naturwissenschaften

(Dr. rer. nat.)

der Fakultät Chemie und Pharmazie

der Universität Regensburg

vorgelegt von

Christian Muhr

aus Roding

im Jahr 2012

Die Arbeit wurde angeleitet von:	Prof. Dr. Achim Göpferich	
Promotionsgesuch eingereicht am:	19.09.2012	
Datum der mündlichen Prüfung:	19.10.2012	
Prüfungsausschuss:	Prof. Dr. S. Elz	(Vorsitzender)
	Prof. Dr. A. Göpferich	(Erstgutachter)
	Prof. Dr. T. Blunk	(Zweitgutachter)
	Prof. Dr. F. Kees	(Drittprüfer)

Für

meine Eltern

Table of Contents

Establishment and Characterization of a Human 3-D Fat Model

Adipogenesis of hASC in a Spheroid Model

3-D Cocultures of Adipocytes and Endothelial Cells

“What we know is a drop, what we don't know is an ocean.”

Isaac Newton (1642 – 1728)

CHAPTER 1

General Introduction

1.1 Adipose tissue: Physiological and pathophysiological aspects

The chronic exposure to elevated amounts of lipids and nutrients in modern society has made obesity an enormous public health problem and a major cause of morbidity and mortality [1–3]. Obesity is defined as an increased adipose tissue accretion to the extent that health may be adversely affected [1,4]. Recent surveys indicated that 33-35% of adults in the USA and 19-21% in Germany can be considered obese, having a body mass index greater than 30 kg/m² [2,5]. Although genetic differences are of importance, and body fat mass is dependent on ethnic background, gender, developmental stage and age, the still increasing prevalence of obesity can be best explained by changes in the behavioral and environmental changes affecting the balance of energy expenditure and intake [4,6,7]. In recent years much progress has been made in understanding the molecular basis of adipose tissue mass regulation. These new insights are likely to accelerate the identification of new targets, eventually leading to the development of safe and effective therapies for obesity [6].

The great importance of such therapeutic methods derives from the severe complications obesity can entail. It is generally accepted that obesity is closely associated with common medical conditions such as type 2 diabetes, dyslipidemia and hypertension, which can be summarized under the term “metabolic syndrome” [2,8]. Besides an increased risk of insulin resistance and cardiovascular disease, an enhanced incidence of liver steatosis, osteoarthritis, Alzheimer’s disease, gallstones, sleep-breathing abnormities and even certain forms of cancer has been detected in obese individuals [3,4,9–12]. Thereby, body fat distribution rather than adiposity *per se* is an important risk factor for obesity-related disorders, yet the mechanisms responsible for this association are still largely unknown [2,3].

Adipose tissue is not only directly involved in the development of obesity, but also influences the physiology and pathophysiology of many other tissues, including hypothalamus, pancreas, liver, skeletal muscle, kidneys, endothelium and immune system, through a complex network of endocrine, paracrine, and autocrine signals [1,11]. Therefore, adipose tissue possesses great pharmacological and therapeutic potential and is increasingly considered as a promising drug discovery target [11,13]. However, in order to use this potential, e.g. for the development of novel strategies for the prevention and treatment of obesity and the diverse disorders associated with it, a thorough understanding of adipose tissue development and adipocyte functions is a prerequisite.

1.1.1 Structure of adipose tissue

Two types of adipose tissue (AT) exist in mammals: Brown adipose tissue (BAT) and white adipose tissue (WAT). In humans, large depots of BAT can only be found during infancy,

while in adults, only small amounts of BAT persist, which are dispersed throughout depots of WAT [14,15]. BAT is transformed into WAT during development, and conversely, WAT can be turned into BAT during cold adaptation or after pharmacological treatment [15]. Brown adipocytes, which are able to dissipate energy as heat without producing ATP, exhibit multiple small lipid droplets and contain numerous mitochondria [1,14].

In this work, however, the focus is on WAT, on which current adipose tissue research is concentrating. While WAT accounts for approx. 16% of total body weight at birth, its total mass is highly variable in adults, ranging from a few percent of body weight in elite athletes to more than half of the total body weight in morbidly obese patients. Normally, fat makes up 10-20% of body mass in males and 20-30% in females [1]. WAT is distributed over various depots throughout the body that can have distinct molecular and physiological properties [14–16]. Total fat mass can be subcategorized into subcutaneous (approx. 80%) and internal (approx. 20%) adipose tissue [1].

In general, adipose tissue represents a loose, highly vascularized and innervated connective tissue, in which adipocytes account for about 35-70% of the mass, but only for 25% of the total cell number. Apart from the adipocytes, AT contains a stromal-vascular fraction (SVF) composed of macrophages, fibroblasts, pericytes, blood cells, endothelial cells, and adipose precursor cells, among others [1]. Mature white adipocytes contain a single large lipid droplet which fills 90% of the cell volume, with the thin cytoplasmic ring pushed against the edge of the cell, causing the nucleus to assume a flattened morphology and leading to the typical unilocular signet-ring form. AT can respond rapidly and dynamically to alterations in nutrient deprivation and excess through adipocyte hypertrophy and hyperplasia, with hypertrophic growth predominating in adult-onset obesity, and hyperplasic growth only occurring when the existing fat cells reach a critical size [1,17]. Depending on the lipid load, the volume of adipocytes can change by several thousand-fold, reaching a maximum of approx. 1000 pl in hypertrophy, while the cellular diameter can vary between 20 and 200 µm [1]. Multiple smaller lipid droplets can be found in developing adipocytes, as well as during periods of nutrient deprivation, when triglycerides are mobilized and the central lipid vacuole disaggregates.

The space between the cells present in adipose tissue is filled up with extracellular matrix (ECM), which is produced by the adipocytes as well as by the SVF cells and is subject to constant turnover, mediated by enzymes promoting construction or involved in the degradation of the ECM. Each adipocyte is surrounded by a thick ECM referred to as basal lamina, which is mainly composed of collagens, most notably collagen IV, but also contains laminin and nidogen, among many other proteins [18–21]. This ECM not only accounts for the integrity of the structural system supporting the cells, but also has an impact on differentiation and cell migration via interactions with cell-surface receptors [22].

1.1.2 Functions of adipose tissue

For many years, the role of adipose tissue was considered to be rather simple. Its main function was seen in the storage of excess energy as triglycerides and its release in the form of free fatty acids (FFA) during periods of nutrient deprivation. For example, the fall in glucose levels during fasting stimulates lipolysis, leading to release of FFA for use by a variety of tissues, such as muscle, liver and kidney [1,23,24]. Apart from this metabolic role in energy homeostasis, functions attributed to fat tissue included the insulation against heat loss through the skin as well as mechanical protection of certain organs by forming a protective padding [1].

However, starting with the identification of leptin in 1994, a paradigm shift has taken place, and it is now widely recognized that adipose tissue also represents an important endocrine organ [24,25]. Over the years, a large number of products secreted by adipocytes have been isolated and characterized, including hormones, growth factors, enzymes, cytokines and complement factors, which have been collectively termed as adipokines, as well as matrix proteins [1,26]. While some of these factors primarily have local auto- or paracrine effects in adipose tissue, others are released into the circulation and exert specific effects on target organs or systemic effects [24]. At the same time, adipocytes express receptors for most of these factors, enabling an extensive crosstalk at a local and systemic level [1]. As a consequence, adipose tissue is now known to participate in many physiological processes, including not only lipid metabolism and energy balance, but also reproduction, immune response, blood pressure control, coagulation, fibrinolysis, and angiogenesis [1,27]. As adipocytes also play a role in the regulation of insulin sensitivity and glucose homeostasis, a dysregulation of the secretion of certain adipokines, as it occurs in obese individuals, can contribute to the development of type 2 diabetes and related disorders, thus representing a link between obesity and its associated co-morbidities [1,13,28–30]. Leptin, which is secreted by mature adipocytes, acts within a negative feedback loop for the maintenance of energy homeostasis by decreasing food intake and increasing energy expenditure. However, although leptin levels are high in obese subjects, these patients have developed a central leptin resistance, prohibiting the hormone’s regulatory role on body weight [24,25,31]. Adiponectin, which is one of the most abundantly expressed genes in adipocytes, has been found to play a protective role against several obesity-related disorders through various insulin-sensitizing effects on different tissues, such as liver and skeletal muscles. Accordingly, in contrast to leptin, the production of adiponectin is reduced in obesity, which has been demonstrated to play a role in the pathogenesis of type 2 diabetes and cardiovascular disease [24,25,32,33]. Other adipose-derived factors involved in energy homeostasis, glucose and lipid metabolism include visfatin, lipoprotein lipase (LPL),

apolipoprotein E (apoE), adipsin, adipocyte protein 2 (aP2/FABP4), glucocorticoids and sex steroids, among others [1,25]. Moreover, factors like TNF-α, IL-6, plasminogen activator inhibitor-1 (PAI-1) or angiotensinogen, play different roles in the regulation of vascular homeostasis as well as in the pathogenesis of atherosclerosis [1,34]. Growth factors released by adipocytes include insulin-like growth factor I (IGF-I), nerve growth factor (NGF), transforming growth factor-β (TGF-β), vascular endothelial growth factor (VEGF) and leukemia inhibitory factor (LIF) [1].

Considering this great variety of adipose-derived factors and their diverse physiological and pathophysiological functions, a better understanding of adipokines gene expression and secretion may facilitate the development of rational approaches to the treatment of the metabolic syndrome and other obesity-related diseases.

1.1.3 Adipocyte differentiation

Adipogenic differentiation, or adipogenesis, not only occurs during embryonic development, but also throughout the lifetime of the organism, both in response to normal cell turnover and when the need for additional fat mass storage arises during periods in which caloric intake exceeds nutritional requirements. In this process, proliferating, mesenchymal, fibroblast-like progenitor cells residing in the SVF become permanently cell cycle-arrested, spherical, lipid-filled and functionally mature adipocytes. Adipogenesis not only involves extensive alterations in cell shape and ECM structure and composition, but is also accompanied by molecular changes that lead to dramatic increases in the ability of the cell for lipid synthesis and in the hormonal responsiveness specific to the specialized role of the adipocyte in energy homeostasis [22,35].

It is widely accepted that adipocyte development can be divided into two phases (Fig. 1-1). The first phase, known as determination, involves the commitment of a pluripotent stem cell to the adipocyte lineage. It results in the conversion of the stem cell to a preadipocyte, which cannot be distinguished morphologically from its precursor cell but has lost the potential to differentiate into other cell types [14]. However, molecular mechanisms regulating this process, as well as the identity of committed preadipocytes, have not been extensively studied up to now and are still poorly understood [36]. In contrast, the second phase, known as terminal differentiation, in which the preadipocyte takes on the characteristics of the mature adipocyte, has been extensively studied, mostly using mouse preadipocyte cell lines such as 3T3-L1, 3T3-F442A or C3H10T1/2. Especially in recent years, also human preadipocyte cell lines as well as human mesenchymal stem cells have been applied for adipogenesis research [14,37].

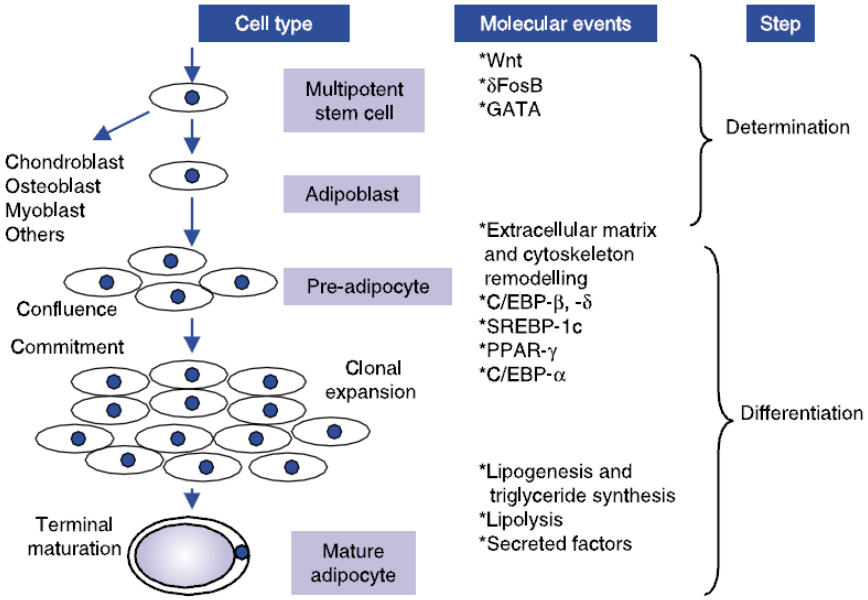

Fig. 1-1: *Adipocyte determination and differentiation: overview (reprinted with permission from [37])*

It is now well established that the differentiation of adipocytes is a complex multi-step process dependent on the strict temporal regulation of inhibitory and stimulatory signaling events [14,22,37]. Using clonal cell lines, it has been found that during the early phase of adipogenesis committed preadipocytes undergo at least one round of mitosis before entering a state of growth arrest. Although there are some controversial reports after experiments with human primary preadipocytes, this step is considered to be required for terminal differentiation [14,22,38]. The whole process of adipogenesis involves a highly regulated cascade of transcriptional events [14,39]. Several transcription factors have been found to play a central role in this cascade, most notably members of the peroxisome proliferator activated receptor (PPAR) and CCAAT-enhancer binding protein (C/EBP) families [14,37,40]. Specifically, C/EBPβ and C/EBPδ are transiently expressed very early during adipogenic differentiation. By binding to the promoters of the corresponding genes, these factors are responsible for the subsequent upregulation of PPARγ and C/EBPα, which represent the key regulators of adipogenesis [14,39]. Interestingly, the continuous expression of these two factors is sustained by a positive feedback loop, which serves to maintain the phenotype of the mature adipocyte [37,41]. PPARγ and C/EBPα directly or indirectly trigger the expression of many adipocyte-specific target genes, e.g. glucose transporter GLUT4 (also known as SLC2A4), fatty-acid-binding protein (FABP4, also known as adipocyte protein 2, aP2), lipoprotein lipase (LPL), perilipin, the adipokines adiponectin and leptin and many more [39]. Apart from those already mentioned, several other transcription factors have been shown to be important for adipogenic differentiation, such as Krox20, Krüppel-like factors, sterol-regulatory element-binding protein (SREBP)-1c, and Stat5, all of which appear to regulate

adipogenesis by regulating the expression or activity of PPARγ or the members of the C/EBP family [41]. For instance, SREBP-1c, a member of the helix-loop-helix family, has been identified to induce PPARγ expression and has been suggested to be responsible for the generation of an as-yet-unknown endogenous PPARγ ligand [14,42,43].

For a better understanding of adipose tissue development it is also important to know which signaling pathways exist upstream of the adipogenic cascade outlined above. *In vivo*, these pathways transduce information about the suitability of intracellular and extracellular conditions for adipogenic differentiation, thereby influencing whether adipogenesis is triggered in stem cells, or not [14,39,44]. Furthermore, such signals are necessary to mediate cross-talk between SVF cells and adipocytes to ensure that growth of existing adipocytes and differentiation of new adipocytes are tightly coupled to energy storage demands [44]. Although these pathways are less well characterized than the adipogenic program itself, many factors have been identified which either promote or block the transcriptional program itself [37]. For example, suppression of the Wnt/β-catenin pathway has been shown to be essential for adipogenesis to proceed *in vitro* and *in vivo* [39,44]. Recently, several other mechanisms controlling adipogenesis have been described, including histone modifications, microRNAs or post-translational modifications, further contributing to illustrate the complexity of the adipogenic program [39].

While it remains to be clarified what exactly triggers adipogenesis *in vivo*, adipogenic differentiation can easily be stimulated using a combination of adipogenic inducers *in vitro*. Although the exact composition varies depending on the cell culture model, these induction cocktails usually contain insulin (or IGF-1), a glucocorticoid (e.g. dexamethasone), an agent increasing intracellular cAMP concentrations (typically 3-isobutyl-1-methylxanthin [IBMX]) and often also a PPARγ-ligand (e.g. thiazolodinediones or indomethacin) [22,45]. Of these, insulin and IGF-1 mediate their adipogenic effect via the IGF-1 receptor pathway, which eventually contributes to the upregulation of PPARγ and C/EBPα [46–48]. While the glucocorticoid dexamethasone has been shown to suppress Pref-1, which inhibits adipogenesis, and to induce the expression of C/EBPδ, IBMX increases intracellular cAMP concentration, which stimulates protein kinase pathways leading to an upregulation of C/EBPβ [22,49–52]. Indomethacin, on the other hand, functions as a direct PPARγ agonist [53]. However, as virtually all studies dealing with the functions of these inducers have been performed in a 2-D *in vitro* system, it is unclear how specific influences of a 3-dimensional microenvironment, e.g. extensive cell-cell contacts or the presence of a prominent ECM, might alter the effectiveness or the necessity of certain components for the induction and maintenance of adipogenic differentiation.

1.2 Adipose tissue vascularization

Native adipose tissue is supplied by an extensive vascular network, with every adipocyte being associated with one or more capillaries [54,55]. Since AT, unlike most other tissues, undergoes continuous expansion and regression during adult life, a parallel remodeling and expansion of the capillary network is required. As a consequence, the formation of new blood vessels (angiogenesis) it tightly linked with adipogenesis [56]. Interestingly, many obesity-related disorders, like diabetic ocular and kidney complications, cardiovascular disease, stroke, and cancer, are closely connected with vascular dysfunctions [54].

During embryonic development, the formation of blood vessels is spatially and temporally associated with adipogenesis, with the arteriolar differentiation usually preceding adipocyte development [57]. The *de novo* formation of a vascular network in the developing embryo involves the differentiation of distinct progenitor cells into endothelial cells and is known as vasculogenesis [58]. In contrast, the process through which new blood vessels arise from preexisting ones, mainly via sprouting of quiescent vascular EC, has been termed angiogenesis. In recent years, it has been found that endothelial progenitor cells are also present in adult bone marrow and circulating blood, suggesting that vasculogenesis is not limited to the embryo, but also contributes to neovascularization in adults [59]. Therefore, it is now recognized that adult neovascularization, as it occurs in adipose tissue, most likely is a more complex process involving both angiogenesis and vasculogenesis simultaneously [60].

The process of angiogenesis involves an extensive cross-talk between vascular cells, the extracellular environment and periendothelial cells, i.e. (pre-)adipocytes in the case of adipose tissue vascularization. It is regulated by a fine balance between pro- and antiangiogenic factors, the “angiogenic switch” [61]. When proangiogenic signals predominate, e.g. in hypoxic conditions, quiescent EC are activated and vessel branching takes place. For a detailed description of the sequential steps during angiogenic sprouting and the molecular mechanisms involved, the reader is referred to comprehensive reviews on this topic, e.g. by Carmeliet and Jain [58] or Herbert and Stainier [62].

There is increasing evidence that (pre-)adipocytes and endothelial cells communicate via paracrine signaling pathways, extracellular components, and direct cell-cell interactions in order to promote and regulate adipose tissue vascularization. Growing adipocytes are known to produce several proangiogenic factors, including VEGF, HGF, IGF-1, bFGF, TGFβ or angiopoietins [54,55]. In recent years, it has been described that also in adipose-derived stem cells (ASC) the secretion of these factors is strongly upregulated when the appropriate molecular stimuli are present [63,64]. Interestingly, not only these classic proangiogenic cytokines, but also some adipokines, like leptin, adiponectin and resistin seem to be involved in the modulation of AT angiogenesis under both physiological and pathological

conditions [61]. For example, leptin has been demonstrated to induce HUVEC migration, proliferation and tube formation *in vitro* [65]. Apart from this direct proangiogenic activity, leptin stimulates neovascularization by upregulating VEGF expression and acting synergistically with VEGF and bFGF [66,67]. Furthermore, leptin facilitates angiogenesis by inducing the activity of MMP-2 and MMP-9. These and other matrix metalloproteinases play an important role in angiogenic sprouting and vessel maturation by contributing to the degradation and remodeling of the ECM, which is not only necessary to adapt matrix structure to the changing cellular geometry, but is also accompanied by the release of matrix-bound angiogenic factors like VEGF [54,55]. Controversial reports exist regarding the influence of adiponectin on angiogenesis. While it has been found to stimulate blood vessel growth in different adipogenesis models [68], inhibiting effects of adiponectin on endothelial cell migration and proliferation have been reported in another study [69].

The cellular cross-talk during the development of vascularized adipose tissue involves a reciprocal regulation of vessel formation and fat cell maturation. However, information about the specific influence of endothelial cell signaling on the process of adipogenic differentiation from *in vitro* culture is scarce and partially conflicting. Depending on the experimental conditions, either an increase or a reduction of adipogenesis was described in the presence of EC (see Chapter 6.5 for a literature overview).

All in all, in many respects our knowledge in the field of adipose tissue angiogenesis is still limited, not only regarding the temporal and spatial interplay between the different cell types during *in vivo* vascularization and vessel remodeling, but also concerning the effects of these interactions on metabolic functions of the cell types [70–72]. Further investigations utilizing model systems more closely resembling the *in vivo* situation are necessary to shed more light on this aspect of adipose tissue development.

1.3 *In vitro* adipose tissue models

Although *in vivo* approaches such as the use of transgenic animals have contributed significantly to our current understanding of adipose tissue development and functions, most of our knowledge in this field is based on *in vitro* model systems, as they represent a powerful and versatile tool for a great variety of applications in basic research [14,22]. In this context it should not be disregarded that *in vitro* models can never represent every ascpect of native tissues, but all have advantages and limitations. Hence, when performing *in vitro* studies, it is not only necessary to choose an appropriate model system depending on the respective research goals, but it would also be desirable that the existing models are continuously refined and new model systems are developed.

Among others, two of the most relevant parameters which influence the validity of results gained from studies applying *in vitro* models of adipose tissue are (a) the cell source on which the culture is based, and (b) the culture dimensionality, both of which will be addressed in this section.

1.3.1 Cell sources for adipose tissue research

In comparison to most other cell types, the isolation and *in vitro* culture of mature adipocytes is difficult and inconvenient to perform. The buoyancy and fragility of these cells resulting from their high lipid content and specific morphology makes conventional cell culture almost impossible. Special culture methods have been developed, such as ceiling culture or floating culture. Interestingly, cultured adipocytes have been found to dedifferentiate and become proliferative again, with the potential to re-differentiate into lipid-filled adipocytes as well as other cell types [73–76]. However, these protocols are not generally applicable for most research purposes [75]. Furthermore, human primary cells only have a limited lifespan in culture leading to a constant need for fresh cell supply.

The introduction of immortalized preadipocyte cell lines in the 1970s represented a great step ahead in adipose tissue research. The 3T3-L1 cell line and other mouse cell lines, which have a fibroblast-like morphology, are not only easy to culture and expand, but can also be efficiently and reproducibly differentiated into adipocytes *in vitro* using specific induction media, even after extensive passaging. Over the years, they have become well-characterized and have proven to be powerful model systems for studying many aspects of adipocyte biology, especially regarding the complex molecular events during adipocyte differentiation [14,22,40,75].

Nevertheless, these cell lines exhibit significant drawbacks. Most importantly, they are unipotent, i.e. already committed to the adipocyte lineage and therefore cannot be used for the study of the early phase of adipogenic differentiation [22,40]. Furthermore, being clonal rodent cell lines, they are aneuploid and may therefore reflect the *in vivo* situation less accurately than diploid primary cells. Moreover, the use of human cells would eliminate the problem of interspecies differences in adipocyte biology that have been shown to exist between humans and, for example, rodents [22,75,77].

Certainly, human embryonic stem cells would be an ideal cell source for adipose tissue research due to their pluripotence and proliferation characteristics. However, their application is limited because of ethical and legal concerns [78–80].

The application of stem cells derived from adult human tissues offers an approach that can help to circumvent these constraints. These adult stem cells, which have been isolated from various tissues including bone marrow, adipose tissue, muscle, liver, brain, umbilical cord

blood, Wharton's jelly from the umbilical cord, placenta, peripheral blood, and pancreas, still have the capacity for self-renewal and are capable of differentiation along multiple lineages (multipotency) [78,80–82]. Until recently, bone marrow has been most commonly used as a source for adult stem cells, termed bone-marrow derived stem cells (BMSC). However, stem cells are rare in bone marrow, as in most other adult tissues, meaning that only small amounts of stem cells can be harvested, with isolation procedures being difficult and painful [79,82].

Only in recent years, adipose tissue has been identified as a source of mesenchymal stem cells (MSC), which reside within its stromal-vascular fraction [36,78,83]. According to a consensus reached by the International Fat Applied Technology Society (IFATS), these cells are termed adipose-derived stem cells (ASC) within this work [84]. In contrast to MSC from other tissues, adipose-derived stem cells are easily available in large quantities, as they can be isolated from lipoaspirates, the waste product of liposuction surgery [82,85–87]. Although an exact phenotypic definition of ASC and a clear discrimination against fibroblasts is difficult and still disputed, it could be demonstrated that ASC, similar to BMSC, have the ability to differentiate into a large variety of cell types, including adipocytes, osteoblasts, chondrocytes, myocytes, endothelial cells and neuronal cells, and even pancreatic and hepatocyte-like cells [36,88]. Furthermore, this multipotency is retained even after serial passaging [89,90]. Especially because of their potential for tissue engineering and regenerative medicine, there has been an explosion in research focusing on ASC in recent years [36,91]. As they are actually part of the stromal-vascular fraction of adipose tissue *in vivo*, ASC represent an ideal cell source for the use in *in vitro* models aiming at the investigation of the whole process of adipose tissue development, starting with the very early stages such as lineage commitment [22,92].

1.3.2 *In vitro* models in two and three dimensions

In most cases, *in vitro* culture of cells is performed as a monolayer on flat and hard tissue culture plastic. As natural tissues are 3-dimensional, it is obvious that these conventional culture models are not able to represent the cellular environment that exists *in vivo* [93,94]. While culturing cells in 2-D is fast and simple, it cannot capture the relevant complexity of the *in vivo* microenvironment, and as a consequence many tissue-specific aspects are lost under these simplified conditions. Among these are the influence of the extracellular matrix (ECM), mechanical and biochemical signals, and cell-cell communication. In contrast, 3-D culture models have the potential to more closely reproduce the complex and dynamic microenvironments of *in vivo* tissues, thereby bridging the gap between traditional cell culture and animal models [94,95]. Up to now a large number of studies using various cell types and

culture systems has clearly demonstrated notable differences between 2-D and 3-D models regarding cellular function and behavior. These differences are not limited to morphology, adhesion, proliferation and differentiation, but also extend to nuclear structure, signal transduction, gene expression and the reaction to external cues as well as mechanical stimulation, among other aspects [93–97]. One of the most important advantages of 3-D culture systems is the presence of a distinct ECM, which contributes to the microenvironmental specificity not only through its mechanical features, but also through its own signaling moieties and its ability to bind growth factors, enzymes and other diffusible molecules [95,98]. Therefore, it plays an important role in the regulation of many cellular functions, as it has for example been shown for WAT differentiation and lipid accumulation [99,100]. Cell–cell and cell–ECM interactions establish a 3-D communication network that maintains the specificity and homeostasis of the tissue and are therefore of pivotal importance for normal cell differentiation and function [93,95,101].

With respect to adipose tissue culture, a variety of 3-D culture systems has been developed. As most of these were intended to serve for tissue engineering applications, they are usually based on the seeding of adipocyte precursor cells on scaffold materials or on encapsulating them in natural or synthetic hydrogels [102,103]. While these systems have proven to be useful also in basic research, especially for investigating the specific influence of ECM components and mechanical signals, they also have certain drawbacks. Among these are the often unknown influence of carrier materials on cellular functions, the still limited cell-cell interactions due to the lack of direct intercellular contacts at least in the first phase of culture, and a gradient in nutrition and oxygen supply caused by a limited diffusion within larger constructs.

The application of multicellular spheroid models can be a way to avoid most of these specific drawbacks. Originally developed as early as in the 1940´s, these spheroid models have been adapted for the investigation of radiation effects in tumor biology in the 1970´s and have since then been used mainly in cancer research [101,104–107]. However, they can be a valuable tool also in other areas of research, using different cell and tissue types [101]. Over the years, various techniques have been developed for the generation and culture of spheroids, as reviewed by Lin and Chang [108], making them a versatile model system for various applications in basic research.

Multicellular spheroids have several advantages in comparison with other 3-D culture systems. The lack of scaffolds or hydrogels as cell carriers not only obliterates the unknown influence of these materials on the cells, but also allows for direct cell-cell contact immediately after self-assembly. Furthermore, they can easily be produced in large numbers, exhibit a defined and reproducible geometry, and their small size leads to sufficient and homogeneous supply with nutrients and oxygen throughout the constructs. Another important

feature of spheroid models is the possibility to cocultivate different cell types in a tissue-like environment to study heterotypic cell-cell interactions [101,107].

Apart from that, it also appears possible to utilize multicellular spheroids for drug screening applications. Today, high-throughput screening (HTS) is used by most pharmaceutical companies in drug lead discovery. However, in the commonly employed 2-D assays cellular response to specific agents may vary considerably from the corresponding *in vivo* effects, which limits their value in predicting clinical outcomes [107]. Only in recent years it has been acknowledged that it is necessary to develop 3-D cell culture systems suitable for drug screening assays [107,109]. In contrast to carrier-based 3-D models, which require complex and labor-intensive handling and often exhibit limited reproducibility, spheroids have the potential to serve as a basis for the development of improved 3-D HTS systems for drug discovery [107].

Finally, spheroids can also be used for applications in tissue engineering and regenerative medicine. They can either be transferred directly into the host, or they can be incorporated into hydrogels, which are subsequently injected or implanted *in vivo* [101,110–112]. It has also been described that spheroids can serve as building blocks for engineering complex tissues using the organ-printing technique [101,113].

In summary, multicellular spheroids represent a stable, reproducible, easy to handle and very versatile 3-D culture system providing a more *in-vivo*-like environment for applications in basic research as compared to conventional monolayer culture, and with the potential to be used as a basis for tissue engineering.

1.4 Adipose tissue engineering

Adipose tissue engineering aims at the generation of transplantable and biologically functional adipose tissue grafts for the application in reconstructive and plastic surgery. The need for adipose tissue reconstruction in regenerative medicine can be the result of soft tissue loss after traumatic injuries or operative removal as well as congenital defects. In this context, reconstruction after tumor resections alone accounts for a large number of surgeries. Moreover, engineered adipose tissue grafts would represent an ideal filling material for plastic and aesthetic surgeries [114].

To avoid problems with biocompatibility, immune response and tissue rejection, the use of autologous fat tissue appears to be ideal for soft tissue reconstruction. However, traditional approaches have been of limited success for several reasons. Single cell injections of liposuctioned tissue have been used for the treatment of smaller defects, but due to the fragility of mature adipocytes, the majority of them are lost during aspiration or preparation. Furthermore, cyst formation, local necrosis and the absorption of cells occur at the injection

site, making repeated treatments necessary. Transplantation of fat grafts in most cases leads to the resorption of large parts of the transplanted tissue, which is mainly caused by insufficient vascularization and the resulting lack of nutrient and oxygen supply, and therefore often repeated surgery is necessary [103,114,115]. The use of pedicled flaps can help to avoid this problem, but involves a complicated and cost-intensive procedure and can cause donor site morbidity [103,116].

Therefore, the development of engineered fat tissue substitutes, which could help to overcome these limitations, provides a new clinical prospective in regenerative medicine. Two general approaches can be distinguished in adipose tissue engineering: acellular and cell-based methods. The former are based on the induction of *de novo* adipogenesis at the site of tissue defects. This has been demonstrated, for example, by the application of Matrigel together with pro-adipogenic growth factors such as bFGF, which can indeed lead to the development of vascularized adipose tissue. However, besides the fact that Matrigel (a mouse tumor product) is unsuitable for clinical applications, size and shape of the developing tissue can hardly be controlled in this process [103].

In cell-based approaches, various carrier materials are seeded with adipocyte precursor cells, which are subsequently implanted *in vivo*, often following a period of *in vitro* preculturing. Those carrier materials can be porous scaffolds, defining the shape of the developing tissue graft. These scaffolds, which should be biocompatible and biodegradable, can be composed of synthetic polymers, such as PLGA, or natural materials, e.g. collagen, hyaluronic acid, or silk. The type of carrier material, but also physical properties, such as pore size and stiffness of these scaffold materials can strongly influence the performance of the cells and the development of a functional tissue and therefore have to be optimized according to the specific application. For example, surface modifications such as the incorporation of cell adhesion proteins can enhance cellular proliferation and tissue growth.

Apart from these scaffold materials, also hydrogels are a common cell carrier for adipose TE approaches. They can either be used in an injectable form, allowing for a minimally invasive procedure, or they are implanted after gelation *in vitro*. It is also possible to combine those hydrogels with a solid support structure or scaffold to enhance mechanical stability of the construct. Hydrogels that have been applied for adipose TE include PEG and its derivatives, but also natural polymers like fibrin, hyaluronan, alginate or collagen. A further approach involves the attachment of cells to microspheres, which can then be injected directly or embedded into a hydrogel for subsequent injection or implantation [103,114,115].

Besides the choice of an appropriate carrier material, the nature of the cells used is an important issue in adipose tissue engineering. Here, the discovery of ASC represented an important step, as they can be easily harvested from autologous tissue in large numbers, are non-immunogenic and have the potential to be expanded and induced to undergo adipogenic

differentiation *in vitro* (see also section 1.3.1). Therefore, ASC are currently seen as the most promising cell source not only for adipose tissue basic research, but also applications in regenerative medicine. In this context, it is important to note that *in vivo* the implanted cells not only represent building blocks that are used to reconstruct the tissue defect, but can also serve as modulators of the local environment at the implantation site, which can contribute to the tissue regeneration e.g. by triggering vascularization and by stimulating host cells to also differentiate into adipocytes [103].

One of the main challenges for tissue engineering in general is the supply of the newly generated tissues with nutrient and oxygen by providing sufficient vascularization. As adipose tissue is highly metabolically active and is therefore strongly vascularized in its native condition, the development of a functional vasculature is of special importance. After implantation, blood vessels from the host tissue usually begin to invade the transplant, but as this process is slow, especially in larger tissue grafts nutrient deficiencies and hypoxia can occur in the center of the tissue. Furthermore, this will lead to nutrient and oxygen gradients, resulting in an inhomogeneous cell differentiation [103,117].

Different strategies are pursued to improve the vascularization of tissue transplants: (1) Scaffold design aims at the development of carrier materials facilitating vessel ingrowth after implantation. This involves for example the adjustment of pore size and interconnectivity, whereas more advanced approaches aim at designing a well-defined complex architecture, e.g. by rapid prototyping or fiber deposition. (2) The delivery of angiogenic factors can also enhance *in vivo* vascularization of tissue grafts. Thereby, growth factors such as VEGF and bFGF are added to the scaffold biomaterials and are released after implantation by diffusion and/or during polymer degradation. (3) *In vivo* prevascularization involves as a first step the implantation of a tissue construct, with an arterio-venous vessel loop being surgically integrated into the new tissue. Within several weeks, a microvascular network develops within the tissue graft, and after this vascularization period the tissue is transplanted to the actual defect site, with the main blood vessel being connected to the existing vasculature. (4) Finally, *in vitro* prevascularization is based on the preformation of vascular structures during an *in vitro* culture period prior to implantation. This can be achieved by coculturing tissue specific progenitor cells (e.g. ASC) with endothelial cells. *In vivo*, the prevascular network can then anastomose with the host vasculature [103,117–119].

Whereas the first two strategies are relatively straightforward and have been proven to be effective in increasing the vascularization of engineered tissues, they still rely on the ingrowth of host vessels. Thus, depending on construct size central areas still are exposed to hypoxia and nutrient deprivation in the first days or weeks. With *in vivo* prevascularization, besides the fact that it involves two elaborate surgical procedures, the problem of slow host vessel

ingrowth is still present during the first stage of the process. In contrast, *in vitro* prevascularization has the potential to provide a much faster perfusion of the whole constructs, as the host vessels only need to grow in until they connect the existing vascular structures within the transplant. Thus, the latter, of course also in combination with the other approaches, appears to be a promising strategy to tackle the problem of vascularization in tissue engineering [117,120]. However, only a limited number of studies have investigated the potential of this strategy in adipose TE up to now [121–123]. As the development of vascularized adipose tissue is a very complex process depending on reciprocal regulation between the involved cell types, the generation of engineered tissue constructs including a functional vasculature is not an easy task. Specifically, one of the major obstacles in finding a suitable *in vitro* coculture system is the adjustment of the culture conditions and protocols to allow for both the development of functional adipocytes and the formation of the vascular network [117,124]. In order to optimize current strategies for vascularization in adipose TE, it is crucial to further improve our understanding of the complex physiological processes involved in the development of native adipose tissue, which include, but are not limited to, adiopogenesis, angiogenesis and their various levels of interplay.

1.5 References

1. Fruhbeck G. Overview of adipose tissue and its role in obesity and metabolic disorders. *Methods Mol Biol* 2008, vol. 456, 1–22.
2. Maury E, Brichard S M. Adipokine dysregulation, adipose tissue inflammation and metabolic syndrome. *Mol Cell Endocrinol* 2010; **314***, 1*, 1–16.
3. Bjørndal B, Burri L, Staalesen V, Skorve J, Berge R K. Different adipose depots: their role in the development of metabolic syndrome and mitochondrial response to hypolipidemic agents. *J Obes* 2011, 15 pages.
4. Kopelman P G. Obesity as a medical problem. *Nature* 2000; **404***, 6778*, 635–643.
5. Berghöfer A, Pischon T, Reinhold T, Apovian C M, Sharma A M, Willich S N. Obesity prevalence from a European perspective: a systematic review. *BMC Public Health* 2008; **8**, 200.
6. Flier J S. Obesity wars: molecular progress confronts an expanding epidemic. *Cell* 2004; **116***, 2*, 337–350.
7. Kiess W, Petzold S, Topfer M, Garten A, Bluher S, Kapellen T, Korner A, Kratzsch J. Adipocytes and adipose tissue. *Best Pract Res Clin Endocrinol Metab* 2008; **22***, 1*, 135–153.
8. Després J-P, Lemieux I. Abdominal obesity and metabolic syndrome. *Nature* 2006; **444***, 7121*, 881–887.
9. Rajala M W, Scherer P E. Minireview: The adipocyte--at the crossroads of energy homeostasis, inflammation, and atherosclerosis. *Endocrinology* 2003; **144***, 9*, 3765–3773.
10. Sharma A M, Chetty V T. Obesity, hypertension and insulin resistance. *Acta Diabetol* 2005; **42**, 3–8.
11. Nawrocki A R, Scherer P E. Keynote review: The adipocyte as a drug discovery target. *Drug Discovery Today* 2005; **10***, 18*, 1219–1230.
12. Gesta S, Tseng Y-H, Kahn C R. Developmental origin ofvan fat: Tracking obesity to its source 2007; **131***, 2*, 242–256.
13. Arner P. The adipocyte in insulin resistance: key molecules and the impact of the thiazolidinediones. *Trends Endocrinol Metab* 2003; **14***, 3*, 137–145.
14. Rosen E D, MacDougald O A. Adipocyte differentiation from the inside out. *Nat Rev Mol Cell Biol* 2006; **7***, 12*, 885–896.
15. Prunet-Marcassus B, Cousin B, Caton D, Andre M, Penicaud L, Casteilla L. From heterogeneity to plasticity in adipose tissues: Site-specific differences. *Exp Cell Res* 2006; **312***, 6*, 727–736.
16. van Harmelen V, Rohrig K, Hauner H. Comparison of proliferation and differentiation capacity of human adipocyte precursor cells from the omental and subcutaneous adipose tissue depot of obese subjects. *Metabolism* 2004; **53***, 5*, 632–637.
17. Sun K, Kusminski C M, Scherer P E. Adipose tissue remodeling and obesity. *J Clin Invest* 2011; **121***, 6*, 2094–2101.
18. Kubo Y, Kaidzu S, Nakajima I, Takenouchi K, Nakamura F. Organization of extracellular matrix components during differentiation of adipocytes in long-term culture. *In Vitro Cell Dev Biol Anim* 2000; **36***, 1*, 38–44.

19. Nakajima I, Muroya S, Tanabe R i, Chikuni K. Extracellular matrix development during differentiation into adipocytes with a unique increase in type V and VI collagen. *Biol Cell* 2002; **94***, 3*, 197–203.

20. Halberg N, Wernstedt-Asterholm I, Scherer P E. The adipocyte as an endocrine cell. *Endocrinol Metab Clin North Am* 2008; **37***, 3*, 753-68, x-xi.

21. Mariman E, Wang P. Adipocyte extracellular matrix composition, dynamics and role in obesity. *Cell Mol Life Sci* 2010; **67***, 8*, 1277–1292.

22. Avram M M, Avram A S, James W D. Subcutaneous fat in normal and diseased states: 3. Adipogenesis: From stem cell to fat cell. *J Am Acad Dermatol* 2007; **56***, 3*, 472–492.

23. Ahima R S, Flier J S. Adipose tissue as an endocrine organ. *Trends Endocrinol Metab* 2000; **11***, 8*, 327–332.

24. Fischer-Posovszky P, Wabitsch M, Hochberg Z. Endocrinology of adipose tissue - an update. *Horm Metab Res* 2007; **39***, 5*, 314–321.

25. Waki H, Tontonoz P. Endocrine functions of adipose tissue. *Annu Rev Pathol Mech Dis* 2007; **2***, 1*, 31–56.

26. Lago F, Gómez R, Gómez-Reino J J, Dieguez C, Gualillo O. Adipokines as novel modulators of lipid metabolism. *Trends Biochem Sci* 2009; **34***, 10*, 500–510.

27. Trayhurn P, Beattie J H. Physiological role of adipose tissue: white adipose tissue as an endocrine and secretory organ. *Proc Nutr Soc* 2001; **60***, 3*, 329–339.

28. Flier J S. Diabetes. The missing link with obesity? *Nature* 2001; **409***, 6818*, 292–293.

29. Kahn S E, Hull R L, Utzschneider K M. Mechanisms linking obesity to insulin resistance and type 2 diabetes. *Nature* 2006; **444***, 7121*, 840–846.

30. Antuna-Puente B, Feve B, Fellahi S, Bastard J-P. Adipokines: the missing link between insulin resistance and obesity. *Diabetes Metab* 2008; **34***, 1*, 2–11.

31. Kelesidis T, Kelesidis I, Chou S, Mantzoros C S. Narrative review: the role of leptin in human physiology: emerging clinical applications. *Ann Intern Med* 2010; **152***, 2*, 93–100.

32. van Gaal L F, Mertens I L, Block C E de. Mechanisms linking obesity with cardiovascular disease. *Nature* 2006; **444***, 7121*, 875–880.

33. Kadowaki T, Yamauchi T. Adiponectin receptor signaling: a new layer to the current model. *Cell Metab* 2011; **13***, 2*, 123–124.

34. Frühbeck G. The adipose tissue as a source of vasoactive factors. *Curr Med Chem Cardiovasc Hematol Agents* 2004; **2***, 3*, 197–208.

35. Lefterova M I, Lazar M A. New developments in adipogenesis. *Trends Endocrinol Metab* 2009; **20***, 3*, 107–114.

36. Cawthorn W P, Scheller E L, MacDougald O A. Adipose tissue stem cells meet preadipocyte commitment: going back to the future. *J Lipid Res* 2011.

37. Feve B. Adipogenesis: cellular and molecular aspects. *Best Pract Res Clin Endocrinol Metab* 2005; **19***, 4*, 483–499.

38. Otto T C, Lane M D. Adipose development: from stem cell to adipocyte. *Crit Rev Biochem Mol Biol* 2005; **40***, 4*, 229–242.

39. Lowe C E, O'Rahilly S, Rochford J J. Adipogenesis at a glance. *J Cell Sci* 2011; **124***, Pt 16*, 2681–2686.

40. Ntambi J M, Young-Cheul K. Adipocyte differentiation and gene expression. *J Nutr* 2000; **130***, 12*, 3122S-3126S.

41. Siersbaek R, Nielsen R, Mandrup S. PPARgamma in adipocyte differentiation and metabolism--novel insights from genome-wide studies. *FEBS Lett* 2010; **584***, 15*, 3242–3249.

42. Kim J B, Spiegelman B M. ADD1/SREBP1 promotes adipocyte differentiation and gene expression linked to fatty acid metabolism. *Genes Dev* 1996; **10***, 9*, 1096–1107.

43. Kim J B, Wright H M, Wright M, Spiegelman B M. ADD1/SREBP1 activates PPARγ through the production of endogenous ligand. *Proc Natl Acad Sci U S A* 1998; **95***, 8*, 4333–4337.

44. Christodoulides C, Lagathu C, Sethi J K, Vidal-Puig A. Adipogenesis and WNT signalling. *Trends Endocrinol. Metab* 2009; **20***, 1*, 16–24.

45. MacDougald O A, Mandrup S. Adipogenesis: forces that tip the scales. *Trends Endocrinol Metab* 2002; **13***, 1*, 5–11.

46. Smith P J, Wise L S, Berkowitz R, Wan C, Rubin C S. Insulin-like growth factor-I is an essential regulator of the differentiation of 3T3-L1 adipocytes. *J Biol Chem* 1988; **263***, 19*, 9402–9408.

47. Rieusset J, Andreelli F, Auboeuf D, Roques M, Vallier P, Riou J P, Auwerx J, Laville M, Vidal H. Insulin acutely regulates the expression of the peroxisome proliferator-activated receptor-gamma in human adipocytes. *Diabetes* 1999; **48***, 4*, 699–705.

48. Miki H, Yamauchi T, Suzuki R, Komeda K, Tsuchida A, Kubota N, Terauchi Y, Kamon J, Kaburagi Y, Matsui J, Akanuma Y, Nagai R, Kimura S, Tobe K, Kadowaki T. Essential role of insulin receptor substrate 1 (IRS-1) and IRS-2 in adipocyte differentiation. *Mol Cell Biol* 2001; **21***, 7*, 2521–2532.

49. Smas C M, Chen L, Zhao L, Latasa M J, Sul H S. Transcriptional repression of pref-1 by glucocorticoids promotes 3T3-L1 adipocyte differentiation. *J Biol Chem* 1999; **274***, 18*, 12632–12641.

50. Shi X M, Blair H C, Yang X, McDonald J M, Cao X. Tandem repeat of C/EBP binding sites mediates PPARgamma2 gene transcription in glucocorticoid-induced adipocyte differentiation. *J Cell Biochem* 2000; **76***, 3*, 518–527.

51. Hamm J K, Park B H, Farmer S R. A role for C/EBPbeta in regulating peroxisome proliferator-activated receptor gamma activity during adipogenesis in 3T3-L1 preadipocytes. *J Biol Chem* 2001; **276***, 21*, 18464–18471.

52. Katafuchi T, Garbers D L, Albanesi J P. CNP/GC-B system: a new regulator of adipogenesis. *Peptides* 2010; **31***, 10*, 1906–1911.

53. Lehmann J M, Lenhard J M, Oliver B B, Ringold G M, Kliewer S A. Peroxisome proliferator-activated receptors alpha and gamma are activated by indomethacin and other non-steroidal anti-inflammatory drugs. *J Biol Chem* 1997; **272***, 6*, 3406–3410.

54. Cao Y. Angiogenesis modulates adipogenesis and obesity. *J Clin Invest* 2007; **117***, 9*, 2362–2368.

55. Lijnen H R. Angiogenesis and obesity. *Cardiovasc Res* 2008; **78***, 2*, 286–293.

56. Christiaens V, Lijnen H R. Angiogenesis and development of adipose tissue. Molecular and cellular aspects of adipocyte development and function. *Mol Cell Endocrinol* 2010; **318***, 1-2*, 2–9.

57. Hausman G J, Richardson R L. Adipose tissue angiogenesis. *J Anim Sci* 2004; **82***, 3*, 925–934.

58. Carmeliet P, Jain R K. Molecular mechanisms and clinical applications of angiogenesis. *Nature* 2011; **473***, 7347*, 298–307.

59. Miranville A, Heeschen C, Sengenes C, Curat C A, Busse R, Bouloumie A. Improvement of postnatal neovascularization by human adipose tissue-derived stem cells. *Circulation* 2004; **110***, 3*, 349–355.

60. Ucuzian A A, Greisler H P. In vitro models of angiogenesis. *World J Surg* 2007; **31***, 4*, 654–663.

61. Ribatti D, Conconi M T, Nussdorfer G G. Nonclassic endogenous novel regulators of angiogenesis. *Pharmacol Rev* 2007; **59***, 2*, 185–205.

62. Herbert S P, Stainier D YR. Molecular control of endothelial cell behaviour during blood vessel morphogenesis. *Nat Rev Mol Cell Biol* 2011; **12***, 9*, 551–564.

63. Rehman J, Traktuev D, Li J, Merfeld-Clauss S, Temm-Grove C J, Bovenkerk J E, Pell C L, Johnstone B H, Considine R V, March K L. Secretion of angiogenic and antiapoptotic factors by human adipose stromal cells. *Circulation* 2004; **109***, 10*, 1292–1298.

64. Kilroy G E, Foster S J, Wu X, Ruiz J, Sherwood S, Heifetz A, Ludlow J W, Stricker D M, Potiny S, Green P, Halvorsen Y D, Cheatham B, Storms R W, Gimble J M. Cytokine profile of human adipose-derived stem cells: expression of angiogenic, hematopoietic, and pro-inflammatory factors. *J Cell Physiol* 2007; **212***, 3*, 702–709.

65. Sierra-Honigmann M R, Nath A K, Murakami C, García-Cardeña G, Papapetropoulos A, Sessa W C, Madge L A, Schechner J S, Schwabb M B, Polverini P J, Flores-Riveros J R. Biological action of leptin as an angiogenic factor. *Science* 1998; **281***, 5383*, 1683–1686.

66. Cao R, Brakenhielm E, Wahlestedt C, Thyberg J, Cao Y. Leptin induces vascular permeability and synergistically stimulates angiogenesis with FGF-2 and VEGF. *Proc Natl Acad Sci USA* 2001; **98***, 11*, 6390–6395.

67. Suganami E, Takagi H, Ohashi H, Suzuma K, Suzuma I, Oh H, Watanabe D, Ojima T, Suganami T, Fujio Y, Nakao K, Ogawa Y, Yoshimura N. Leptin stimulates ischemia-induced retinal neovascularization: possible role of vascular endothelial growth factor expressed in retinal endothelial cells. *Diabetes* 2004; **53***, 9*, 2443–2448.

68. Ouchi N, Kobayashi H, Kihara S, Kumada M, Sato K, Inoue T, Funahashi T, Walsh K. Adiponectin stimulates angiogenesis by promoting cross-talk between AMP-activated protein kinase and Akt signaling in endothelial cells. *J Biol Chem* 2004; **279***, 2*, 1304–1309.

69. Bråkenhielm E, Veitonmäki N, Cao R, Kihara S, Matsuzawa Y, Zhivotovsky B, Funahashi T, Cao Y. Adiponectin-induced antiangiogenesis and antitumor activity involve caspase-mediated endothelial cell apoptosis. *Proc Natl Acad Sci USA* 2004; **101***, 8*, 2476–2481.

70. Fukumura D, Ushiyama A, Duda D G, Xu L, Tam J, Krishna V, Chatterjee K, Garkavtsev I, Jain R K. Paracrine regulation of angiogenesis and adipocyte differentiation during in vivo adipogenesis. *Circ Res* 2003; **93***, 9*, e88-97.

71. Nishimura S, Manabe I, Nagasaki M, Hosoya Y, Yamashita H, Fujita H, Ohsugi M, Tobe K, Kadowaki T, Nagai R, Sugiura S. Adipogenesis in obesity requires close interplay between differentiating adipocytes, stromal cells, and blood vessels. *Diabetes* 2007; **56***, 6*, 1517–1526.

72. Choi J H, Bellas E, Gimble J M, Vunjak-Novakovic G, Kaplan D L. Lipolytic Function of Adipocyte/Endothelial Cocultures. *Tissue Eng Part A* 2011.

73. Fernyhough M E, Vierck J L, Hausman G J, Mir P S, Okine E K, Dodson M V. Primary adipocyte culture: adipocyte purification methods may lead to a new understanding of adipose tissue growth and development. *Cytotechnology* 2004; **46***, 2-3*, 163–172.

74. Dodson M V, Fernyhough M E. Mature adipocytes: are there still novel things that we can learn from them? *Tissue Cell* 2008; **40***, 4*, 307–308.

75. Poulos S P, Dodson M V, Hausman G J. Cell line models for differentiation: preadipocytes and adipocytes. *Exp Biol Med (Maywood)* 2010; **235***, 10*, 1185–1193.

76. Asada S, Kuroda M, Aoyagi Y, Fukaya Y, Tanaka S, Konno S, Tanio M, Aso M, Satoh K, Okamoto Y, Nakayama T, Saito Y, Bujo H. Ceiling culture-derived proliferative adipocytes retain high adipogenic potential suitable for use as a vehicle for gene transduction therapy. *Am J Physiol Cell Physiol* 2011; **301***, 1*, C181-5.

77. Ryden M, Dicker A, van Harmelen V, Hauner H, Brunnberg M, Perbeck L, Lonnqvist F, Arner P. Mapping of early signaling events in tumor necrosis factor-alpha -mediated lipolysis in human fat cells. *J Biol Chem* 2002; **277***, 2*, 1085–1091.

78. Gimble J, Guilak F. Adipose-derived adult stem cells: isolation, characterization, and differentiation potential. *Cytotherapy* 2003; **5***, 5*, 362–369.

79. Rodriguez A M, Elabd C, Amri E Z, Ailhaud G, Dani C. The human adipose tissue is a source of multipotent stem cells. *Biochimie* 2005; **87***, 1*, 125–128.

80. Spencer N D, Gimble J M, Lopez M J. Mesenchymal stromal cells: past, present, and future. *Vet Surg* 2011; **40***, 2*, 129–139.

81. Guilak F, Lott K E, Awad H A, Cao Q, Hicok K C, Fermor B, Gimble J M. Clonal analysis of the differentiation potential of human adipose-derived adult stem cells. *J Cell Physiol* 2006; **206***, 1*, 229–237.

82. Locke M, Windsor J, Dunbar P R. Human adipose-derived stem cells: isolation, characterization and applications in surgery. *ANZ J Surg* 2009; **79***, 4*, 235–244.

83. Zuk P A, Zhu M, Mizuno H, Huang J, Futrell J W, Katz A J, Benhaim P, Lorenz H P, Hedrick M H. Multilineage cells from human adipose tissue: implications for cell-based therapies. *Tissue Eng* 2001; **7***, 2*, 211–228.

84. Gimble J M, Katz A J, Bunnell B A. Adipose-derived stem cells for regenerative medicine. *Circ Res* 2007; **100***, 9*, 1249–1260.

85. Dubois S G, Floyd E Z, Zvonic S, Kilroy G, Wu X, Carling S, Halvorsen Y D, Ravussin E, Gimble J M. Isolation of human adipose-derived stem cells from biopsies and liposuction specimens. *Methods Mol Biol* 2008; **449**, 69–79.

86. Bunnell B A, Flaat M, Gagliardi C, Patel B, Ripoll C. Adipose-derived stem cells: isolation, expansion and differentiation. *Methods* 2008; **45***, 2*, 115–120.

87. Wilson A, Butler P E, Seifalian A M. Adipose-derived stem cells for clinical applications: a review. *Cell Prolif* 2011; **44***, 1*, 86–98.

88. Schaeffler A, Buechler C. Concise review: adipose tissue-derived stromal cells-basic and clinical implications for novel cell-based therapies. *Stem Cells (Durham, NC, United States)* 2007; **25***, 4*, 818–827.

89. Wall M E, Bernacki S H, Loboa E G. Effects of serial passaging on the adipogenic and osteogenic differentiation potential of adipose-derived human mesenchymal stem cells. *Tissue Eng* 2007; **13***, 6*, 1291–1298.

90. Gonda K, Shigeura T, Sato T, Matsumoto D, Suga H, Inoue K, Aoi N, Kato H, Sato K, Murase S, Koshima I, Yoshimura K. Preserved proliferative capacity and multipotency of human adipose-derived stem cells after long-term cryopreservation. *Plast Reconstr Surg* 2008; **121***, 2*, 401–410.

91. Gimble J M, Nuttall M E. Adipose-derived stromal/stem cells (ASC) in regenerative medicine: pharmaceutical applications. *Curr Pharm Des* 2011; **17***, 4*, 332–339.

92. Nakamura T, Shiojima S, Hirai Y, Iwama T, Tsuruzoe N, Hirasawa A, Katsuma S, Tsujimoto G. Temporal gene expression changes during adipogenesis in human mesenchymal stem cells. *Biochem Biophys Res Commun* 2003; **303***, 1*, 306–312.

93. Pampaloni F, Reynaud E G, Stelzer E HK. The third dimension bridges the gap between cell culture and live tissue. *Nat Rev Mol Cell Biol* 2007; **8***, 10*, 839–845.

94. Yamada K M, Cukierman E. Modeling tissue morphogenesis and cancer in 3D. *Cell* 2007; **130***, 4*, 601–610.

95. Mazzoleni G, Di Lorenzo D, Steimberg N. Modelling tissues in 3D: the next future of pharmaco-toxicology and food research? *Genes Nutr* 2009; **4***, 1*, 13–22.

96. Griffith L G, Swartz M A. Capturing complex 3D tissue physiology in vitro. *Nat Rev Mol Cell Biol* 2006; **7***, 3*, 211–224.

97. Green J A, Yamada K M. Three-dimensional microenvironments modulate fibroblast signaling responses. *Adv Drug Deliv Rev* 2007; **59***, 13*, 1293–1298.

98. Bosman F T. Functional structure and composition of the extracellular matrix. *J Pathol* 2003; **200***, 4*, 423–428.

99. O'Connor K C, Song H, Rosenzweig N, Jansen D A. Extracellular matrix substrata alter adipocyte yield and lipogenesis in primary cultures of stromal-vascular cells from human adipose. *Biotechnol Lett* 2003; **25***, 23*, 1967–1972.

100. Chun T H, Hotary K B, Sabeh F, Saltiel A R, Allen E D, Weiss S J. A pericellular collagenase directs the 3-dimensional development of white adipose tissue. *Cell* 2006; **125***, 3*, 577–591.

101. Lin R Z, Chang H Y. Recent advances in three-dimensional multicellular spheroid culture for biomedical research. *Biotechnol J* 2008; **3***, 9-10*, 1172–1184.

102. Khetani S R, Bhatia S N. Engineering tissues for in vitro applications. *Curr Opin Biotechnol* 2006; **17***, 5*, 524–531.

103. Bauer-Kreisel P, Goepferich A, Blunk T. Cell-delivery therapeutics for adipose tissue regeneration. *Adv Drug Deliv Rev* 2010; **62***, 7-8*, 798–813.

104. Sutherland R M, McCredie J A, Inch W R. Growth of multicell spheroids in tissue culture as a model of nodular carcinomas. *J Natl Cancer Inst* 1971; **46***, 1*, 113–120.

105. Mueller-Klieser W. Three-dimensional cell cultures: from molecular mechanisms to clinical applications. *Am J Physiol Cell Physiol* 1997; **273***, 4*, C1109-C1123.

106. Santini M T, Rainaldi G. Three-dimensional spheroid model in tumor biology. *Pathobiology* 1999; **67***, 3*, 148–157.

107. Kunz-Schughart L A, Freyer J P, Hofstaedter F, Ebner R. The use of 3-D cultures for high-throughput screening: the multicellular spheroid model. *J Biomol Screen* 2004; **9***, 4*, 273–285.

108. Lin T M, Tsai J L, Lin S D, Lai C S, Chang C C. Accelerated growth and prolonged lifespan of adipose tissue-derived human mesenchymal stem cells in a medium using reduced calcium and antioxidants. *Stem Cells Dev* 2005; **14***, 1*, 92–102.

109. Abbott A. Cell culture: biology's new dimension. *Nature* 2003; **424***, 6951*, 870–872.

110. Ota K, Saito S, Hamasaki K, Tanaka N, Orita K. Transplantation of xenogeneic hepatocytes: three-dimensionally cultured hepatocyte (spheroid) transplantation into the spleen. *Transplant Proc* 1996; **28***, 3*, 1430–1432.

111. Laib A M, Bartol A, Alajati A, Korff T, Weber H, Augustin H G. Spheroid-based human endothelial cell microvessel formation in vivo. *Nat Protoc* 2009; **4***, 8*, 1202–1215.

112. Verseijden F, Posthumus-van S SJ, Farrell E, van Neck J W, Hovius S E, Hofer S O, van Osch G J. Prevascular structures promote vascularization in engineered human adipose tissue constructs upon implantation. *Cell Transplant* 2010; **19***, 8*, 1007–1020.

113. Mironov V, Visconti R P, Kasyanov V, Forgacs G, Drake C J, Markwald R R. Organ printing: tissue spheroids as building blocks. *Biomaterials* 2009; **30***, 12*, 2164–2174.

114. Weiser B, Neubauer M, Göpferich A, Blunk T. Tissue Eegineering, fat. in *Encyclopedia of Biomaterials and Biomedical Engineering* 2008, pp 2725-2736.

115. Gomillion C T, Burg K JL. Stem cells and adipose tissue engineering. *Biomaterials* 2006; **27***, 36*, 6052–6063.

116. Findlay M W, Messina A, Thompson E W, Morrison W A. Long-term persistence of tissue-engineered adipose flaps in a murine model to 1 year: an update. *Plast Reconstr Surg* 2009; **124***, 4*, 1077–1084.

117. Rouwkema J, Rivron N C, van Blitterswijk C A. Vascularization in tissue engineering. *Trends Biotechnol* 2008; **26***, 8*, 434–441.

118. Lokmic Z, Mitchell G M. Engineering the microcirculation. *Tissue Eng Part B Rev* 2008; **14***, 1*, 87–103.

119. Kaully T, Kaufman-Francis K, Lesman A, Levenberg S. Vascularization--the conduit to viable engineered tissues. *Tissue Eng Part B Rev* 2009; **15***, 2*, 159–169.

120. Laschke M W, Harder Y, Amon M, Martin I, Farhadi J, Ring A, Torio-Padron N, Schramm R, Rucker M, Junker D, Haufel J M, Carvalho C, Heberer M, Germann G, Vollmar B, Menger M D. Angiogenesis in tissue engineering: breathing life into constructed tissue substitutes. *Tissue Eng* 2006; **12***, 8*, 2093–2104.

121. Frerich B, Lindemann N, Kurtz-Hoffmann J, Oertel K. In vitro model of a vascular stroma for the engineering of vascularized tissues. *Int J Oral Maxillofac Surg* 2001; **30***, 5*, 414–420.

122. Borges J, Müller M C, Momeni A, Stark G B, Torio-Padron N. In vitro analysis of the interactions between preadipocytes and endothelial cells in a 3D fibrin matrix. *Minim Invasive Ther Allied Technol* 2007; **16***, 3*, 141–148.

123. Kang J H, Gimble J M, Kaplan D L. In vitro 3D model for human vascularized adipose tissue. *Tissue Eng Part A* 2009; **15***, 8*, 2227–2236.

124. Kirkpatrick C J, Fuchs S, Unger R E. Co-culture systems for vascularization--learning from nature. *Adv Drug Deliv Rev* 2011; **63***, 4-5*, 291–299.

CHAPTER 2

Goals of the Thesis

The main goal of this work was the development and characterization of a 3-dimensional (3-D) adipose tissue model based on human adipose-derived stem cells (hASC). The intention was to design a culture system which serves as a tool for basic research to improve our understanding of adipose tissue functions, development and pathophysiology. Apart from its use in basic research, this model system should not only have the potential to be used for applications in tissue engineering and regenerative medicine, but also to be utilized as a basis for 3-D drug screening assays. The experimental work performed to achieve this goal can be divided into two major parts:

- The first part involved the establishment of culture conditions for a hASC spheroid model, which was subsequently applied to investigate differences in adipogenic differentiation between 2-D and 3-D culture systems.

- The second part focused on the development of a coculture system of hASC and human microvascular endothelial cells (hMVEC) based on the monoculture spheroids developed in the first part. These coculture spheroids were then applied to investigate the interactions between the two cell types during adipose tissue development, primarily focusing on the influence of the endothelial cells on hASC adipogenesis.

ASC monoculture spheroids

The vast majority of our knowledge regarding adipose tissue biology is based on conventional monolayer cell culture models [1,2]. It is, however, well recognized that many tissue-inherent factors, such as the presence of extracellular matrix, cell-cell contact and interaction, as well as the complex 3-dimensional microenvironment, are represented by these 2-D culture systems only to a very limited extent [3,4]. 3-D *in vitro* cell culture using multicellular spheroids provides a possibility to overcome these limitations. At the same time, some of the disadvantages of scaffold- or hydrogel-based systems, such as the unknown influence of the carrier material or the absence of direct cell-cell-contact during the first phase of culture, do not apply for spheroid culture [5–7]. In our group, such a 3-D spheroid model using the 3T3-L1 mouse preadipocyte cell line has been established previously [8]. To resemble the physiology of human adipose tissue even more closely, it would be desirable to develop a spheroid model based on human ASC. These cells are multipotent, can easily be harvested in large numbers by liposuction, and can be readily differentiated into adipocytes, making them an ideal cell source for basic research as well as adipose tissue engineering [9,10]. Thus, the first goal of this thesis was the establishment of a culture

method for hASC spheroids **(Chapter 3)**. We aimed at the development of a stable, easy-to-handle and versatile 3-D model system suitable for basic research, drug screening and tissue engineering applications.

To develop therapeutic strategies against adipose tissue-associated diseases, it is of great importance to increase our understanding of the complex processes involved in adipogenic differentiation. Our newly developed hASC spheroid model was therefore applied to investigate adipogenesis on a functional and molecular level **(Chapter 4)**. Specifically, we focused on the differences between 3-D spheroids and conventional 2-D monolayer cultures regarding their response to and dependence on exogenous stimulation. This was done by investigating the influence of different adipogenic induction protocols on lipid accumulation and the expression of various marker genes associated with adipogenesis.

ASC/MVEC coculture spheroids

Native fat is a highly vascularized tissue, and it is well known that adipogenesis and angiogenesis are closely associated with each other *in vivo* [11–13]. Although it has been demonstrated that adipocytes as well as their progenitors produce several angiogenic factors, the molecular basis of the complex interaction between these two processes during adipose tissue development is still poorly understood. Furthermore, most of the studies addressing the crosstalk between (pre-)adipocytes and endothelial cells have been performed using 2-D monolayer culture [14,15]. Therefore, it was our goal to develop a 3-D coculture system consisting of hASC and hMVEC, which could then serve as a more *in-vivo*-like model system for studying the interactions between the two cell types. Thus, based on the ASC monoculture spheroid model developed during the first part of this work, we aimed at establishing culture conditions and protocols for ASC/MVEC coculture spheroids which allowed for the ASC to be induced to undergo adipogenesis without compromising MVEC viability and proliferation **(Chapter 5)**.

Subsequently, this 3-D coculture spheroid model was characterized with a special focus set on the interactions between the two cell types. Specifically, parameters such as spheroid morphology, cell viability, triglyceride accumulation, tissue homogeneity and cellular self-organization were investigated under mono- and coculture conditions. After establishing a method to dissociate the coculture spheroids and separate the cell types, a gene expression array was performed on the ASC to study the influence of the MVEC on adipogenesis within a 3-D environment on a molecular level **(Chapter 6)**.

References

1. MacDougald O A, Mandrup S. Adipogenesis: forces that tip the scales. *Trends Endocrinol Metab* 2002; **13***, 1*, 5–11.
2. Rosen E D, MacDougald O A. Adipocyte differentiation from the inside out. *Nat Rev Mol Cell Biol* 2006; **7***, 12*, 885–896.
3. Yamada K M, Cukierman E. Modeling tissue morphogenesis and cancer in 3D. *Cell* 2007; **130***, 4*, 601–610.
4. Mazzoleni G, Di Lorenzo D, Steimberg N. Modelling tissues in 3D: the next future of pharmaco-toxicology and food research? *Genes Nutr* 2009; **4***, 1*, 13–22.
5. Kunz-Schughart L A, Freyer J P, Hofstaedter F, Ebner R. The use of 3-D cultures for high-throughput screening: the multicellular spheroid model. *J Biomol Screen* 2004; **9***, 4*, 273–285.
6. Pampaloni F, Reynaud E G, Stelzer E HK. The third dimension bridges the gap between cell culture and live tissue. *Nat Rev Mol Cell Biol* 2007; **8***, 10*, 839–845.
7. Lin R Z, Chang H Y. Recent advances in three-dimensional multicellular spheroid culture for biomedical research. *Biotechnol J* 2008; **3***, 9-10*, 1172–1184.
8. Weiser B. Adipose tissue engineering - Precultivation strategies towards clinical applications & A novel 3-D model of adipogenesis for basic research. *Dissertation, University of Regensburg* 2008.
9. Bunnell B A, Flaat M, Gagliardi C, Patel B, Ripoll C. Adipose-derived stem cells: isolation, expansion and differentiation. *Methods* 2008; **45***, 2*, 115–120.
10. Gimble J M, Katz A J, Bunnell B A. Adipose-derived stem cells for regenerative medicine. *Circ Res* 2007; **100***, 9*, 1249–1260.
11. Cao Y. Angiogenesis modulates adipogenesis and obesity. *J Clin Invest* 2007; **117***, 9*, 2362–2368.
12. Lijnen H R. Angiogenesis and obesity. *Cardiovasc Res* 2008; **78***, 2*, 286–293.
13. Christiaens V, Lijnen H R. Angiogenesis and development of adipose tissue. Molecular and cellular aspects of adipocyte development and function. *Mol Cell Endocrinol* 2010; **318***, 1-2*, 2–9.
14. Rehman J, Traktuev D, Li J, Merfeld-Clauss S, Temm-Grove C J, Bovenkerk J E, Pell C L, Johnstone B H, Considine R V, March K L. Secretion of angiogenic and antiapoptotic factors by human adipose stromal cells. *Circulation* 2004; **109***, 10*, 1292–1298.
15. Kilroy G E, Foster S J, Wu X, Ruiz J, Sherwood S, Heifetz A, Ludlow J W, Stricker D M, Potiny S, Green P, Halvorsen Y D, Cheatham B, Storms R W, Gimble J M. Cytokine profile of human adipose-derived stem cells: expression of angiogenic, hematopoietic, and pro-inflammatory factors. *J Cell Physiol* 2007; **212***, 3*, 702–709.

CHAPTER 3

Establishment of a 3-D Spheroid Model using Human Adipose-Derived Stem Cells (hASC)

3.1 Abstract

Adipose tissue plays an important role in many physiological and pathophysiological processes. Current knowledge about adipocyte biology and development is mainly based on *in vitro* monolayer cell culture models. However, three-dimensional (3-D) culture systems much better resemble the *in vivo* situation in terms of cell-cell contact and interactions with the extracellular matrix (ECM). The goal of this study was the development of a 3-D cell culture model based on the generation of multicellular spheroids from human adipose-derived stem cells (ASC).

Using the liquid overlay technique, ASC were seeded in agarose-coated 96-well-plates. This method was successfully employed to produce mechanically stable spheroids of defined size, in which ASC could be induced to undergo adipogenic differentiation. Cryopreservation and multiple passaging did not impair triglyceride accumulation during adipogenesis. Different culture conditions were evaluated with the goal of improving flexibility and cost effectiveness for routine culture. Spheroids sizes could be adjusted by varying the cell numbers seeded per well. After increasing seeding densities from 750 to 5000 cells per well, constructs still accumulated lipids homogeneously, while the larger spheroid sizes facilitated practical handling. Effective spheroid formation and adipogenic differentiation proved to be also possible when ASC from a different provider were applied, with cells remaining viable within the constructs.

The established ASC spheroid model can not only be applied as a drug screening tool providing a more *in-vivo*-like context, but can also serve as a powerful model for the investigation and characterization of adipogenesis and adipocyte functions in a 3-D environment. Moreover, these spheroids have the potential to serve as building blocks for applications in adipose tissue engineering.

3.2 Introduction

In recent years, the relevance of adipose tissue in many physiological processes, but also in the pathogenesis of diseases like type 2 diabetes and the metabolic syndrome, has been increasingly acknowledged [1–6]. Therefore, a thorough understanding of adipose tissue function and development is of great importance.

The differentiation of multipotent precursor cells towards mature adipocytes is a complex process involving a coordinated transcriptional program as well as massive functional and morphological changes [7]. This process has been extensively studied *in vitro*, mainly using conventional two-dimensional (2-D) culture models [8–10]. However, in these 2-D systems, several aspects of the *in vivo* situation, especially tissue-inherent factors like cell-cell contacts and interactions with the extracellular matrix (ECM), are represented to a very limited extent only [11–14]. Three-dimensional (3-D) cultures can provide a model system resembling the *in vivo* context more closely [15]. Mainly for tissue engineering approaches, several 3-D culture systems for the cultivation of adipocyte precursor cells have been developed. In these models, cells are usually cultured in a 3-D environment either by seeding on porous scaffolds made of materials such as PLGA or collagen, or by encapsulating cells in hydrogels, predominantly based on PEG or fibrin [16,17]. These systems have proven to be useful for the development of implantable or injectable adipose tissue constructs in various *in-vivo* studies [18–22]. However, they exhibit several drawbacks for their use in basic research, when the focus is on elucidating the role of cell-cell communication, ECM influences and 3-dimensional architecture on adipocyte biology, or simply when the effects of certain (pharmacological) substances need to be evaluated in a more *in-vivo*-like context during screening processes. Notably, the presence of scaffold or carrier materials may not only affect cell functions and behavior [23], but also limits direct interactions with neighboring cells and the ECM, as cells are situated separated from each other, at least in the early stages of culture. Also, due to the size of the constructs, a cellular inhomogeneity resulting from insufficient nutrient and oxygen supply can occur [18], making cellular and molecular analytics difficult and inaccurate.

One approach to overcome these limitations is the culture of multicellular spheroids. This model system, which has been applied in cancer research for many years, is based on the formation of cellular aggregates due to the absence of cell-adherent surfaces [24,25]. Although various spheroid model systems have been applied not only for tumor cells, but also for different types of primary cells [26], literature reports involving adipocyte spheroids are still scarce. A 3-dimensional model system based on the generation of such spheroids from 3T3-L1 preadipocytes was developed by our group. Characterization of these 3T3-L1 spheroids, which could be induced to undergo adipogenic differentiation, has already

revealed several differences in adipogenic maturation and adipocyte functionality as compared to 2-D monolayer cultures [27]. 3T3-L1 cells, an immortalized cell line, are a well-characterized and reliable model for studying the conversion of preadipocytes into adipocytes, representing a homogenous population of cells that are all at the same stage of differentiation and can be passaged indefinitely [28,29]. However, there are various metabolic and physiologic differences in the aneuploid mouse cell line 3T3-L1 as compared to human primary cells, e.g. regarding intracellular signaling pathways, the expression of transcription factors or the response to endocrine stimulation [30,31]. Furthermore, 3T3-L1 cells have already undergone determination and can only be differentiatied towards adipose tissue [29].

In contrast, human adipose-derived stem cells (hASC), which can be isolated from the stromal-vascular fraction of adipose tissue, are still multipotent, having the potential to undergo differentiation into adipocytes, osteoblasts, chondrocytes, myocytes, endothelial cells and neuronal cells, among others [32–35]. As a consequence, ASC may be a better model to explore especially the early molecular events during adipogenesis, including the lineage commitment [36]. Unlike bone marrow-derived stem cells (BMSC), they are easily available and can be harvested in large numbers, e.g. from liposuctions [34,37].

In some reports, hASC have already been cultured as spheroids generated by hanging-drop culture [38–40], by culturing in spinner flasks [41] or as centrifugation pellet culture [42]. However, these methods contain several drawbacks [26].

The aim of this chapter was to establish an *in vitro* hASC spheroid model suitable for long-term culture and screening applications, in which cells can be easily induced to undergo adipogenic differentiation. As these spheroids could also be embedded and further cultured within hydrogels, they would not only be a valuable tool for basic research, but also have great potential as building blocks for the use in adipose tissue engineering.

At first, it was evaluated if ASC spheroids can be generated and differentiated using the liquid overlay technique. Secondly, in an attempt to make 3-D culture easier, more flexible and cost effective, we investigated the influence of cryoconservation and multiple passaging as well as different culture conditions on ASC performance. Furthermore, spheroid sizes were optimized by variation of the seeding density followed by a histological evaluation of tissue homogeneity. After a necessary change of the cell provider due to patent issues, spheroid formation, adipogenic differentiation and cell viability were assessed using the new cell source.

3.3 Materials and Methods

3.3.1 Materials

Human adipose derived stem cells (ASC) were obtained from Lonza (Walkersville, MD, USA; lot 7F4308) and from PromoCell (Heidelberg, Germany; lot 8073006.12); Preadipocyte Growth Medium 2 (PGM2, consisting of PBM2, 10% FBS and 1% penicillin/streptomycin solution) and PGM2 SingleQuots (IBMX, insulin, indomethacin, dexamethasone) were from Lonza (Verviers, Belgium). DMEM/Ham´s F12 was purchased from Biochrom (Berlin, Germany). Fetal bovine serum (FBS, lot 40A0044K), penicillin-streptomycin solution, 0.25% trypsin/EDTA solution and phosphate buffered saline (PBS) were from Invitrogen (Darmstadt, Germany). Minimum Essential Medium alpha modification (MEM alpha), agarose, indomethacin, dexamethasone, glycerol standard solution, bovine serum albumin (BSA), propidiumiodide solution, dimethylsulfoxide (DMSO), calf thymus DNA, Oil Red O, Nile Red and osmium tetroxide were purchased from Sigma-Aldrich (Munich, Germany). 3-isobutyl-methylxanthine (IBMX) was bought from Serva (Heidelberg, Germany), Thesit from Gepepharm (Siegburg, Germany). Hoechst 33258 dye was obtained from Polysciences (Warrington, PA, USA). Bovine insulin was kindly provided by Sanofi-Aventis (Frankfurt a. M., Germany). All other chemicals were from Merck (Darmstadt, Germany). All cell culture plastics were from Corning (Bodenheim, Germany).

3.3.2 Methods

3.3.2.1 Cell culture

3.3.2.1.1 2-D cell culture

For 2-D monolayer cultures, human adipose-derived stem cells (ASC) were thawed after cryopreservation (passage 3, if not stated otherwise) and seeded in culture flasks. They were expanded at 37°C, 5% CO_2 in growth medium (GM), i.e. Preadipocyte Basal Medium 2 (PBM2) containing 10% FBS, penicillin (100 U/ml) and streptomycin (100 µg/ml). At 90% confluence cells were trypsinized, seeded in 24-well plates at a density of 30000 cells/cm² and cultured in GM for 2 days before adipogenic differentiation was induced.

3.3.2.1.2 3-D cell culture

For the generation of 3-D spheroid cultures the liquid overlay technique was used (Fig. 3-1) [25,27]. ASC were expanded as described in the previous section. After trypsinization, cells were resuspended in GM and seeded into 96-well plates coated with 1.5% agarose at a distinct number of cells per well, ranging from 750 to 15000 cells

depending on the experiment. As evaporation is higher in the outermost rows and columns during prolonged culture, those wells were not seeded with cells, but only filled with PBS containing penicillin (100 U/ml) and streptomycin (100 µg/ml) (Fig. 3-1). Culture plates were kept on an orbital shaker at 50 rpm during incubation. After 1 day, a single spheroid had developed in each well. Like in 2-D culture, adipogenesis was induced after 2 days in GM. As spheroids would be lost with complete removal of medium from the wells, all medium changes were performed by replenishing only half of the medium volume. For comparability, 2-D cultures were treated in the same way.

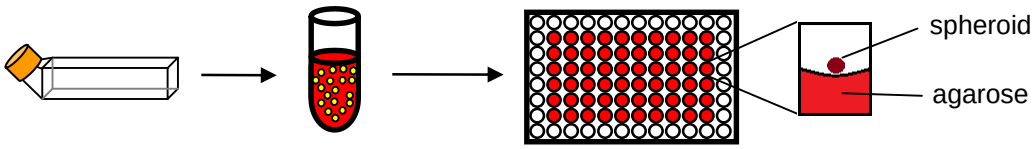

Figure 3-1: *Generation of hASC spheroids using the liquid overlay technique (from [27], modified). Cells were expanded in 2-D culture, trypsinized and seeded into agarose-coated 96-well plates at a distinct number of cells per well. As cells cannot adhere to the agarose surface, they accumulated in the center of the well and, by attaching to each other, formed a single multicellular spheroid in each well.*

3.3.2.1.3 Adipogenic differentiation

In both culture systems (2-D and 3-D), cells were induced to undergo adipogenesis 2 days after seeding by exchanging half of the medium with induction medium (IM), consisting of GM supplemented with a hormonal cocktail, resulting in final concentrations of 1.7 µM insulin, 1 µM dexamethasone, 200 µM indomethacin and 500 µM 3-isobutyl-1-methylxanthine (IBMX). The time point of induction was always referred to as day 0. Cells were kept in IM over the whole culture period.

3.3.2.1.4 Evaluation of culture conditions

In order to determine optimal culture conditions, the general culture protocol described above was modified in several ways.

Hormonal cocktail:

The induction cocktail (IBMX, dexamethasone, insulin, indomethacin) originally supplied together with PBM2 (“SingleQuots”) was replaced by a self-prepared hormonal mixture containing the same substances in corresponding concentrations to induce adipogenesis in 2-D cultures.

Feeding strategy:

As in the manufacturer´s protocol supplied together with the cells no recommendations were given regarding the frequency of medium changes after induction, intervals of 7 or 3-4 days were applied and compared in 2-D.

Basal media and fetal bovine serum:

Besides PGM2, alternative basal media were tested with respect to differentiation efficiency. ASC were seeded either in PGM2, in DMEM/Ham´s F12 or in MEM alpha and kept in the same media during adipogenic differentiation. Additionally, two different lots of FBS were used to supplement the media, keeping the FBS concentration at 10% at all times.

Spheroid sizes:

To investigate the influence of different cell numbers on spheroid formation and differentiation, cells were seeded in agarose-coated 96-well plates with 1500, 3000, 5000, 10000 or 15000 cells per well. Adipogenic differentiation was induced as described above.

3.3.2.2 Microscopical determination of spheroid size

At specific time points, microscopical bright field images of the spheroids were acquired using a CCD camera (DS-5M, Nikon, Düsseldorf, Germany) attached to an inverted microscope (Leica DM IRB, Leica Microsystems, Wetzlar, Germany). Cross-sectional areas of at least 10 randomly selected spheroids were determined with ImageJ software (NIH, Bethesda, MD, USA). Equivalent diameters and spheroid volumes were calculated thereof.

3.3.2.3 Lipid staining with Oil Red O or osmium tetroxide

To visualize triglyceride accumulation, cultures were harvested and staining with Oil Red O (ORO) or osmium tetroxide (OsO_4) was performed. For this purpose, spheroids were pooled in PBS, transferred to microcentrifuge tubes, washed with PBS, fixed in 10% formalin (1h, 4°C), stained with ORO (3 mg/ml solution in 60% isopropanol) for 4h or with OsO_4 (1% aqueous solution) for 1 h on ice and washed three times with PBS. Stained spheroids were embedded in Tissue-Tek (Hartenstein Laborbedarf, Würzburg, Germany), snap frozen and cut into 10-µm-thick cryosections. After removal of Tissue-Tek by washing in water, the sections were mounted in glycerol. Serial sections were prepared from all spheroids and sections from the center region were used for histological evaluation. For 2-D cultures, staining was performed directly in the 24-well plates. Microscopical bright field images were acquired using a CCD camera (DS-5M, Nikon, Düsseldorf, Germany) attached to an inverted microscope (Leica DM IRB, Leica Microsystems, Wetzlar, Germany).

3.3.2.4 Lipid staining with Nile Red

Nile Red Staining was performed according to a protocol adapted from Greenspan et al. [43]. Spheroids were harvested, fixed in 10% formalin and transferred to angiogenesis slides (Ibidi, Martinsried, Germany). Remaining medium was removed carefully, followed by the addition of the dye solution, which was prepared by adding 10 µl of a Nile Red stock solution (500 µg/ml in Acetone) to 1 ml of 75% glycerol. After 1h of incubation at room temperature the staining was evaluated with a confocal laser scanning microscope (Zeiss Axiovert 200M microscope coupled to a Zeiss LSM 510 scanning device, Carl Zeiss MicroImaging, Jena, Germany). Nile Red fluorescence was excited at 488 nm and detected using a 505-550 nm band-pass filter. Z-stacks were performed to visualize lipid distribution within the spheroids.

3.3.2.5 Quantitative determination of the intracellular triglyceride (TG) content

For analysis of the intracellular TG content, 2-D monolayers were washed twice with PBS and harvested in 0.5% aqueous Thesit solution. 3-D spheroids were pooled, washed twice with PBS and resuspended in 0.5% aqueous Thesit solution. For both culture systems, cells were sonicated and spectroscopic quantification of TG was performed using the enzymatic Serum Triglyceride Determination Kit from Sigma-Aldrich (Munich, Germany) according to the manufacturer's instructions. Beforehand, assay conditions were adjusted to 96-well plate format in a series of comparative measurements. For calibration, different glycerol standard dilutions were used. All TG data were acquired from three biological replicates; one replicate was derived from one well for 2-D cultures and an exact number of approximately 20 spheroids for 3-D cultures, respectively. TG contents per spheroid or per well were calculated and normalized to the DNA content, which was determined as described below.

3.3.2.6 Determination of the DNA content

2-D monolayers were washed twice with PBS, harvested in lysis buffer (2 mM EDTA, 2M NaCl, 50 mM Na_3PO_4, pH 7,4) and sonicated. 3-D spheroids were pooled, washed twice with PBS, resuspended in lysis buffer and sonicated as well. DNA content was determined using the intercalating Hoechst 33258 dye (0.1 µg/ml in 0.1 M NaCl, 1 mM EDTA, 10 mM Tris, pH 7.4). Fluorescence intensities were determined at an excitation wavelength of 365 nm and an emission wavelength of 458 nm with a LS 55 fluorescence spectrometer (PerkinElmer, Wiesbaden, Germany) and correlated to DNA contents using standard dilutions of double-stranded DNA (from calf thymus). All measurements were performed in three biological replicates; one replicate was derived from one well for 2-D cultures and an exact number of approximately 10 spheroids for 3-D cultures, respectively.

3.3.2.7 Live/Dead Assay

Cell viability within the spheroids was assessed with the Live/Dead Cell Staining Kit II (PromoCell, Heidelberg, Germany). Spheroids were pooled, washed three times with PBS and incubated with the staining solution (4 µM EthD-III, 2 µM Calcein AM) for 45 min. The staining was evaluated by imaging with a confocal laser scanning microscope (Zeiss Axiovert 200M microscope coupled to a Zeiss LSM 510 scanning device, Carl Zeiss MicroImaging, Jena, Germany). Live cells showed green calcein fluorescence (ex. 488 nm, em. 505-550 BP), dead cells were indicated by red fluorescence of DNA-intercalating EthD-III in the nuclei (ex. 543 nm, em. LP 560). The z-stack mode was used to investigate viability inside the spheroids.

3.3.2.8 Statistics

All quantitative results are expressed as mean values ± standard deviations. Differences between multiple groups were analyzed for significance using one-way analysis of variances (ANOVA) with subsequent multiple comparisons according to Tukey´s post-hoc test. A value of $p<0.05$ was regarded as statistically significant. Statistical analysis was performed using PASW Statistics 18 software (SPSS Inc., Chicago, IL, USA).

3.4 Results and Discussion*

3.4.1 hASC spheroids – proof of principle

In order to evaluate the general suitability of the liquid overlay technique for the generation of 3-D ASC spheroids, in a first attempt cells from passage 1 were seeded into agarose-coated 96-well plates at 750 cells per well. This seeding density was selected based on previous results with 3T3-L1 spheroids. In these, a starting cell number of 750 per well had been found to be optimal, while larger spheroid sizes had led to gradients in triglyceride accumulation after adipogenic induction [27]. The culture conditions were chosen according to the cell supplier´s recommendations: PGM2 was used as basic medium, and adipogenic induction was performed with the provided SingleQuots kit, with the inducers remaining in the medium over the complete culture time.

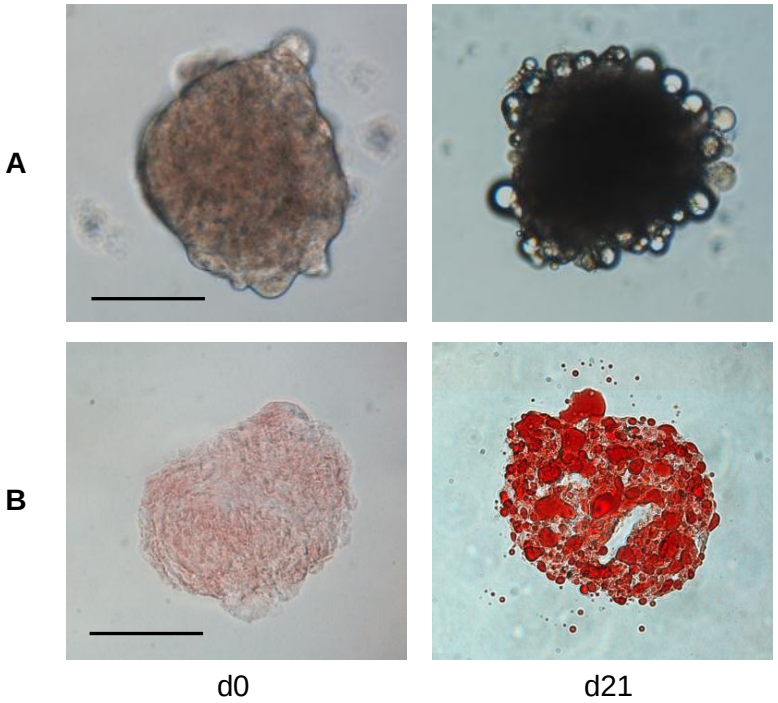

Figure 3-2: *Adipogenic differentiation of passage 1 ASC spheroids, 750 cells per well* ***A)*** *Bright field images of the whole spheroids at the time point of induction (d0) and after 3 weeks of adipogenic differentiation (d21).* ***B)*** *Cryosections of d0 and d21 spheroids, stained for triglycerides with Oil Red O (ORO). Scale bars are 100 µm.*

One day after seeding, cells had aggregated to form a single spheroid in each well (Fig. 3-2 A). These compact 3-D tissue constructs remained mechanically stable over a prolonged culture period, independent of a subsequent hormonal induction or cultivation in growth medium only. When adipogenesis was induced on day 0, cells started to accumulate

* *As the establishment of the hASC spheroid model was a multi-step process, with each experiment being based on the results of the previous one, results and discussion are combined in one section.*

more and more triglycerides in droplets up to day 21, which was clearly observable via bright field microscopy (Fig 3-2 A). In contrast to day 0, where virtually no triglycerides could be detected, Oil Red O staining revealed that on day 21, numerous lipid droplets were homogeneously distributed throughout the spheroids (Fig. 3-2 B).

On day 0, the spheroids had equivalent diameters of under 200 µm, which was comparable to 3T3-L1 spheroids which have been generated previously in our group [27]. Interestingly, the hASC spheroid diameters did not increase significantly during adipogenic differentiation. 21 days after induction, they were still in the same range as on day 0. In contrast, 3T3-L1 spheroids had strongly increased in size when they were induced to undergo adipogenesis, which was mainly attributed to the accumulation of lipid droplets [27]. 3T3-L1 is a mouse cell line, and the much higher growth rate of the induced spheroids can be explained by the faster metabolism and therefore strongly increased speed of adipogenic differentiation as compared to human ASC [44].

In general, for most applications a higher seeding density leading to a larger number of cells per spheroid would be advantageous with regard to practical handling, as the total number of constructs needed in one experiment would be reduced. As already mentioned, for the 3T3-L1 spheroids, 750 cells per well had been determined to be optimal, as on account of the strong volume increase during adipogenesis higher seeding numbers had led to partially inhomogeneous differentiation of the constructs. This was attributed to the limited diffusion of oxygen into the center of the spheroids with increasing size [27]. As in the hASC spheroids no significant volume increase took place, higher seeding densities may be possible for them without compromising construct homogeneity after differentiation. The optimization of spheroid sizes will be further addressed in chapter 3.4.4.

In summary, these first results proved that the spheroid model based on the liquid overlay technique is a suitable culture system for the 3-dimensional cultivation of hASC. For our intended applications, it bears several advantages over other methods for the generation of multicellular spheroids [26]. With hanging drop culture, medium changes, which are inevitable during long-term culture or for the induction of adipogenesis, can only be performed by transferring the constructs to new well plates, whereas in our model, spheroids remain in the culture plates, while half of the medium is exchanged with a multi-channel pipette. By seeding a distinct number of cells into each well, spheroids of controlled and reproducible sizes can be generated, which is not the case for the culture in spinner flasks or rotary systems, or even when cells are cultured on non-adhesive surfaces of larger scale, like in petri dishes. As compared to pellet culture in centrifuge tubes, with the model system described here a much higher throughput is possible, because it is easier to produce large numbers of spheroids and media exchanges can be performed more rapidly.

3.4.2 Influence of cryoconservation and multiple passaging

Since the goal of this project was the establishment of a 3-D culture system suitable for routine use and in screening applications, the generation of differentiated constructs should also be possible when ASC in higher passages and/or after cryoconservation are applied. To characterize cell performance after serial passaging, in a 2-D experiment adipogenic differentiation was performed with passage 4 (P4) cells, which had been stored in liquid nitrogen after an initial expansion phase at passage 1.

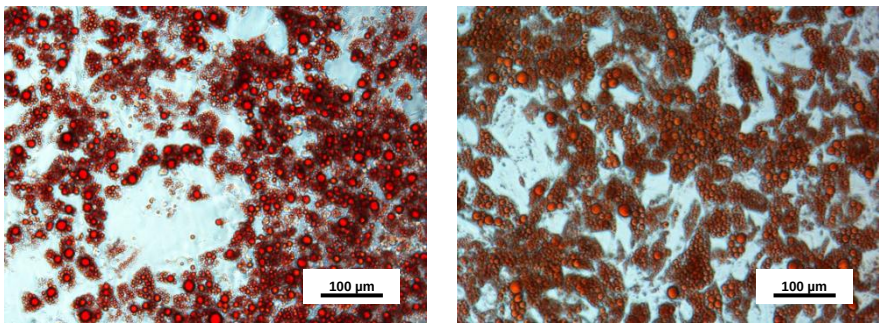

Figure 3-3: *2-D cultures of passage 1 (P1) and passage 4 (P4) ASC on day 21 after induction of adipogenesis. Triglycerides stained red using ORO. Scale bars are 100 µm.*

After seeding in 24-well plates and adipogenic induction, these cells performed comparably to those in P1, leading to a similar differentiation rate and lipid accumulation, as determined by ORO staining on day 21 (Fig. 3-3). This result was in accordance with literature reports, indicating that adipogenic differentiation of ASC can be induced at least up to P10, independent of previous cryoconservation [45,46].

As a consequence, all following experiments were performed with P4 cells, leading to an improved flexibility, cost effectiveness and inter-experimental comparability, as cryoconserved cells from one batch could be used for several independent experiments.

3.4.3 Evaluation of culture conditions

The culture protocol which was applied in the first experiments could effectively differentiate the ASC towards the adipocyte lineage, but has some drawbacks with regard to routine culturing, like a poorly defined hormonal cocktail provided with the PGM2 medium (SingleQuots kit) and high cost. Therefore, in a set of 2-D experiments, it was tested whether comparable performance and differentiation could also be achieved using alternative culture conditions.

On the one hand, the SingleQuots kit (SQ) was replaced by a self-prepared hormonal cocktail (HC), which was composed of the same components as in the SQ (IBMX,

dexamethasone, indomethacin, insulin). Concentrations were chosen as described in literature [45,47–51]. Differentiation rate and triglyceride content after 21 days of culture were comparable in both groups, with a tendency to even stronger adipogenesis when the self-prepared cocktail (HC) was used (Fig. 3-4, groups 2 and 3). As the self-prepared HC provided defined conditions and led to an enhanced flexibility, it was used in all following experiments.

A

Group	1	2	3	4
Induction	-	SQ	HC	SQ
Interval	3-4	7	7	3-4

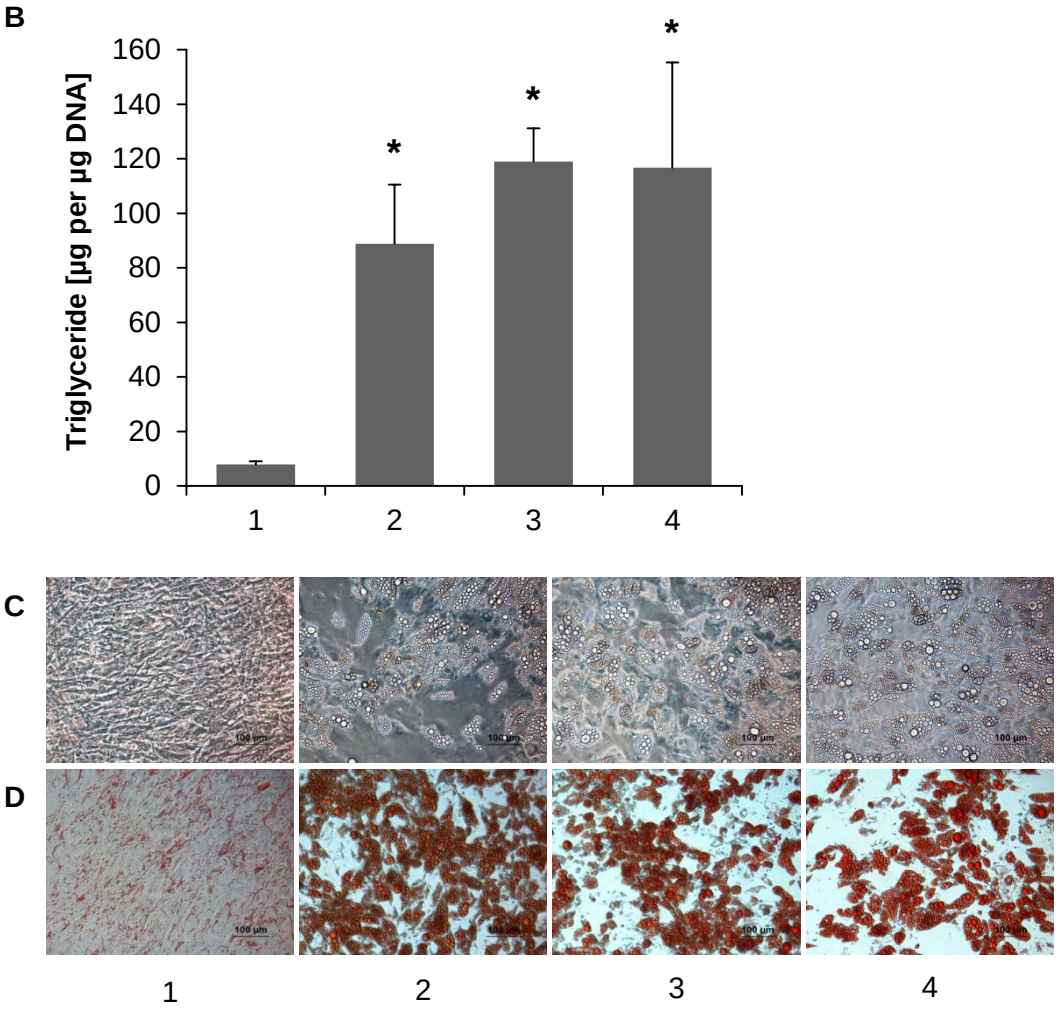

Figure 3-4: *Evaluation of culture conditions:* ***A)*** *2-D cultures in different groups were induced using either the SingleQuots Kit (SQ) supplied with PGM2 or a corresponding self-mixed hormonal cocktail (HC). Medium change intervals were either 3-4 days or 7 days.* ***B)*** *Cellular triglyceride contents on day 21 after induction; * indicates statistically significant differences vs. group 1 (p<0,05)* ***C)*** *Phase contrast images and* ***D)*** *ORO staining of the cultures on day 21. Scale bars are 100 µm.*

On the other hand, medium changes were performed not only every 7 days as in the first experiments, but alternatively with a 3-to-4-day interval. The frequency of medium exchanges did not influence cell triglyceride accumulation significantly, as determined by ORO staining and TG quantification (Fig. 3-4, groups 2 and 4). However, in the majority of subsequent experiments, media were exchanged every 3-4 days, as this is more common for the cultivation of human primary cells.

In general, ASC are most frequently cultured using a 1:1-mixture of DMEM and Ham´s F12 as a basic medium [52–55]. In order to determine if the PGM2, which has been used in the previous experiments, can be replaced with the chemically defined DMEM/Ham´s F12 without compromising adipogenic differentiation, a comparative study was conducted. In addition, MEM alpha was included in the experiment as a further alternative medium, which has occasionally been used for the culture of mesenchymal stem cells [56,57].

Not only the basic media, but also the supplemented fetal bovine serum (FBS) can have substantial influence on cell proliferation and differentiation [58]. Therefore, in this study two different batches of FBS were added to each of the media.

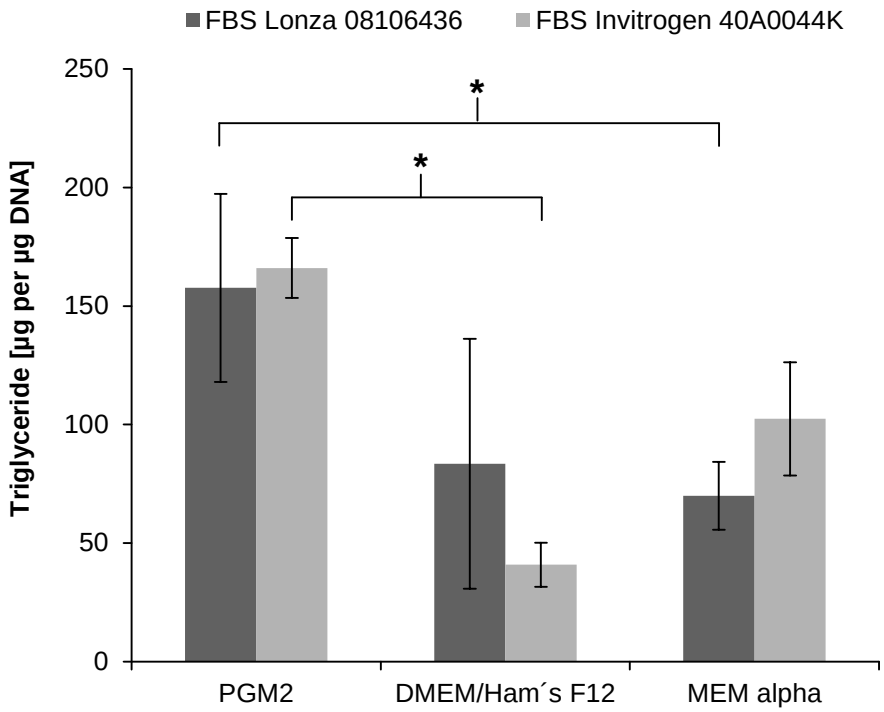

Figure 3-5: *Influence of different combinations of basic media and FBS batches on adipogenic differentiation. TG contents are shown for day 21 after induction. * indicates statistically significant differences between the respective groups (p<0,05).*

The determination of triglyceride contents on day 21 after induction showed that cells had accumulated the largest amount of lipids when cultured with PGM2, independent of the supplemented FBS (Fig. 3-5). The exact composition of PGM2 was not revealed by the

manufacturer, making it impossible to identify possible reasons for its better performance. However, as the establishment of standard conditions leading to an effective adipogenic differentiation was an aim of this project, PGM2 was continuously used as basic medium in all further steps.

In summary, it was determined that optimal ASC culture conditions for the current project included the basic medium PBM2, containing 10% FBS (batch 40A0044K, Invitrogen), medium changes every 3-4 days and adipogenic induction with the hormonal cocktail composed of IBMX, dexamethasone, indomethacin and insulin.

In a next step, this optimized protocol was used for the culture and differentiation of ASC spheroids. Here, seeding into the 96-well plates was not only performed with 750 cells per well, like in the initial experiments, but also with 1500 cell per well. In both cases, extensive lipid accumulation could be observed throughout the constructs, indicating that spatially homogeneous adipogenic conversion of the ASC had taken place. This proved that the optimized culture conditions could successfully be applied for ASC spheroid differentiation.

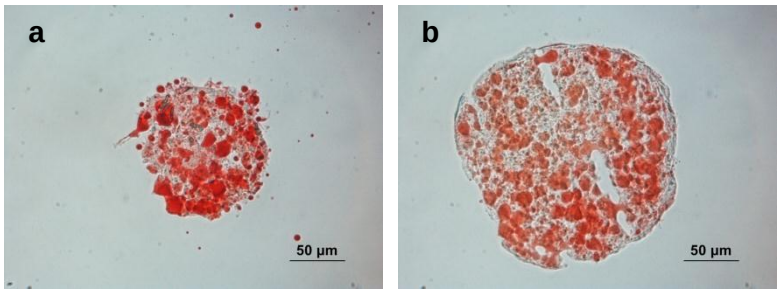

Figure 3-6: *3-D ASC spheroids cultured according to the optimized protocol. Seeding density was 750 cells (a) or 1500 cells (b) per well, respectively. Lipid accumulation on day 21 after induction was determined by ORO staining. Scale bars are 50 µm.*

3.4.4 Evaluation of optimal spheroid sizes

As already mentioned in chapter 3.4.1, with regard to the 3-D spheroid system, it was desirable to increase the number of cells seeded per well, which would lead to higher construct volumes. This would not only facilitate practical handling, but also reduce the number of spheroids that have to be pooled for subsequent analytics. Since results from chapter 3.4.1 had demonstrated that ASC spheroids, in contrast to 3T3-L1 spheroids, did not increase significantly in volume up to 3 weeks of culture, we hypothesized that the generation and adipogenic conversion of constructs larger than 750 cells should be possible without compromising homogeneous adipocyte maturation. In the previous chapter, it could already be demonstrated that this was true for a doubling of the seeding density to 1500 cells (Fig. 3-6). In a new study, the influence of the cell number per spheroid was investigated in more detail. ASC were seeded into agarose-coated 96-well plates with 1500, 3000, 5000,

10000 or 15000 cells per well. In all cases, a single spheroid had formed in each well within 24h. On the day of adipogenic induction (d0), spheroid volumes increased linearly with the cell numbers up to 5000 cells. In contrast, spheroids generated from 10000 or 15000 cells had volumes slightly smaller than expected, with higher inter-spheroid variability (Fig. 3-7 A).

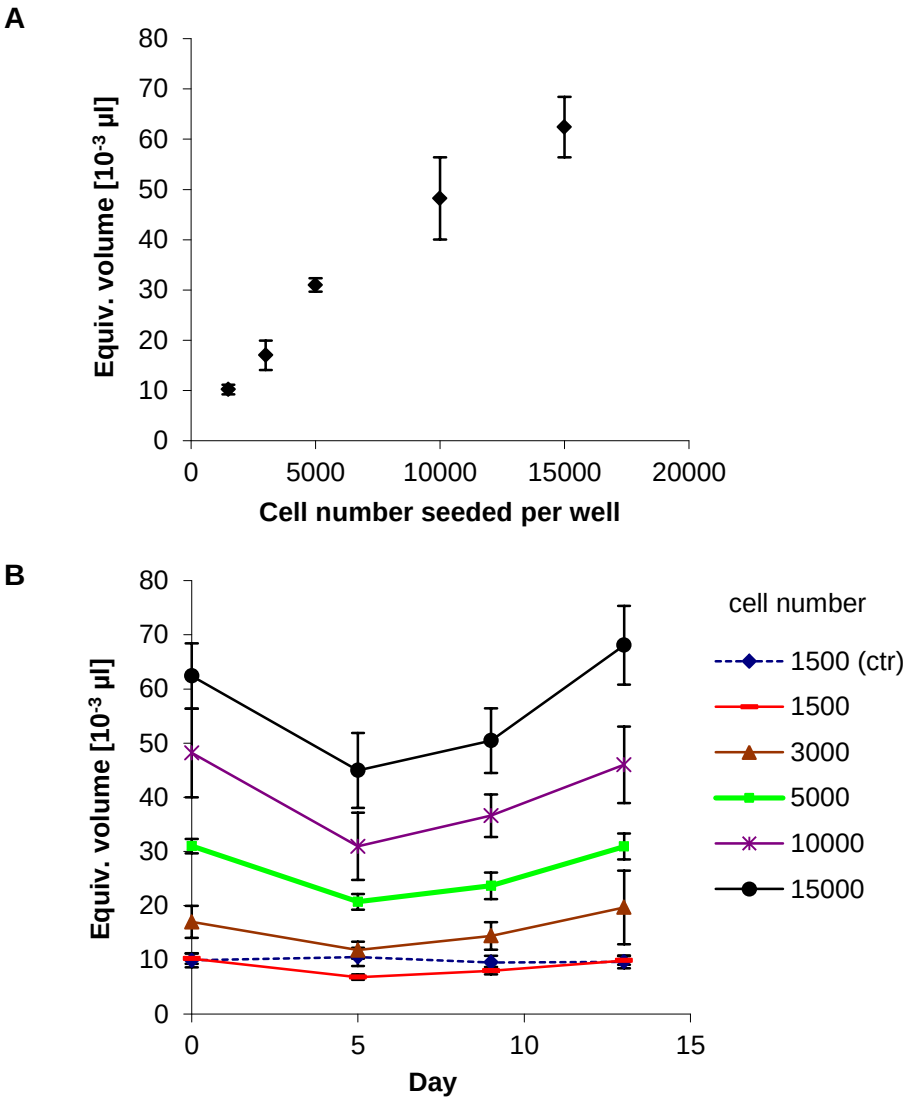

Figure 3-7: A) *Equivalent spheroid volumes on day 0 in dependence of the cell number seeded per well.* ***B)*** *Growth kinetics of the spheroids up to day 13 after induction.*

This could be a hint that in these groups, not all of the seeded cells in each well were included into the aggregation of the spheroids. Another explanation might be a stronger compaction of the constructs in the first phase of culture, which has also been observed for 3T3-L1 spheroids of larger sizes [27] and for MSC spheroids generated by hanging-drop culture [38]. During adipogenic differentiation, spheroids of all groups initially decreased in size (as detected on day 5, Fig. 3-7 B). Subsequently, up to day 13 a volume increase of about 50% as compared to day 5 could be observed for all spheroids, independent of the cell

numbers seeded (Fig. 3-7 B). Interestingly, after about 16 days, the largest constructs, generated from 15000 cells, in some cases began to show signs of mechanical instability and desaggregation.

On day 16 after induction, cells in all groups treated with the hormonal cocktail had accumulated lipids in all areas of the constructs, whereas uninduced groups contained no lipid droplets, as determined by staining with OsO_4. However, in the spheroids generated from 10000 or 15000 cells, adipogenic conversion had occurred to a slightly lesser extent in the center regions of the constructs, whereas for the smaller spheroids, triglyceride accumulation was homogeneous (Fig. 3-8).

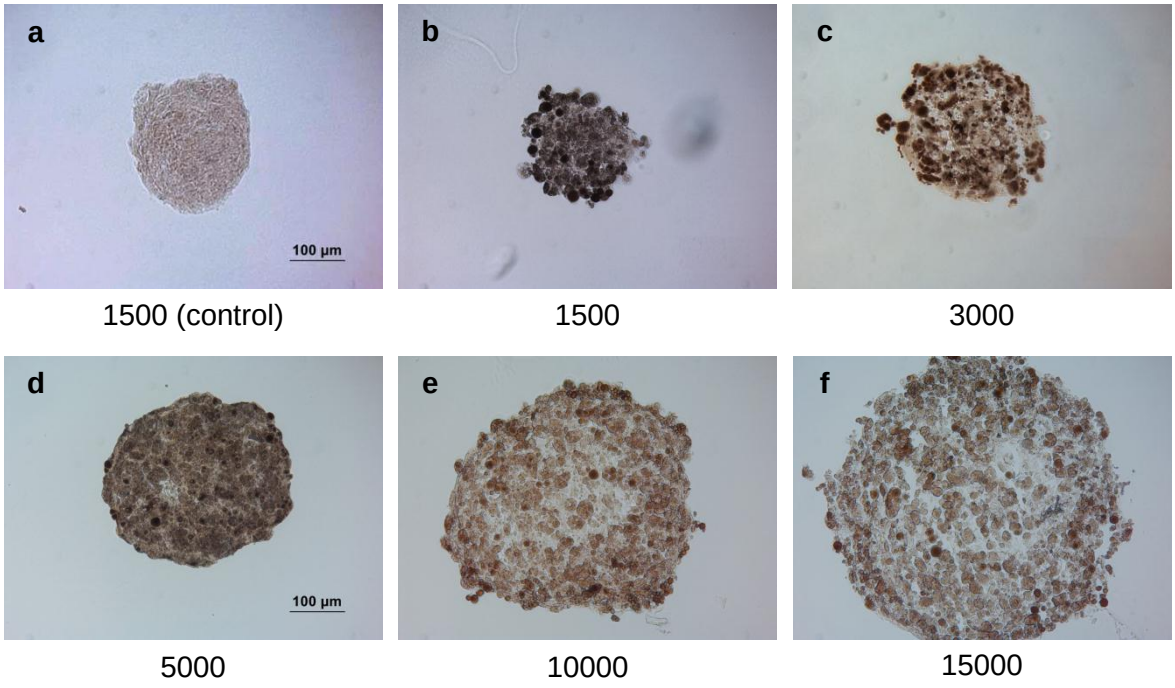

Figure 3-8: *Cryosections of ASC spheroids on day 16 after induction, stained with OsO_4. a) uninduced control b-f) induced with hormonal cocktail. Scale bars are 100 µm.*

In summary, spheroids generated from 3000 or 5000 cells appeared to have optimal properties for routine culture. These constructs represent a 3-D model system small enough to allow for reproducible construct sizes, adipocyte maturation without spatial gradients and long term mechanical stability, but large enough to facilitate practical handling and to reduce the number of spheroids required for standard analytics.

3.4.5 Introduction of a new cell source

Due to patent issues, the ASC from Lonza (Verviers, Belgium) were no longer available for purchase after the establishment phase of the spheroid culture, which was described in the previous sections. Thus, for all future steps of this work, ASC were acquired from PromoCell

(Heidelberg, Germany). Before cells from the new provider were applied for routine experiments, it was tested whether their performance under the previously established conditions was comparable regarding proliferation, spheroid formation and adipogenic differentiation.

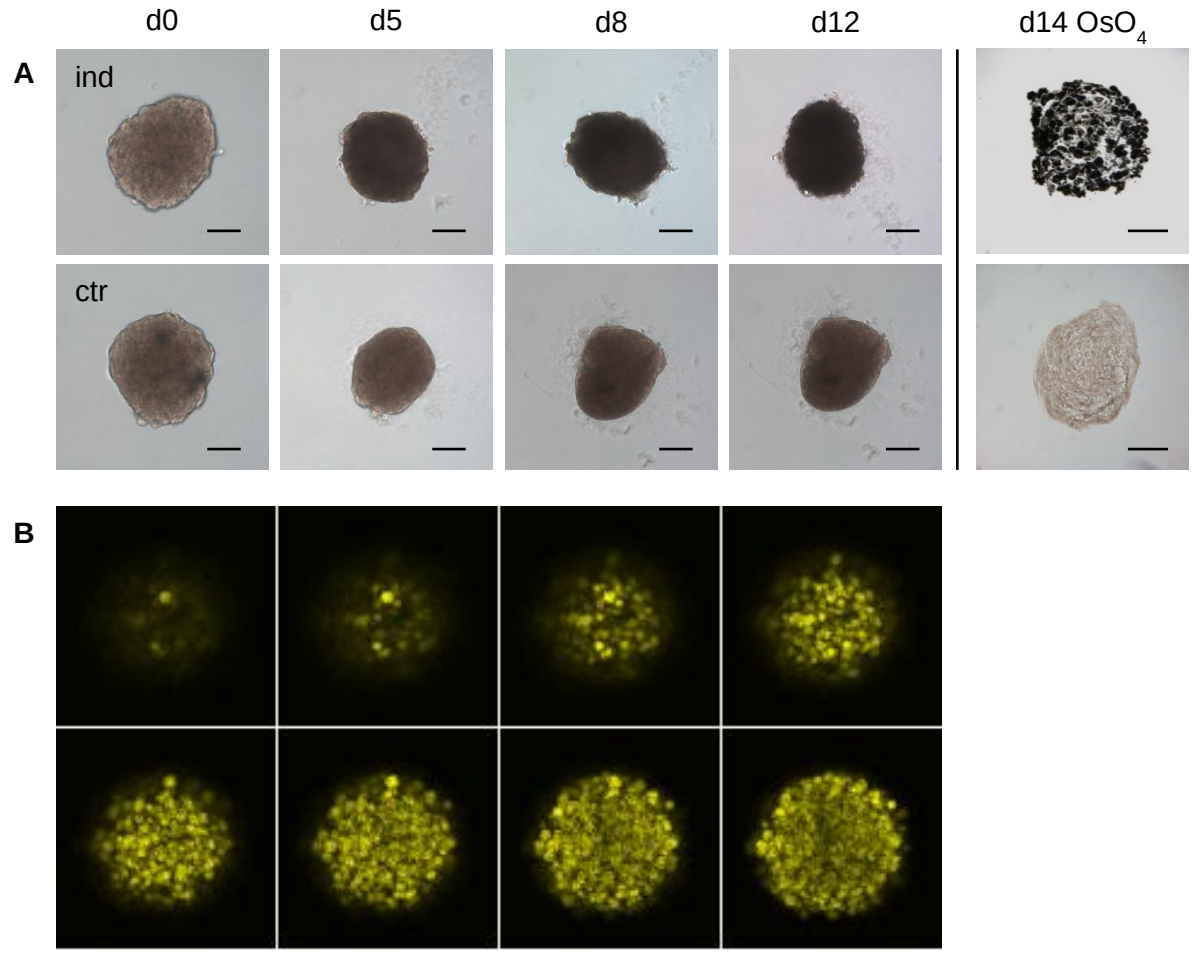

Figure 3-9: *Adipogenic differentiation of spheroids consisting of 3000 ASC (PromoCell)* ***A)*** *Bright field images of the whole spheroids and OsO_4-stained cryosections (right) of induced (upper row) and control (lower row) spheroids at different time points. Scale bars are 100 µm.* ***B)*** *CLSM images of induced spheroids on day 14; Lipids stained with Nile Red. To visualize TG distribution inside the constructs, the image shows a series of consecutive optical sections (z-stack) with 10 µm intervals (top left to bottom right).*

When seeded with 3000 cells per well into agarose-coated 96-well plates, cell aggregation, initial volume decrease and subsequent accumulation of lipid droplets were observed via bright field microscopy and appeared to be very similar to the Lonza cells. OsO_4 staining on day 14 after induction revealed extensive and homogeneous adipogenic conversion within the constructs when treated with adipogenic induction medium (Fig. 3-9 A).

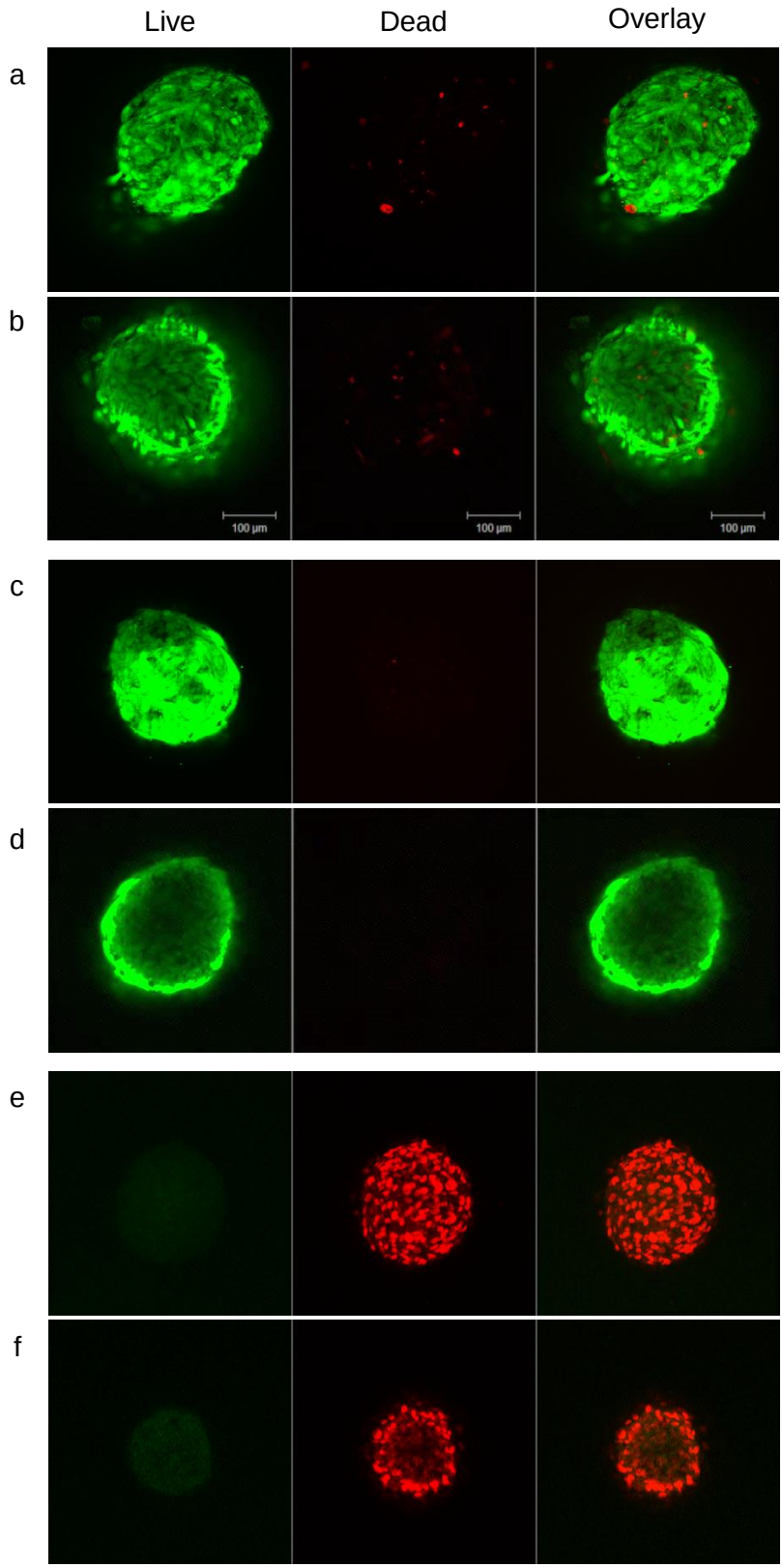

Figure 3-10: *Live/Dead-staining of ASC spheroids (d7). Optical sections acquired by confocal microscopy are depicted. In each row, green calcein fluorescence indicating live cells is shown on the left, red EthD-III fluorescence indicating dead cells in the middle and the overlay image on the right. a, c, and e show 3-dimensional projections obtained from z-stacks, b, d and f show single optical sections from areas within the spheroids.* ***a/b)*** *uninduced controls* ***c/d)*** *induced spheroids* ***e/f)*** *dead control (cells treated with DMSO for 2h). Scale bar is 100 µm.*

Additionally, day 14 spheroids were stained with Nile Red and optical sections were acquired via confocal laser scanning microscopy (CLSM) by using the z-stack function, which confirmed that lipid inclusions were evenly distributed throughout the constructs (Fig. 3-9 B).
Live/dead staining was performed on day 7 after induction to assess cell viability within the 3-D constructs. In both induced and uninduced spheroids, the vast majority of cells showed green fluorescence indicating viability (Fig. 3-10).

3.5 Conclusion

A 3-D spheroid model capable of adipogenic differentiation after hormonal induction and suitable for long-term culture and screening applications was successfully established. It was demonstrated with cells from two different providers that, by applying the liquid overlay technique in agarose-coated 96-well plates, hASC form mechanically stable spheroids of defined size and can be induced to undergo adipogenesis. Subsequently, the influence of multiple passaging, FBS supplementation and the type of hormonal induction cocktail was assessed, and culture conditions were optimized regarding culture protocol and basic media in order to improve flexibility and cost effectiveness without decreasing lipid accumulation during adipogenesis. The seeding density could be increased from 750 up to 5000 cells per well, resulting in larger spheroids, which still homogeneously accumulated triglycerides when induced to undergo adipogenesis, while bearing several advantages with regard to routine culture.
The established human ASC spheroid model not only provides a system for screening the effects of pharmacological substances on adipose tissue in a more *in-vivo*-like context as compared to conventional 2-D culture, but can also serve as a powerful tool for the investigation and characterization of adipogenesis and adipocyte functions in a 3-D environment. It may be useful in order to gain new insights into the way how tissue-inherent factors like cell-cell-contact and the influence of ECM, which are much better represented in a 3-D model, affect adipose tissue development and adipocyte biology. Furthermore, it opens up perspectives for applications in adipose tissue engineering, because the spheroids can also serve as building blocks for the generation of coherent tissue, e.g. after embedding in hydrogels or by applying the organ printing technique.

3.6 References

1. Trayhurn P, Beattie J H. Physiological role of adipose tissue: white adipose tissue as an endocrine and secretory organ. *Proc Nutr Soc* 2001; **60***, 3*, 329–339.
2. Arner P. The adipocyte in insulin resistance: key molecules and the impact of the thiazolidinediones. *Trends Endocrinol Metab* 2003; **14***, 3*, 137–145.
3. Fruhbeck G. Overview of adipose tissue and its role in obesity and metabolic disorders. *Methods Mol Biol* 2008, vol. 456, 1–22.
4. Bjørndal B, Burri L, Staalesen V, Skorve J, Berge R K. Different adipose depots: their role in the development of metabolic syndrome and mitochondrial response to hypolipidemic agents. *J Obes* 2011, 15 pages.
5. Nawrocki A R, Scherer P E. Keynote review: The adipocyte as a drug discovery target. *Drug Discovery Today* 2005; **10***, 18*, 1219–1230.
6. Maury E, Brichard S M. Adipokine dysregulation, adipose tissue inflammation and metabolic syndrome. *Mol Cell Endocrinol* 2010; **314***, 1*, 1–16.
7. DeLany J P, Floyd Z E, Zvonic S, Smith A, Gravois A, Reiners E, Wu X, Kilroy G, Lefevre M, Gimble J M. Proteomic analysis of primary cultures of human adipose-derived stem cells: modulation by Adipogenesis. *Mol Cell Proteomics* 2005; **4***, 6*, 731–740.
8. Rosen E D, MacDougald O A. Adipocyte differentiation from the inside out. *Nat Rev Mol Cell Biol* 2006; **7***, 12*, 885–896.
9. MacDougald O A, Mandrup S. Adipogenesis: forces that tip the scales. *Trends Endocrinol Metab* 2002; **13***, 1*, 5–11.
10. Tong Q, Hotamisligil G S. Molecular mechanisms of adipocyte differentiation. *Rev Endocr Metab Disord* 2001; **2***, 4*, 349–355.
11. Cukierman E, Pankov R, Stevens D R, Yamada K M. Taking cell-matrix adhesions to the third dimension. *Science* 2001; **294***, 5547*, 1708–1712.
12. Pedersen J A, Swartz M A. Mechanobiology in the third dimension. *Ann Biomed Eng* 2005; **33***, 11*, 1469–1490.
13. Mazzoleni G, Di Lorenzo D, Steimberg N. Modelling tissues in 3D: the next future of pharmaco-toxicology and food research? *Genes Nutr* 2009; **4***, 1*, 13–22.
14. Boudreau N, Weaver V. Forcing the third dimension. *Cell* 2006; **125***, 3*, 429–431.
15. Abbott A. Cell culture: biology's new dimension. *Nature* 2003; **424***, 6951*, 870–872.
16. Khetani S R, Bhatia S N. Engineering tissues for in vitro applications. *Curr Opin Biotechnol* 2006; **17***, 5*, 524–531.
17. Bauer-Kreisel P, Goepferich A, Blunk T. Cell-delivery therapeutics for adipose tissue regeneration. *Adv Drug Deliv Rev* 2010; **62***, 7-8*, 798–813.
18. Fischbach C, Spruss T, Weiser B, Neubauer M, Becker C, Hacker M, Gopferich A, Blunk T. Generation of mature fat pads in vitro and in vivo utilizing 3-D long-term culture of 3T3-L1 preadipocytes. *Exp Cell Res* 2004; **300***, 1*, 54–64.
19. Neubauer M, Hacker M, Bauer-Kreisel P, Weiser B, Fischbach C, Schulz M B, Goepferich A, Blunk T. Adipose tissue engineering based on mesenchymal stem cells and basic fibroblast growth factor in vitro. *Tissue Eng* 2005; **11***, 11-12*, 1840–1851.
20. Weiser B, Prantl L, Schubert T EO, Zellner J, Fischbach-Teschl C, Spruss T, Seitz A K, Tessmar J, Goepferich A, Blunk T. In vivo development and long-term survival of

engineered adipose tissue depend on in vitro precultivation strategy. *Tissue Eng Part A* 2008; **14***, 2*, 275–284.

21. Kimura Y, Ozeki M, Inamoto T, Tabata Y. Adipose tissue engineering based on human preadipocytes combined with gelatin microspheres containing basic fibroblast growth factor. *Biomaterials* 2003; **24***, 14*, 2513–2521.
22. Torio-Padron N, Baerlecken N, Momeni A, Stark G B, Borges J. Engineering of adipose tissue by injection of human preadipocytes in fibrin. *Aesthetic Plast Surg;* **31***, 3*, 285–293.
23. O'Connor K C, Song H, Rosenzweig N, Jansen D A. Extracellular matrix substrata alter adipocyte yield and lipogenesis in primary cultures of stromal-vascular cells from human adipose. *Biotechnol Lett* 2003; **25***, 23*, 1967–1972.
24. Kunz-Schughart L A, Freyer J P, Hofstaedter F, Ebner R. The use of 3-D cultures for high-throughput screening: the multicellular spheroid model. *J Biomol Screen* 2004; **9***, 4*, 273–285.
25. Santini M T, Rainaldi G. Three-dimensional spheroid model in tumor biology. *Pathobiology* 1999; **67***, 3*, 148–157.
26. Lin R Z, Chang H Y. Recent advances in three-dimensional multicellular spheroid culture for biomedical research. *Biotechnol J* 2008; **3***, 9-10*, 1172–1184.
27. Weiser B. Adipose tissue engineering - Precultivation strategies towards clinical applications & A novel 3-D model of adipogenesis for basic research. *Dissertation, University of Regensburg* 2008.
28. Avram M M, Avram A S, James W D. Subcutaneous fat in normal and diseased states: 3. Adipogenesis: From stem cell to fat cell. *J Am Acad Dermatol* 2007; **56***, 3*, 472–492.
29. Ntambi J M, Young-Cheul K. Adipocyte differentiation and gene expression. *J Nutr* 2000; **130***, 12*, 3122S-3126S.
30. Ryden M, Dicker A, van Harmelen V, Hauner H, Brunnberg M, Perbeck L, Lonnqvist F, Arner P. Mapping of early signaling events in tumor necrosis factor-alpha -mediated lipolysis in human fat cells. *J Biol Chem* 2002; **277***, 2*, 1085–1091.
31. Poulos S P, Dodson M V, Hausman G J. Cell line models for differentiation: preadipocytes and adipocytes. *Exp Biol Med (Maywood)* 2010; **235***, 10*, 1185–1193.
32. Zuk P A, Zhu M, Mizuno H, Huang J, Futrell J W, Katz A J, Benhaim P, Lorenz H P, Hedrick M H. Multilineage cells from human adipose tissue: implications for cell-based therapies. *Tissue Eng* 2001; **7***, 2*, 211–228.
33. Gimble J, Guilak F. Adipose-derived adult stem cells: isolation, characterization, and differentiation potential. *Cytotherapy* 2003; **5***, 5*, 362–369.
34. Gimble J M, Katz A J, Bunnell B A. Adipose-derived stem cells for regenerative medicine. *Circ Res* 2007; **100***, 9*, 1249–1260.
35. Guilak F, Lott K E, Awad H A, Cao Q, Hicok K C, Fermor B, Gimble J M. Clonal analysis of the differentiation potential of human adipose-derived adult stem cells. *J Cell Physiol* 2006; **206***, 1*, 229–237.
36. Nakamura T, Shiojima S, Hirai Y, Iwama T, Tsuruzoe N, Hirasawa A, Katsuma S, Tsujimoto G. Temporal gene expression changes during adipogenesis in human mesenchymal stem cells. *Biochem Biophys Res Commun* 2003; **303***, 1*, 306–312.
37. Bunnell B A, Flaat M, Gagliardi C, Patel B, Ripoll C. Adipose-derived stem cells: isolation, expansion and differentiation. *Methods* 2008; **45***, 2*, 115–120.

38. Bartosh T J, Ylostalo J H, Mohammadipoor A, Bazhanov N, Coble K, Claypool K, Lee R H, Choi H, Prockop D J. Aggregation of human mesenchymal stromal cells (MSCs) into 3D spheroids enhances their antiinflammatory properties. *Proc Natl Acad Sci U S A* 2010; **107***, 31*, 13724–13729.

39. Potapova I A, Gaudette G R, Brink P R, Robinson R B, Rosen, Cohen I S, Doronin S V. Mesenchymal stem cells support migration, extracellular matrix invasion, proliferation, and survival of endothelial cells in vitro. *Stem Cells* 2007; **25***, 7*, 1761–1768.

40. Verseijden F, Posthumus-van Sluijs S J, Pavljasevic P, Hofer S O, van Osch G J, Farrell E. Adult human bone marrow- and adipose tissue-derived stromal cells support the formation of prevascular-like structures from endothelial cells in vitro. *Tissue Eng Part A* 2010; **16***, 1*, 101–114.

41. Bhang S H, Cho S W, La W G, Lee T J, Yang H S, Sun A Y, Baek S H, Rhie J W, Kim B S. Angiogenesis in ischemic tissue produced by spheroid grafting of human adipose-derived stromal cells. *Biomaterials* 2011; **32***, 11*, 2734–2747.

42. Verseijden F, Posthumus-van S SJ, Farrell E, van Neck J W, Hovius S E, Hofer S O, van Osch G J. Prevascular structures promote vascularization in engineered human adipose tissue constructs upon implantation. *Cell Transplant* 2010; **19***, 8*, 1007–1020.

43. Greenspan P, Mayer E P, Fowler S D. Nile red: a selective fluorescent stain for intracellular lipid droplets. *J Cell Biol* 1985; **100***, 3*, 965–973.

44. Lahnalampi M, Heinäniemi M, Sinkkonen L, Wabitsch M, Carlberg C. Time-resolved expression profiling of the nuclear receptor superfamily in human adipogenesis. *PLoS One* 2010; **5***, 9*, e12991.

45. Wall M E, Bernacki S H, Loboa E G. Effects of serial passaging on the adipogenic and osteogenic differentiation potential of adipose-derived human mesenchymal stem cells. *Tissue Eng* 2007; **13***, 6*, 1291–1298.

46. Gonda K, Shigeura T, Sato T, Matsumoto D, Suga H, Inoue K, Aoi N, Kato H, Sato K, Murase S, Koshima I, Yoshimura K. Preserved proliferative capacity and multipotency of human adipose-derived stem cells after long-term cryopreservation. *Plast Reconstr Surg* 2008; **121***, 2*, 401–410.

47. Jing K, Heo J Y, Song K S, Seo K S, Park J H, Kim J S, Jung Y J, Jo D Y, Kweon G R, Yoon W H, Hwang B D, Lim K, Park J I. Expression regulation and function of Pref-1 during adipogenesis of human mesenchymal stem cells (MSCs). *Biochim Biophys Acta* 2009; **1791***, 8*, 816–826.

48. Kakudo N, Shimotsuma A, Kusumoto K. Fibroblast growth factor-2 stimulates adipogenic differentiation of human adipose-derived stem cells. *Biochem Biophys Res Commun* 2007; **359***, 2*, 239–244.

49. Janderova L, McNeil M, Murrell A N, Mynatt R L, Smith S R. Human mesenchymal stem cells as an in vitro model for human adipogenesis. *Obesity* 2003; **11***, 1*, 65–74.

50. Xiang Y, Zheng Q, Jia B B, Huang G P, Xu Y L, Wang J F, Pan Z J. Ex vivo expansion and pluripotential differentiation of cryopreserved human bone marrow mesenchymal stem cells. *J Zhejiang Univ Sci B* 2007; **8***, 2*, 136–146.

51. Li W, Vogel C F, Fujiyoshi P, Matsumura F. Development of a human adipocyte model derived from human mesenchymal stem cells (hMSC) as a tool for toxicological studies on the action of TCDD. *Biol Chem* 2008; **389***, 2*, 169–177.

52. Bouloumie A, Sengenes C, Portolan G, Galitzky J, Lafontan M. Adipocyte produces matrix metalloproteinases 2 and 9: involvement in adipose differentiation. *Diabetes* 2001; **50***, 9*, 2080–2086.

53. Lacasa D, Taleb S, Keophiphath M, Miranville A, Clement K. Macrophage-secreted factors impair human adipogenesis: involvement of proinflammatory state in preadipocytes. *Endocrinology* 2007; **148***, 2*, 868–877.

54. Bujalska I J, Walker E A, Hewison M, Stewart P M. A switch in dehydrogenase to reductase activity of 11 beta-hydroxysteroid dehydrogenase type 1 upon differentiation of human omental adipose stromal cells. *J Clin Endocrinol Metab* 2002; **87***, 3*, 1205–1210.

55. Hemmrich K, Heimburg D von, Rendchen R, Di Bartolo C, Milella E, Pallua N. Implantation of preadipocyte-loaded hyaluronic acid-based scaffolds into nude mice to evaluate potential for soft tissue engineering. *Biomaterials* 2005; **26***, 34*, 7025–7037.

56. Morgan S M, Ainsworth B J, Kanczler J M, Babister J C, Chaudhuri J B, Oreffo R OC. Formation of a human-derived fat tissue layer in P(DL)LGA hollow fibre scaffolds for adipocyte tissue engineering. *Biomaterials* 2009; **30***, 10*, 1910–1917.

57. Ninomiya Y, Sugahara-Yamashita Y, Nakachi Y, Tokuzawa Y, Okazaki Y, Nishiyama M. Development of a rapid culture method to induce adipocyte differentiation of human bone marrow-derived mesenchymal stem cells. *Biochem Biophys Res Commun* 2010; **394***, 2*, 303–308.

58. Price P J, Gregory E A. Relationship between in vitro growth promotion and biophysical and biochemical properties of the serum supplement. *In Vitro* 1982; **18***, 6*, 576–584.

CHAPTER 4

Characterization of hASC Spheroids – Adipogenesis in 2-D and 3-D Cultures

4.1 Abstract

For the development of therapies against diseases associated with fat tissue, but also for applications in adipose tissue engineering, it is important to shed light on the process of adipogenesis. The conversion of mesenchymal stem cells to mature adipocytes is known to involve a highly regulated cascade of gene expression events. However, the three-dimensional (3-D) microenvironment of native tissue is barely represented in monolayer cell culture. Therefore, a 3-D spheroid model using human adipose-derived stem cells (ASC), which had been established previously, was applied to characterize adipogenesis on a functional and molecular level, especially in comparison with conventional 2-D culture.

Applying short-term adipogenic induction (common hormonal cocktail containing dexamethasone, insulin, 3-isobutyl-methylxanthine (IBMX) and indomethacin applied for two days only), a strong adipogenic response with a high lipid content on day 14 was observed in 3-D spheroids, whereas lipid content was only minimal in 2-D culture. Gene expression data reflected these results: In 2-D culture, several genes associated with lipid synthesis and transport (FASN, ACLY, FATP1) were very weakly expressed, in contrast to high expression in 3-D spheroids. Also other fat cell markers and adipokines (e.g., adiponectin, apelin, LPL) were more strongly expressed in 3-D. Strikingly, already on day 2, increased expression of important transcription factors (PPARγ, C/EBPβ, SREBF1) was determined in 3-D culture, which represents, at least in part, a likely explanation for the observed 2-D/3-D-differences at later time points. In 2-D, additional exogenous stimulation after day 2 was necessary to achieve significant adipogenic differentiation, while the 3-D context provided conditions rendering further stimulation unnecessary. Moreover, hormonal induction without either IBMX or indomethacin still led to significant lipid accumulation and expression of marker genes like PPARγ in the ASC spheroids, but not in 2-D cultures, providing insights into possible molecular mechanisms leading to the observed differences.

In conclusion, adipogenesis in the spheroid system proved to be less dependent on external stimulation than in conventional 2-D culture. The characterization of the 3-D spheroids provided valuable information for their use in adipose tissue engineering as well as in basic research.

4.2 Introduction

The role of white adipose tissue (WAT) is not limited to storing excess energy in the form of fat, as it was the established opinion decades ago. On the contrary, it is now known that WAT contributes to the regulation of many physiological and pathophysiological processes through endocrine, paracrine, and autocrine signals [1–4]. A thorough understanding of adipose tissue function and the process of adipogenesis is not only a prerequisite for the development of therapeutic strategies against diseases associated with obesity and the metabolic syndrome [4–6], but can also help to improve methods in adipose tissue engineering.

The conversion of mesenchymal stem cells towards adipocytes involves a determination phase, in which commitment to the adipocyte lineage takes place, followed by terminal differentiation. Especially the latter phase, in which cells gradually adopt adipocyte morphology and start to express typical fat cell markers and adipokines, has been characterized in numerous studies. This has helped to identify more and more genes and regulatory mechanisms involved in adipocyte differentiation and maturation [1,2,7–9]. It is now well known that adipogenesis is accompanied by a temporally regulated set of gene expression events, in which transcription factors like PPARγ, the so called master regulator of adipogenesis, and members of the CCAAT-enhancer-binding protein family (C/EBPs) play an important role [10,11].

The vast majority of studies in this field was performed using conventional two-dimensional (2-D) *in vitro* culture. However, it is well recognized that cells are strongly influenced by tissue-specific aspects such as multiple cell-cell and cell-ECM interactions and the 3-dimensional structure itself, all of which are not accurately represented in 2-D culture [12–16].

Therefore, the main goal of this study was to characterize the process of adipogenesis in a 3-D culture system in comparison to conventional 2-D culture on a functional and molecular level. For this purpose, our previously established hASC spheroid model was applied, as it provides a well-defined, homogeneous, scaffold-free 3-D environment, in which adipogenic differentiation can be investigated in a more *in-vivo*-like context (chapter 3).

Specifically, the main focus of this chapter was set on the influence of a reduced hormonal stimulation on adipogenesis in 2-D and 3-D culture. Most common protocols for the *in vitro* adipogenic differentiation of hASC include the application of a hormonal induction cocktail consisting of the 4 components dexamethasone, 3-isobutyl-methylxanthine (IBMX), insulin and indomethacin [17–21]. Usually, these inducers remain in the medium over the whole culture period (permanent induction, IND-P). There have been hints that protocols involving only a short-term induction lead to a severely impaired differentiation efficiency in 2-D

culture, but this behavior was not further investigated [19]. However, preliminary experiments with our spheroid model indicated that such a short-term protocol (IND-S), in which the hormonal cocktail was removed at day 2, could be sufficient to induce adipogenic differentiation in the 3-D environment. This would mean that adipogenesis is less dependent on exogenous stimulation in our spheroid system than in conventional 2-D culture.

To investigate this hypothesis, lipid accumulation and gene expression of monolayers and 3-D spheroids were assessed, when cells were induced to undergo adipogenic differentiation using either permanent or short-term induction. Moreover, in a different experiment, both culture systems were exposed to altered induction cocktails, in which certain components were omitted, which also represents conditions with a reduced exogenous stimulus.

The *in vitro* pretreatment of cell constructs is also an important issue in adipose tissue regeneration, which can significantly influence their subsequent *in vivo* performance. Interestingly, in several studies adipogenic induction performed prior to implantation led to strongly increased adipogenesis and better adipose tissue development *in vivo* [22,23]. With regard to clinical applications in regenerative medicine, it is desirable to keep *in vitro* preconditioning as short as possible. Therefore, a further goal of this study was to evaluate the suitability of the spheroid model, in combination with modified induction protocols, for a possible future use in tissue engineering applications.

4.3 Materials and Methods

4.3.1 Materials

Human adipose derived stem cells (ASC) were obtained from PromoCell (Heidelberg, Germany; lot 8073006.12); Preadipocyte Growth Medium 2 (PGM2) was from Lonza (Verviers, Belgium). Fetal bovine serum (FBS, lot 40A0044K), penicillin-streptomycin solution, 0.25% trypsin/EDTA solution, phosphate buffered saline (PBS) and Trizol reagent were from Invitrogen (Darmstadt, Germany). Agarose, indomethacin, dexamethasone, glycerol standard solution, bovine serum albumin (BSA), propidiumiodide solution, dimethylsulfoxide (DMSO), calf thymus DNA, Oil Red O, osmium tetroxide, formaldehyde solution, MOPS, RNA sample loading buffer, EDTA, sodium acetate and DEPC water were purchased from Sigma-Aldrich (Munich, Germany). 3-isobutyl-methylxanthine (IBMX) was bought from Serva (Heidelberg, Germany), Thesit from Gepepharm (Siegburg, Germany). Hoechst 33258 dye was obtained from Polysciences (Warrington, PA, USA). Bovine insulin was kindly provided by Sanofi-Aventis (Frankfurt a. M., Germany). Turbo DNase and the TaqMan Gene Expression Master Mix were from Applied Biosystems (Darmstadt, Germany).

All other chemicals were from Merck (Darmstadt, Germany). All cell culture plastics were from Corning (Bodenheim, Germany).

4.3.2 Methods

4.3.2.1 Cell culture

4.3.2.1.1 2-D cell culture

Human adipose-derived stem cells (hASC) were thawed after cryopreservation (Passage 3) and seeded in culture flasks. They were expanded at 37°C, 5% CO_2 in growth medium (GM), i.e. Preadipocyte Basal Medium (PBM2) containing 10% FBS, penicillin (100 U/ml) and streptomycin (100 µg/ml). At 90% confluence cells were trypsinized, seeded in 24-well plates at a density of 30,000 cells/cm² and cultured in GM for 2 days before adipogenic differentiation was induced.

4.3.2.1.2 3-D cell culture

For the generation of 3-D spheroid cultures the liquid overlay technique was used. hASC were expanded as described in the previous section. After trypsinization, cells were resuspended in GM and seeded into 96-well plates coated with 1.5% agarose at 3,000 cells per well. Culture plates were kept on an orbital shaker at 50 rpm during incubation. After 1 day, a single spheroid had developed in each well. Like in 2-D culture, adipogenesis was induced after 2 days in GM. As spheroids would be lost with complete removal of medium from the wells, all medium changes were performed by replenishing only half of the medium volume. For comparability, 2-D cultures were treated in the same way.

4.3.2.1.3 Adipogenic differentiation under permanent and short-term induction

In both culture systems (2-D and 3-D), adipogenic differentiation was performed using two different induction protocols (see Fig. 4-1 for an illustration of the experimental design): permanent induction (IND-P) and short-term induction (IND-S).

In both cases, on day 0 (i.e. the day of induction) adipogenesis was induced by exchanging half of the medium with induction medium (IM), consisting of GM supplemented with a hormonal cocktail, resulting in final concentrations of 1.7 µM insulin, 1 µM dexamethason, 200 µM indomethacin and 500 µM 3-isobutyl-1-methylxanthine (IBMX). When permanent induction (IND-P) was applied, cells were kept in IM over the whole culture period up to day 14. Using short-term induction (IND-S), IM was replaced by maintenance medium (MM) on day 2 after induction by exchanging half of the medium for three times (in 2-D and 3-D) in

order to reduce the concentration of the hormonal inducers. MM consisted of GM supplemented with 1.7 µM insulin (final concentration). For both 2-D and 3-D culture, a control group (CTRL) was kept in GM for the whole culture time without adipogenic induction, but otherwise treated in the same way as the other groups.

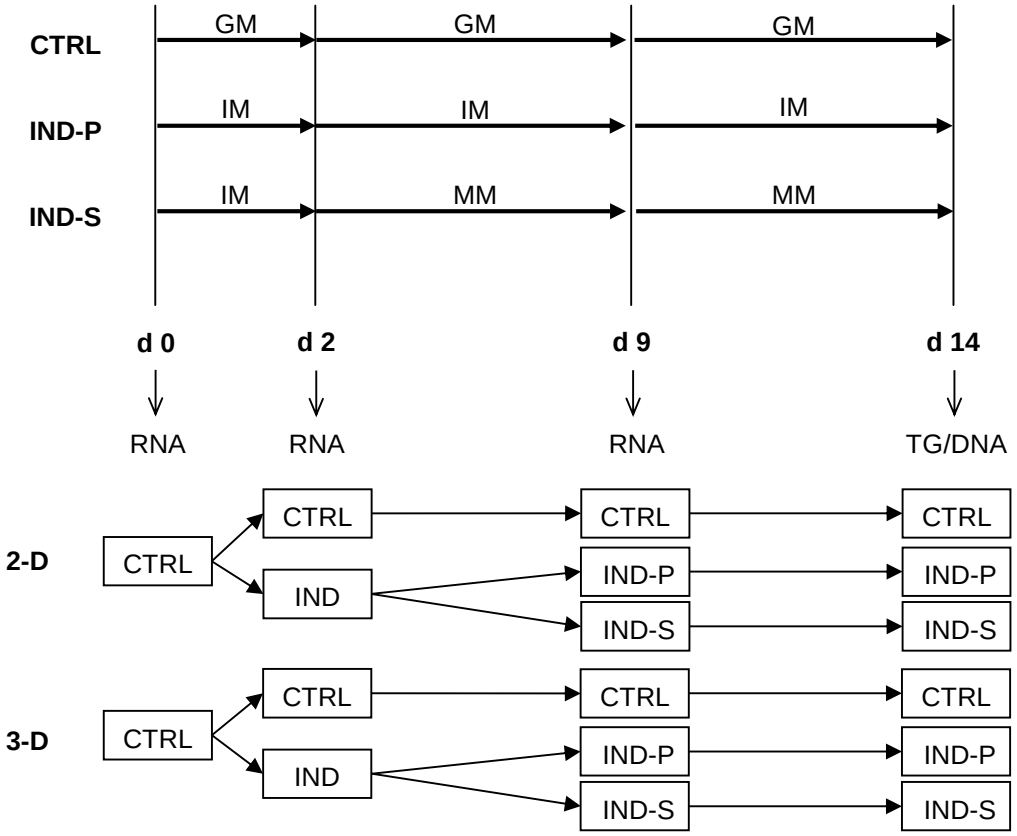

Figure 4-1: *Experimental design. hASC were seeded as 2-D monolayers or 3-D spheroids. In both culture systems, adipogenic differentiation was performed using two different induction protocols: permanent induction (IND-P) and short-time induction (IND-S). In both cases, on day 0 induction medium (IM) was applied. Using IND-P, cells were kept in IM over the whole culture period up to day 14, while for the IND-S groups, IM was replaced by maintenance medium (MM) on day 2 after induction. A control group (CTRL) for each culture system (2-D and 3-D) was kept in growth medium (GM) for the whole culture time without adipogenic induction. Samples for the analysis of triglyceride and DNA contents were taken from each group on day 14 after induction. RNA was isolated on days 0, 2 and 9. Please note that on day 0 only one group existed in each culture system, because samples were taken before the start of the adipogenic induction. Up to day 2, treatment of the groups IND-P and IND-S was identical, so that on day 2 we could only distinguish between control (CTRL) and induced (IND) groups.*

2-D and 3-D cultures were harvested on days 0, 2 and 9 for RNA isolation in triplicates. For one biological replicate, one well (2-D) or a pool of 60 spheroids (3-D) were used, respectively. On day 14, cells were harvested for the analysis of triglyceride (TG) and DNA contents as well as histological staining.

4.3.2.1.4 Adipogenic differentiation with altered hormonal cocktails

2 days after seeding (i.e. on day 0), 2-D and 3-D cultures were treated with 2 different induction media, which were equivalent to standard IM (as described above), except that either IBMX or indomethacin were not included. Half of the medium was exchanged at day 2 and then again every 3-4 days. One group of cells was kept in IM without IBMX over the whole culture time up to day 14, the other in IM without indomethacin. For both 2-D and 3-D culture, a control group (CTRL) was kept in GM for the whole culture time without adipogenic induction, but otherwise treated in the same way as the other groups. 2-D and 3-D cultures were harvested on days 0, 2 and 9 for RNA isolation and subsequent qRT-PCR analysis in triplicates. For one biological replicate, one well (2-D) or a pool of 20 spheroids (3-D) were used, respectively. On day 14, cells were harvested for the analysis of triglyceride (TG) and DNA contents as well as histological staining.

4.3.2.2 Histological staining and preparation of cryosections

To visualize triglyceride accumulation, cultures were harvested on day 14 after induction and staining with osmium tetroxide (OsO_4) or Oil Red O (ORO) was performed. For this purpose, spheroids were transferred to microcentrifuge tubes, washed with PBS, fixed in 10% formalin (1h, 4°C), stained with OsO_4 (1% aqueous solution) or with ORO (3 mg/ml solution in 60% isopropanol) for 1h on ice and washed three times with PBS. Stained spheroids were embedded in Tissue-Tek, snap-frozen and cut into 10 µm cryosections. After removal of Tissue-Tek by washing in water, the sections were mounted in glycerol. Serial sections were prepared from all spheroids and sections from the center region were used for histological evaluation. For 2-D cultures, staining was performed directly in the 24-well plates.

4.3.2.3 Analysis of intracellular triglyceride (TG) accumulation

For analysis of the intracellular TG content, 2-D monolayers and 3-D spheroids were washed twice with PBS and harvested in 0.5% aqueous Thesit solution. After sonication, spectroscopic quantification of TG was performed using the enzymatic Serum Triglyceride Determination Kit from Sigma-Aldrich (Taufkirchen, Germany) according to the manufacturer's instructions. All measurements were performed in three biological replicates; one replicate was derived from one well for 2-D cultures and an exact number of approximately 20 spheroids for 3-D cultures, respectively. TG contents per spheroid or per well were calculated and normalized to the DNA content, which was determined as described below.

4.3.2.4 Determination of DNA content

2-D monolayers and 3-D spheroids were washed twice with PBS, harvested in lysis buffer (2 mM EDTA, 2M NaCl, 50 mM Na_3PO_4, pH 7,4) and sonicated. DNA content was determined using the intercalating Hoechst 33258 dye (0.1 µg/ml in 0.1 M NaCl, 1 mM EDTA, 10 mM Tris, pH 7.4). Fluorescence intensities were determined at 365 nm excitation wavelength and 458 nm emission wavelength and correlated to DNA contents using standard dilutions of double-stranded DNA (from calf thymus). All measurements were performed in three biological replicates; one replicate was derived from one well for 2-D cultures and an exact number of approximately 10 spheroids for 3-D cultures, respectively.

4.3.2.5 Low Density Gene Expression Array

Prior to RNA isolation, 2-D monolayers as well as whole spheroids were washed with PBS. Total RNA was extracted from the samples using RNeasy Mini Kit (Qiagen, Hilden, Germany) according to the manufacturer's instructions. For one biological replicate, 60 spheroids were pooled and lysed by addition of RLT lysis buffer. 2-D cultures were lysed directly in the wells. Genomic DNA was eliminated using TURBO DNase according to the manufacturer's instructions. DNase was subsequently removed by phenol-chloroform extraction. RNA concentration was determined spectrophotometrically with a NanoDrop analyzer (Thermo Fisher Scientific, Wilmington, DE, USA). RNA quality was tested by agarose gel electrophoresis.

cDNA was synthesized from 100 ng total RNA per sample using High Capacity cDNA Reverse Transcription Kit (Applied Biosystems, Darmstadt, Germany) according to the manufacturer´s protocol.

qRT-PCR using custom-made TaqMan Low Density Arrays (Applied Biosystems, Darmstadt, Germany) containing primers and probes for a variety of adipogenesis-related genes in 384-well micro fluidic cards was performed according to the manufacturer's instructions. cDNA samples were mixed with TaqMan Gene Expression Master Mix and filled into the ports of the micro fluidic cards. After centrifugation in order to distribute the cDNA samples to the reaction wells, the cards were sealed and RT-PCR was performed on a 7900HT Fast Real-Time System (Applied Biosystems, Darmstadt, Germany) over 40 cycles. Evaluation of expression data was carried out according to the ΔΔCt method. All Ct values were normalized to GAPDH. Expression values of 2-D cultures on day 0 were used as reference for all other groups. If a gene was not detectable in the reference group, a Ct value of 40 was assumed (corresponding to one cDNA replicate in the sample). Relative expression levels (RQ) were calculated as $2^{-\Delta\Delta Ct}$. All measurements were performed with three biological replicates. Genes specifically mentioned in the text are listed in Table 4-1.

Table 4-1: *List of gene names, gene symbols, and TaqMan Assay ID's.*

Gene name	Gene symbol	Assay ID#
ATP citrate lyase	ACLY	Hs00153764_m1
adiponectin	ADIPOQ	Hs00605917_m1
angiotensinogen	AGT	Hs00174854_m1
apelin	APLN	Hs00175572_m1
apolipoprotein E	APOE	Hs00171168_m1
CCAAT/enhancer binding protein (C/EBP), alpha	CEBPA	Hs00269972_s1
CCAAT/enhancer binding protein (C/EBP), beta	CEBPB	Hs00270923_s1
CCAAT/enhancer binding protein (C/EBP), delta	CEBPD	Hs00270931_s1
complement factor D (adipsin)	CFD	Hs00157263_m1
fatty acid binding protein 4 (aP2)	FABP4	Hs01086177_m1
fatty acid synthase	FASN	Hs00188012_m1
fatty acid transporter 1	FATP1	Hs01587917_m1
glyceraldehyde-3-phosphate dehydrogenase	GAPDH	Hs99999905_m1
facilitated glucose transporter 4	GLUT4	Hs00168966_m1
lipoprotein lipase	LPL	Hs00173425_m1
nicotinamide phosphoribosyltransferase (visfatin)	NAMPT	Hs00237184_m1
peroxisome proliferator-activated receptor gamma	PPARG	Hs00234592_m1
sterol regulatory element binding transcription factor 1	SREBF1	Hs01088691_m1

4.3.2.6 Quantitative real-time PCR (qRT-PCR)

Cells were harvested with Trizol reagent and the total RNA was isolated according to the manufacturer's instructions. For one biological replicate, one well (2-D) or a pool of 20 spheroids was used, respectively. All measurements were performed with three biological replicates. RNA concentrations were determined spectrophotometrically with a NanoDrop analyzer (Thermo Fisher Scientific, Wilmington, DE, USA).

First strand cDNA was synthesized from total RNA using ImProm-II Reverse Transcription System (Promega, Mannheim, Germany) according to the manufacturer's protocol. qRT-PCR was performed with MESA Blue qPCR MasterMix Plus for SYBR® Assay (Eurogentec, Köln, Germany) on a Opticon 2 Real-Time PCR Detection System (Bio-Rad, München, Germany) using the following cycling conditions: 95 °C for 15 minutes, followed by 40 cycles at 95 °C for 15 seconds, 55 °C for 30 seconds and 72 °C for 30 seconds. Amplification was carried out using specific primers for PPARγ (QT00029841), C/EBPα (QT00203357), aP2 (=FABP4, QT01667694) and GLUT4 (=SLC2A4, QT00097902) from Qiagen (Hilden,

Germany). Evaluation of expression data was carried out according to the ΔΔCt method. All Ct values were normalized to beta-actin (QT01680476) as a housekeeping gene. Expression levels were calculated relative to 2-D cultures on day 0. Relative expression levels (RQ) were calculated as $2^{-\Delta\Delta Ct}$.

4.3.2.7 Statistics

All quantitative results are presented as mean value ± standard deviation. Differences between 2-D and 3-D culture at each time point were analyzed for significance using unpaired Student's t-test. Differences within each culture system between time points were analyzed for significance using one-way analysis of variances (ANOVA) with subsequent multiple comparisons according to Tukey's post-hoc test. A value of $p<0.05$ was regarded statistically significant. Statistical analysis was performed using PASW Statistics 18 software (SPSS Inc., Chicago, IL, USA).

4.4 Results

4.4.1 Effect of short-term hormonal induction on lipid accumulation in 2-D and 3-D cultures

3-D spheroid cultures and conventional 2-D cultures of hASC were induced to undergo adipogenesis using two different induction protocols (Fig. 4-1). After 14 days, 2-D cultures treated according to the permanent induction protocol (IND-P) showed substantial triglyceride accumulation which became obvious in phase contrast microscopy and after staining with OsO_4 (Fig. 4-2 A). Under the same conditions, OsO_4-stained cryosections revealed that 3-D spheroids also contained many lipid droplets, which were distributed over all areas of the constructs (Fig. 4-2 A). However, when the complete hormonal induction cocktail (IBMX, dexamethason, indomethacin, insulin) was applied for only 2 days (short-term induction protocol, IND-S), only a minimal number of lipid droplets could be detected in monolayers, whereas in 3-D spheroids triglyceride accumulation was comparable to the group treated with the protocol IND-P (Fig. 4-2 A). Uninduced control groups stained negative for triglycerides.

Quantification of the triglyceride (TG) content confirmed these results. Using permanent induction, in both culture systems ASC had accumulated triglycerides on day 14, with TG levels in 3-D cultures being even higher than in 2-D. With short-time induction a TG level comparable to that under IND-P treatment had been reached in 3-D, while in 2-D virtually no TG could be detected at all (Fig. 4-2 B).

4.4.2 Adipogenesis in 2-D and 3-D cultures: Gene expression

To investigate if the observed morphological and functional differences between 2-D and 3-D cultures during adipogenesis were also reflected on gene expression level, and to elucidate possible reasons for this behavior, qRT-PCR was performed using a TaqMan Low Density Array. The custom-made array included several genes related to adipogenesis and adipocyte functions like transcription factors, adipokines and other fat cell markers. Samples of the 2-D and 3-D cultures were taken at three time points: on day 0, i.e. immediately before hormonal induction was performed, to obtain a reference value; on day 2, an early time point during adipogenesis at which the groups IND-P and IND-S were still identical (both had received the complete hormonal cocktail until then) and were therefore labeled as IND; and finally on day 9 to represent a later stage of adipogenesis (Fig. 4-1).

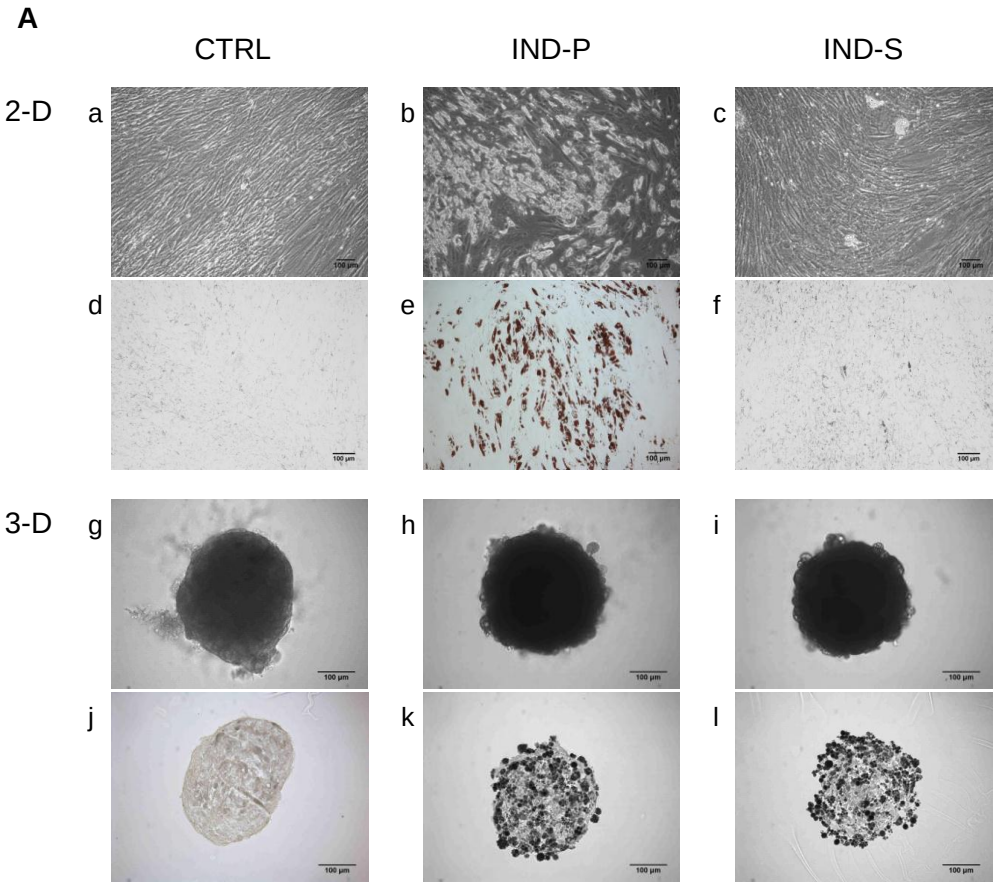

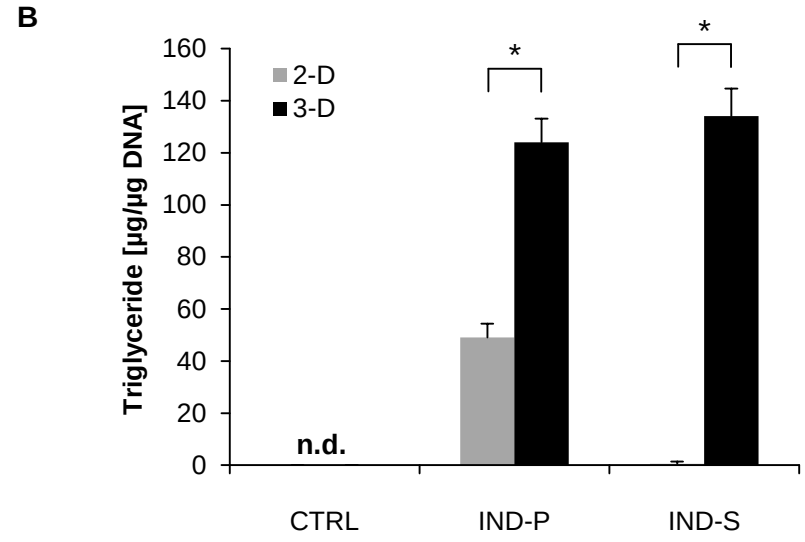

Figure 4-2: A) *Histological analysis of the triglyceride (TG) accumulation in 2-D and 3-D hASC cultures on day 14 after adipogenic induction using the protocols IND-P (middle) or IND-S (right). Uninduced controls (CTRL) are shown on the left. 2-D cultures: unstained, viewed with phase contrast (a-c) and stained with OsO_4 to visualize triglycerides (d-e). 3-D cultures: brightfield images of whole spheroids (g-i) and cryosections (from central regions of the constructs) stained with OsO4 (j-l). Scale bars are 100 µm.* ***B)*** *Quantification of intracellular TG content on day 14 (n=3). TG contents were normalized to DNA contents. 5 independent experiments were performed; representative results from one experiment are shown here. Statistically significant differences between 2-D and 3-D cultures are indicated by * ($p<0.05$).*

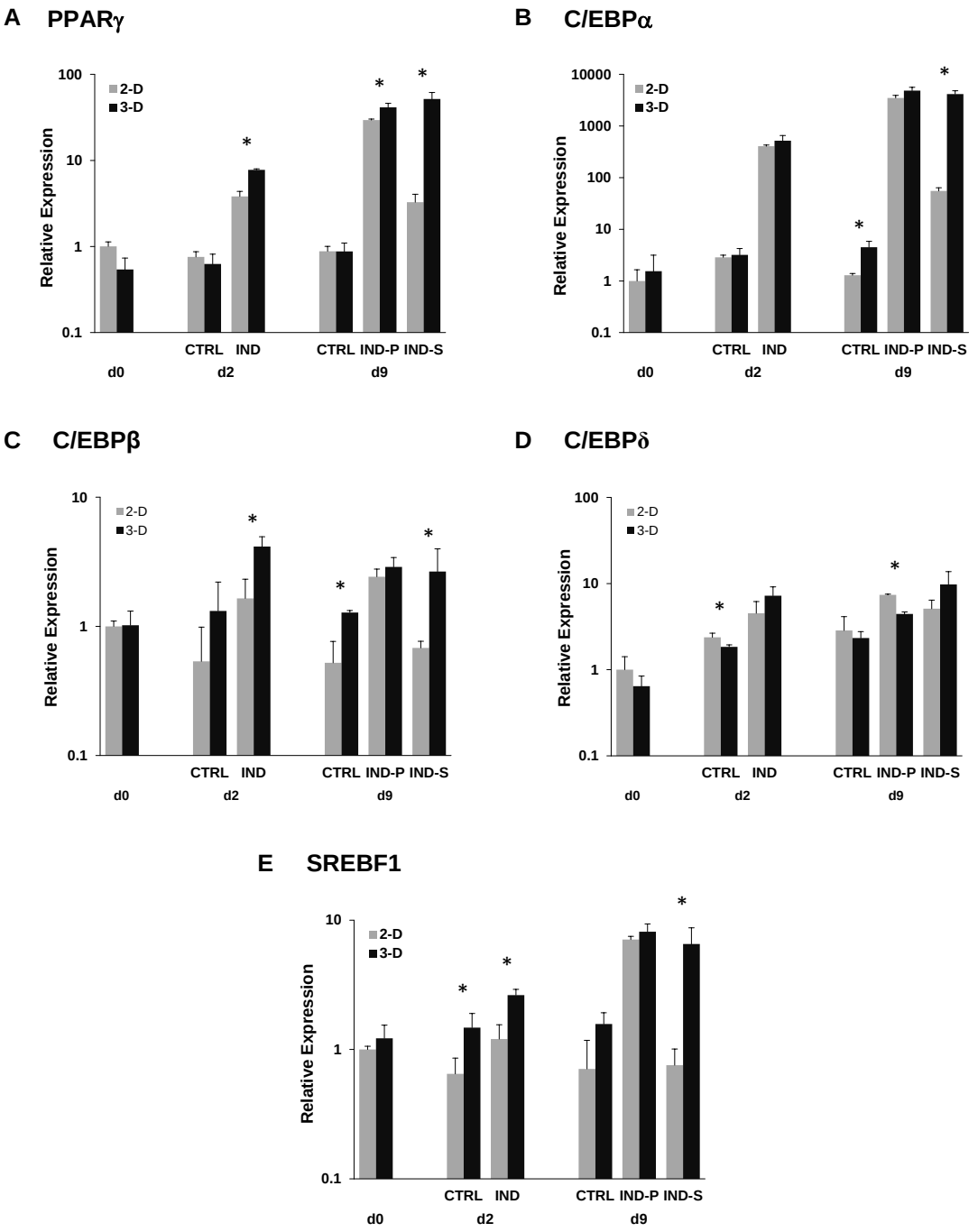

Figure 4-3: *Relative gene expression data (n=3) of the adipogenesis-related transcription factors PPARγ, C/EBPα, C/EBPβ, C/EBPδ and SREBF1 as determined by qRT-PCR using TaqMan Low Density Arrays. All mRNA levels are expressed relative to the value at d0 in 2-D culture. Statistically significant differences between 2-D and 3-D cultures are indicated by * (p<0.05).*

Expression of the transcription factor PPARγ, the master regulator of adipogenesis, was low on day 0 and in all uninduced controls, but highly upregulated by day 9 when permanent induction (IND-P) was performed, with the mRNA level in spheroid cultures being only slightly higher than in 2-D (Fig. 4-3 A). However, with short-time induction (IND-S) the difference between the two culture systems was much more pronounced. Here, expression in 2-D was greatly reduced as compared to 3-D culture, for which a similar expression level

to IND-P was measured, leading to a prominent difference between the two culture systems. Strikingly, already on day 2 PPARγ expression was significantly higher in 3-D cultures than in 2-D. Moreover, for IND-S, gene expression in 2-D was still on the same level on day 9 as it had been on day 2, whereas in 3-D it was further upregulated from day 2 to day 9.

C/EBPα, another important transcription factor for adipogenesis, in general showed a similar expression pattern (Fig. 4-3 B). Here, gene expression was strongly upregulated by day 2 independent of culture dimensionality. With IND-P, it was further increased by day 9 and reached comparable levels in 2-D and 3-D cultures. By contrast, using IND-S, C/EBPα expression in 2-D cultures was lower on day 9 than on day 2, but higher in 3-D spheroids, where by day 9 it had reached similar values as with IND-P.

C/EBPβ and C/EBPδ are usually upregulated in the early phase of adipogenic differentiation. On day 2 after induction, a significantly higher expression of C/EBPβ (Fig. 4-3 C), but not C/EBPδ (Fig. 4-3 D) could be detected in 3-D as compared to 2-D cultures.

Expression of the SREBF1 gene in 2-D cultures treated according to IND-S was not higher than in uninduced controls on day 9 (Fig. 4-3 E). In 3-D however, mRNA levels at that time point were comparable to those differentiated under the IND-P protocol. This pattern was again similar to the results for PPARγ and C/EBPα. Furthermore, like for PPARγ and C/EBPβ, also for SREBF1 gene expression data revealed a significant difference between 2-D and 3-D culture already on day 2 after induction.

In principle, comparable expression patterns could also be observed for several fat cell marker genes associated with lipid synthesis and lipid or glucose transport, like FAS, ACLY, FATP1, GLUT4 and aP2 (Fig. 4-4 A-E). For all of those genes an enormous difference between 2-D and 3-D cultures was detected regarding expression levels on day 9 after induction, when IND-S was used. In almost all cases, in 3-D spheroids those marker genes were nearly equally expressed with IND-S as with IND-P. In contrast, 2-D cultures contained much less mRNA of these genes when IND-S was used, but not when IND-P was applied. Interestingly, in 2-D cultures for some of these marker genes (FAS, ACLY and FATP1) mRNA levels with IND-S on day 9 were barely higher than in uninduced controls (CTRL). In contrast, expression of GLUT4 and aP2, while being still much lower than in 3-D cultures treated the same way, showed substantial upregulation on day 9 as compared to controls (Fig. 4-4). On day 2, significant differences in gene expression during adipogenic differentiation could be detected for FATP1 and GLUT4, while this was not the case for FAS, ACLY and aP2.

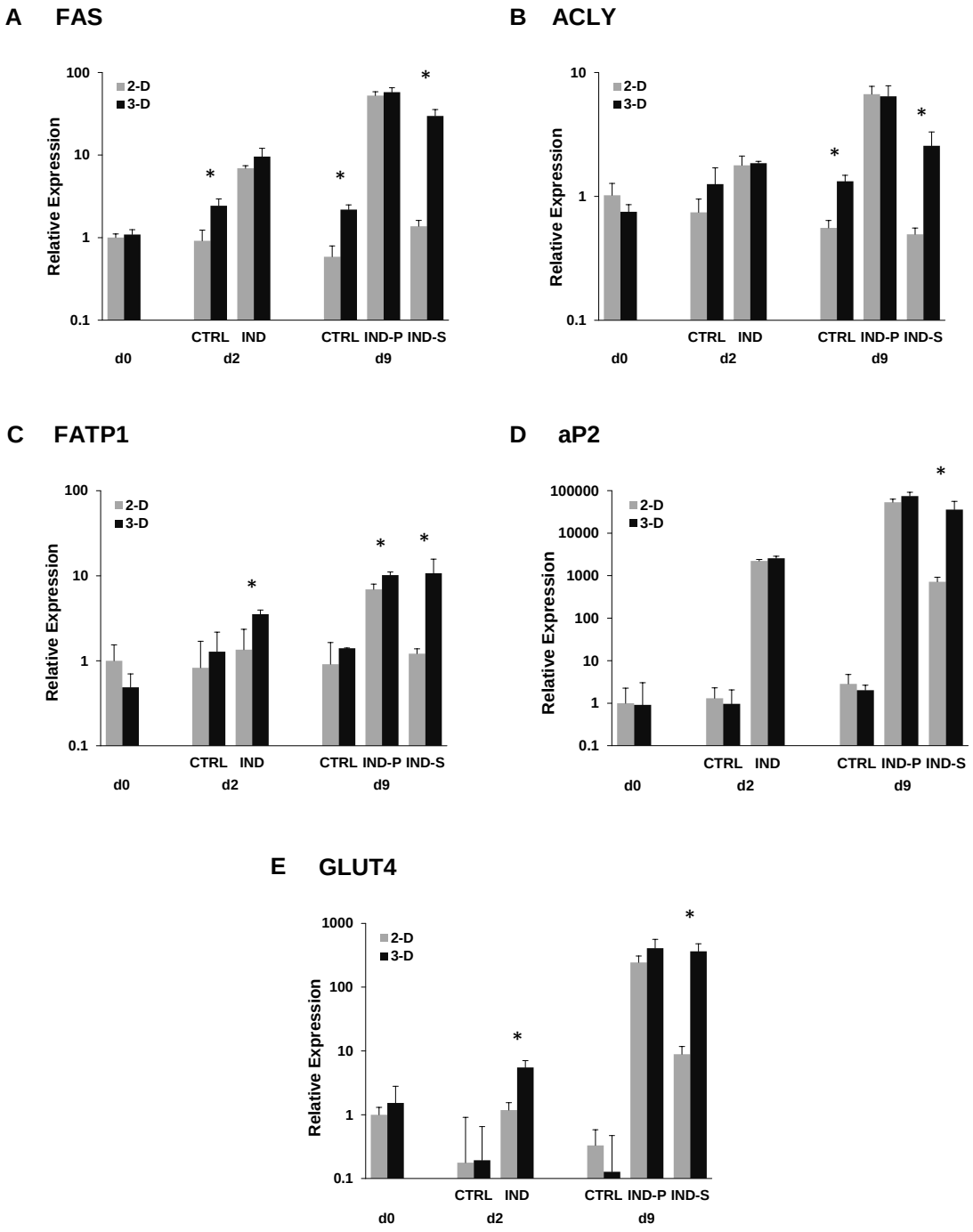

Figure 4-4: *Relative gene expression data (n=3) of several genes associated with lipid synthesis and lipid or glucose transport as determined by qRT-PCR using TaqMan Low Density Arrays: FAS (fatty acid synthase), ACLY (ATP citrate lyase), FATP1 (fatty acid transport protein 1), aP2 (fatty acid binding protein 4, FABP4) and GLUT4 (glucose transporter type 4). All mRNA levels are expressed relative to the value at d0 in 2-D culture. Statistically significant differences between 2-D and 3-D cultures are indicated by * ($p<0.05$).*

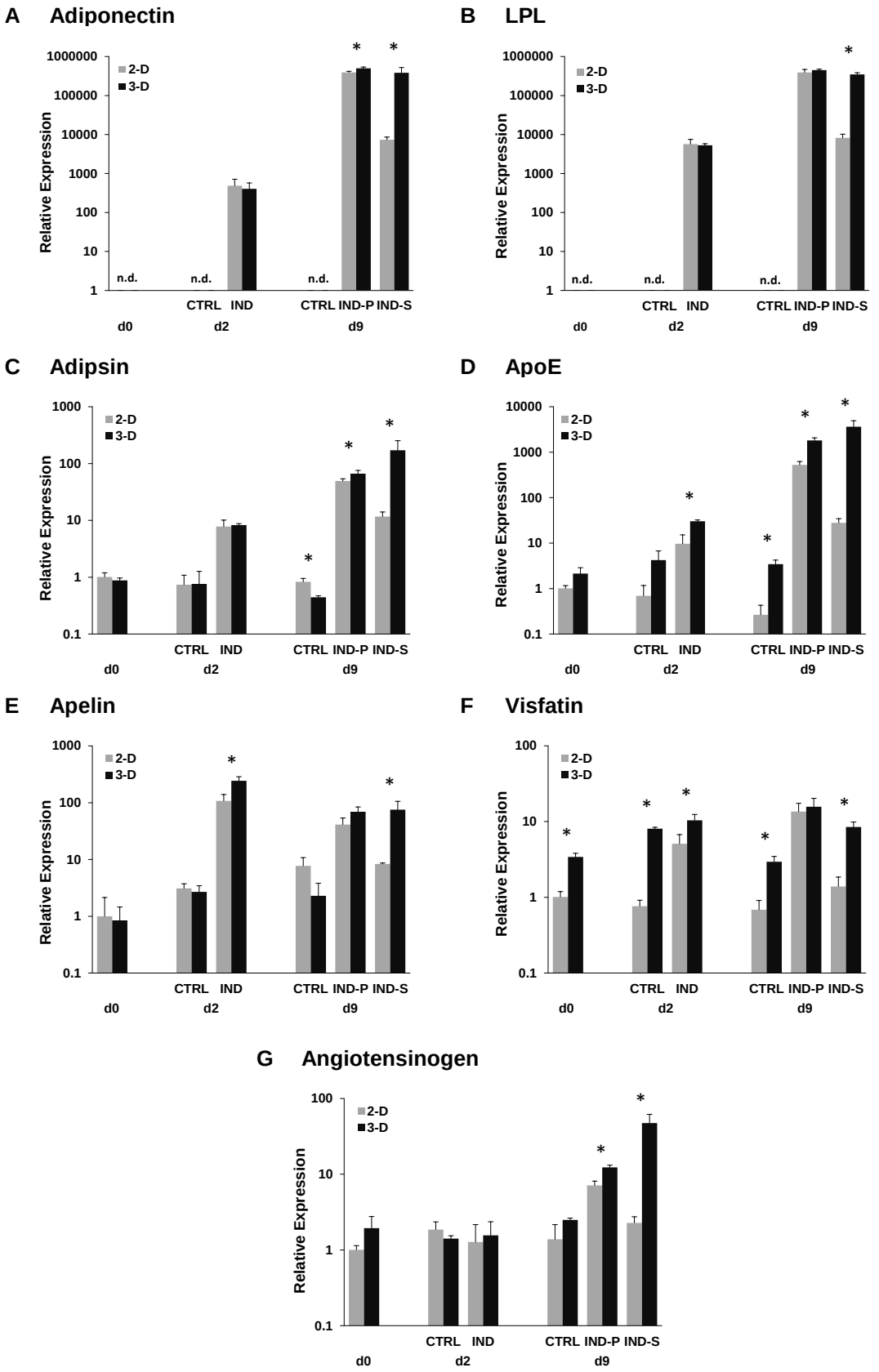

Figure 4-5: *Relative gene expression data (n=3) of the adipokines adiponectin, LPL (lipoprotein lipase), adipsin (complement factor D, CFD), apoE (Apolipoprotein E), apelin, visfatin (=NAMPT) and angiotensinogen as determined by qRT-PCR using TaqMan Low Density Arrays. All mRNA levels are expressed relative to the value at d0 in 2-D culture. Statistically significant differences between 2-D and 3-D cultures are indicated by * (p<0.05).*

Several biologically active substances secreted by adipocytes, known as adipokines [3,24–27], were also included in our Low Density Array. Adiponectin and LPL could not be detected at all on day 0 and in all control groups. When adipogenic induction was performed, these genes were upregulated on day 2 and even more on day 9 (Fig. 4-5 A,B). For both genes, mRNA levels on day 9 showed large differences between the culture systems only when IND-S was used. Again, expression in 2-D, but not in 3-D, was strongly reduced under these conditions, although still significantly higher than in the control groups, where no expression of these genes was detectable. Expression of adipsin, apoE, apelin, visfatin and angiotensinogen also was much higher in 3-D than in 2-D cultures on day 9 when IND-S was applied (Fig. 4-5 C-G). For apoE and apelin, a significantly higher expression in 3-D was already detectable on day 2. For visfatin, LDA data revealed a higher gene expression in 3-D cultures also in the control groups and on d0 (Fig. 4-5 F). Nevertheless, by day 9 mRNA values reached the same level in both culture systems when IND-P was applied. With IND-S however, expression in 2-D, but not in 3-D, was again much lower.

4.4.3 Induction without IBMX or indomethacin: Effect on adipogenesis in 2-D and 3-D cultures

To investigate the influences of a reduced hormonal induction in 2-D and 3-D cultures, we not only utilized alternative induction protocols involving short-term induction, as described above, but also evaluated the effects of modified cocktail compositions providing a reduced stimulus. In preliminary experiments, 2-D and 3-D cultures were exposed to induction cocktails containing only 3 of the 4 components of the standard mixture over a period of 14 days. Interestingly, when dexamethasone was omitted from the induction medium, neither in 2-D nor in 3-D cultures any lipid accumulation occurred. In contrast, after induction without insulin substantial development of lipid droplets could be observed in both culture systems (data not shown). However, when the ASC were induced without IBMX or without indomethacin, the response was different for 2-D and 3-D cultures, respectively. Therefore, these two groups were analyzed more closely.

After induction without IBMX and also without indomethacin, histological staining with Oil Red O at day 14 revealed only minimal lipid inclusions in 2-D cultures (Fig. 4-6 A). Only very few cells appeared to have accumulated triglycerides at all. However, in spheroid cultures treated in the same way numerous lipid droplets could be detected; here, ORO-positive cells seemed to be present mainly in the outer regions of the constructs, becoming fewer towards the center.

Determination of triglyceride contents supported those observations. For both groups, i.e. induction without IBMX or without indomethacin, TG levels on day 14 were significantly higher in 3-D than in 2-D (Fig 4-6 B).

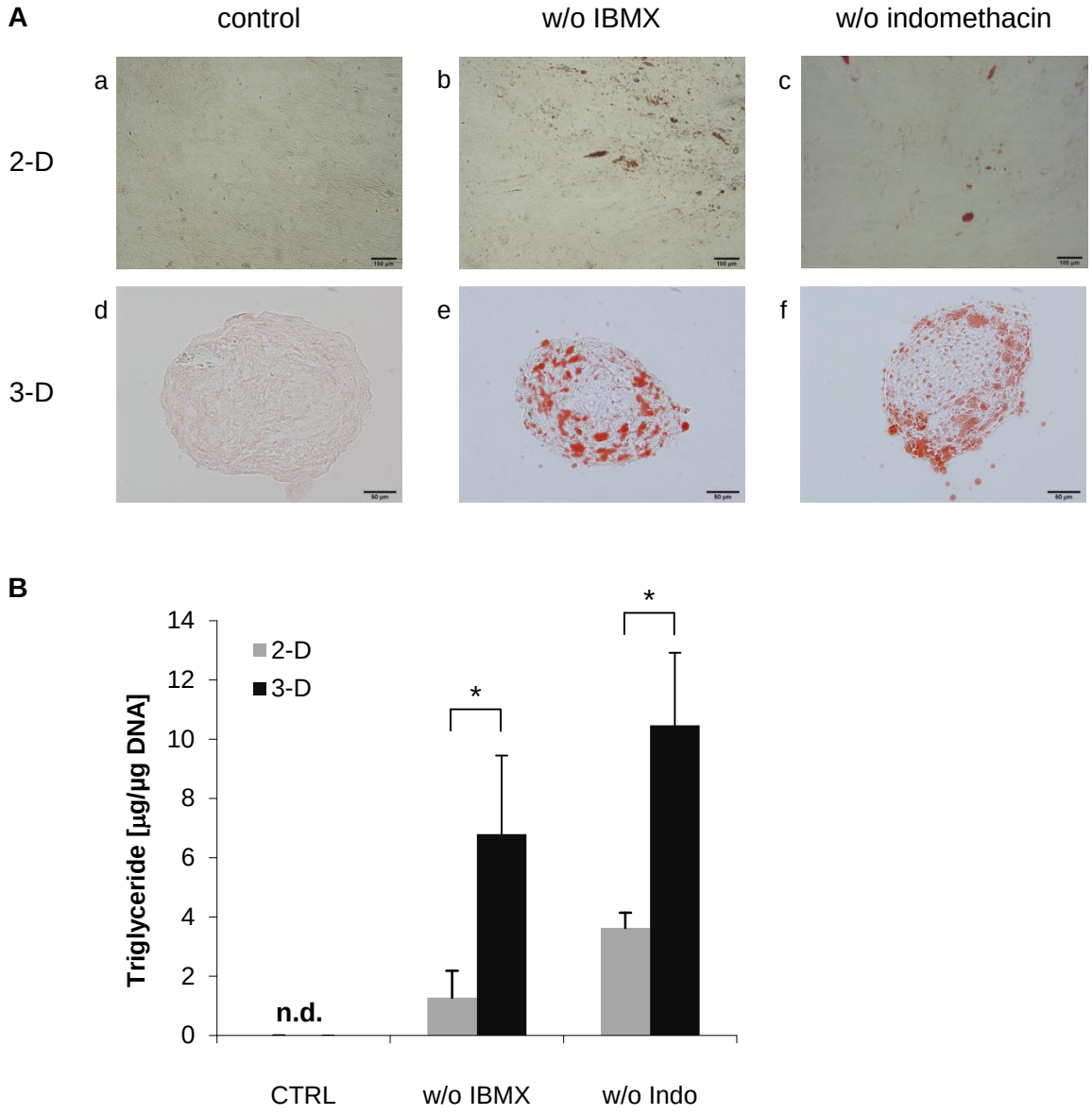

Figure 4-6: A) *Histological analysis of the triglyceride (TG) accumulation in 2-D and 3-D hASC cultures at day 14 after treatment with induction medium, either without IBMX (middle) or without indomethacin (right). Uninduced controls are shown on the left. 2-D cultures: stained with ORO to visualize triglycerides (a-c). Scale bars are 100 µm. 3-D cultures: cryosections (from central regions of the constructs) stained with ORO (d-f). Scale bars are 50 µm.* ***B)*** *Quantification of intracellular TG accumulation on day 14 (n=3). TG contents were normalized to DNA contents. 2 independent experiments were performed; representative results from one experiment are shown here. Statistically significant differences between 2-D and 3-D cultures are indicated by * ($p<0.05$).*

qRT-PCR was performed at days 0, 2 and 9 to investigate how the mRNA expression of four important adipogenesis-related genes was regulated under these conditions. Expression of the transcription factors PPARγ and C/EBPα was clearly elevated in 3-D cultures at days 2

and 9 for both cocktail mixtures (w/o IBMX and w/o indomethacin) as compared to 2-D (Fig. 4-7 A,B). When cells were cultured without IBMX in 2-D, expression levels more or less remained at the level of uninduced controls, whereas in 3-D they were strongly upregulated. Interestingly, when indomethacin was omitted, also in 2-D PPARγ and C/EBPα expression was somewhat higher than in controls by day 2, but mRNA levels did not increase further until day 9, as it was the case for the 3-D cultures, leading to even larger differences between the culture systems at the later time point. The adipocyte marker GLUT4 was initially upregulated in 2-D and 3-D when cells were cultivated without indomethacin, but only in 3-D expression a further increase up to day 9 could be observed (Fig. 4-7 C). For cultures not receiving IBMX, large differences in GLUT4 expression were already detectable on day 2, which had become even more prominent at day 9. aP2, another important adipocyte marker, also was expressed to a much higher level in spheroid cultures than in 2-D cultures by day 9, when either IBMX- or indomethacin-free induction was performed (Fig. 4-7 D).

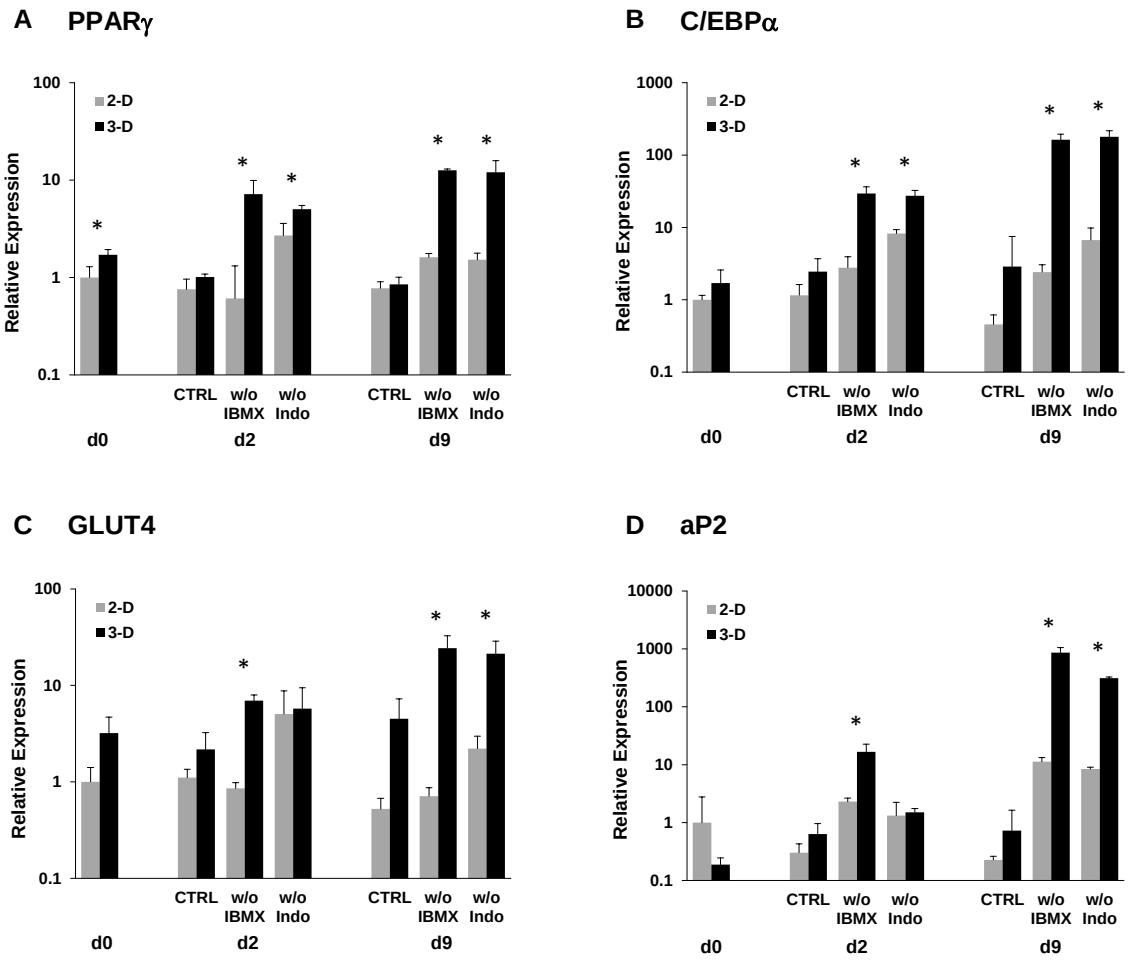

Figure 4-7: *Relative gene expression data (n=3) of PPARγ, C/EBPα, GLUT4 and aP2 as determined by qRT-PCR. All mRNA levels are expressed relative to the value at d0 in 2-D culture. Statistically significant differences between 2-D and 3-D cultures are indicated by * (p<0.05).*

4.5 Discussion

It is increasingly acknowledged that tissue-inherent factors like cell-cell interactions or the influence of the extracellular matrix (ECM) can strongly affect the biology of various cell types. However, these and other typical aspects of a 3-D microenvironment are barely present in conventional 2-D *in vitro* culture models [16,28,29]. Recently, multicellular spheroids, originally applied mainly as tumor models, have become popular as a more *in-vivo*-like model system also for primary or progenitor cells [30].

In this study, we applied our previously established spheroid model of human ASC to investigate adipogenic differentiation in a 3-dimensional (3-D) environment in comparison to conventional 2-D culture. This model system offers defined and reproducible conditions for ASC culture and adipocyte conversion in a 3-D environment (chapter 3). In contrast to most scaffold or gel-based approaches, our spheroid model allows direct cell-cell contacts shortly after seeding and, due to small construct sizes, provides sufficient nutrient and oxygen supply also in central areas of the agglomerates. Moreover, the possible influence of carrier materials on cell functions is also eliminated.

In some studies, similar spheroid cultures of human mesenchymal stem cells (hMSC) were compared to 2-D monolayers with respect to their influence on endothelial cells [31], their anti-inflammatory properties [32] or their therapeutic potential in ischemic disease [33]. However, to our knowledge this is the first time that the process of adipogenesis and its dependence on culture conditions are characterized in 3-D spheroid cultures as well as 2-D monolayers on a functional and molecular level.

Many common protocols for adipogenic differentiation of hASC include the application of a hormonal induction cocktail consisting of the 4 components dexamethasone, 3-isobutyl-methylxanthine (IBMX), insulin and indomethacin [17–21]. Here, in both 2-D and 3-D culture, we used two different induction protocols for the adipogenic differentiation: With permanent induction (IND-P), the 4 inducers remained in the medium over the whole culture period, whereas with short-term (IND-S) induction, the hormonal cocktail was removed at day 2, and was replaced by insulin only for the rest of the culture time. In a previous study employing 2-D culture only, protocols similar to IND-S led to only minimal differentiation efficiency in 2-D culture [19].

Our results supported these observations: For hASC cultured as 2-D monolayers, only with IND-P extensive lipid accumulation could be detected after 14 days, as assessed by histological staining and determination of the triglyceride content. Using IND-S, TG levels were only minimal at the same time point. However, this huge difference with respect to the induction protocol was completely absent in the 3-D spheroid culture, where both IND-S and IND-P led to substantial TG accumulation, which proved to be even higher than the value

reached in 2-D culture with IND-P. Obviously, short-term application of the hormonal cocktail was sufficient for the development of adipocyte morphology in the 3-D environment of the spheroids, but not in conventional monolayers of hASC.

To further investigate this striking difference between 2-D and 3-D models on a molecular level, a gene expression low density array (LDA) was used to determine the expression levels of several adipogenesis-related genes. When IND-P was applied, many genes, including the transcription factors PPARγ, C/EBPα and SREBF1, showed an expression pattern which was, in general, comparable between 2-D and 3-D cultures and typical for adipogenic differentiation as reported in the literature. For example, expression of PPARγ, the master regulator of adipogenesis, which is involved in the regulation of many adipocyte marker genes [2,34,35], had strongly increased by day 9 in both culture systems. With IND-S, however, expression was much lower in monolayers than in spheroids, in which it reached a similar level as under IND-P. A similar mRNA expression could be detected for other central adipogenic transcription factors like C/EBPα, another key player in adipogenesis which is regulated by PPARγ and vice versa [34], and SREBF1. The latter mainly codes for SREBP1-c in fat tissue, which is known to directly or indirectly increase the production of an endogenous ligand for PPARγ [36–38].

Furthermore, many genes associated with fat and glucose metabolism and transport, such as FASN, FATP1, aP2 and GLUT4, which are known to be partially regulated via PPARγ [1] were expressed much higher in 3-D cultures than in 2-D under short-term induction. The low expression level of these genes in monolayer cultures at day 9 may provide an explanation for the observed minimal lipid accumulation under IND-S. In addition, also many adipokines, which are usually produced by developing and mature adipocytes [3,24–27], were upregulated to a much lower degree in 2-D cultures than in 3-D with IND-S, whereas with IND-P expression levels were similar between the two culture systems or differed only slightly. All of these results on mRNA level support the lipid accumulation data in suggesting that under short-term induction, normal adipogenesis involving the differentiation of a large fraction of cells and leading to a typical adipocyte morphology is only possible in the 3-D spheroids, but not in conventional 2-D culture of ASC.

In this context it is noteworthy that under IND-S expression levels of some marker genes, like GLUT4 and aP2, but also adiponectin and LPL were indeed much lower in 2-D than in 3-D at day 9, but nevertheless significantly upregulated as compared to uninduced controls. This was also true for the transcription factors PPARγ and C/EBPα. However, this upregulation obviously did not lead to the ASC adopting adipocyte morphology. This suggests that in these cultures, the adipogenic cascade was not taking place to its full extent, but only partially, so that the expression levels of typical marker genes could not reach the level

necessary for the cells to become functional adipocytes. An upregulation of PPARγ without adipogenic conversion of the cell has, e.g., also been observed in C/EBPβ-deficient preadipocytes, when an exogenous PPARγ ligand was not present [39], as well as in 3T3-L1 preadipocytes, when they were cultured with pyruvate instead of glucose [40].

Gene expression data from day 2 can give further insight into the differentiation process. At that time point, permanent and short-term induction protocols were still identical. Interestingly, mRNA levels of PPARγ and SREBF1 showed a significantly higher expression in spheroid culture already at day 2. This was also the case for C/EBPβ, a transcription factor which is especially important in the early phase of adipogenesis and, together with C/EBPδ, induces the expression of PPARγ and C/EBPα [2,35]. Furthermore, it has been reported that C/EBPβ activates a program, which leads to the synthesis of molecules that can act as activators of PPARγ, conceivably via the activation of SREBP-1 [39]. These findings could possibly explain the higher TG accumulation in 3-D cultures as compared to 2-D by day 14 even when permanent induction was performed, because the higher expression levels of these genes at day 2 may have led to an earlier onset of TG accumulation in 3-D cultures, so that over time more lipids were stored in the differentiating cells.

Without further exogenous stimulation via the hormonal cocktail (under IND-S), in most cases mRNA levels did not show a further increase up to day 9 in 2-D cultures, but rather stayed on the same level as on day 2 or even decreased with time. In 3-D spheroids, however, expression levels further increased from day 2 on, independent of the continual presence of hormonal inducers.

We can conclude from these facts that the 3-dimensional environment of the ASC in spheroid culture is responsible for its differential response to reduced exogenous adipogenic stimulation. This suggests that certain tissue-specific aspects of the 3-D culture provide conditions for the cells that make adipogenic differentiation of ASC possible even in a setup that is not sufficient for normal adipogenesis in conventional 2-D culture.

To further elucidate the tissue-inherent properties causing this behavior, we also used a different approach to reduce the adipogenic stimulus besides a short-term induction protocol. By changing the composition of the hormonal induction cocktail, i.e. omitting specific substances from the mixture, we aimed at getting further insight into the different prerequisites for adipogenic differentiation in 3-D and 2-D cultures.

The glucocorticoid dexamethasone, which has been reported to induce the expression of C/EBPδ in preadipocytes [9,39], proved to be essential for adipogenic induction in both culture systems. In contrast, when IBMX or indomethacin were excluded from the hormonal cocktail, both lipid accumulation and the expression of PPARγ and C/EBPα as well as GLUT4 and aP2, as assessed by qRT-PCR, were significantly higher in spheroids than in

monolayer culture at days 14 and 9, respectively. In fact, in 2-D cultures almost no lipid-containing cells could be detected by day 14, while there was a substantial amount of TG detectable in 3-D. On gene expression level, the trends mentioned above could already be observed at day 2. These results indicate that the adipogenic cascade can be initiated in our spheroid culture without the presence of specific components which are essential for the differentiation of ASC monolayers. Thus, it can be concluded that adipogenesis in 3-D spheroids is less dependent on exogenous stimulation than in 2-D culture, not only regarding the length of the induction period, but also concerning the complete presence or absence of certain factors.

As already mentioned, the treatment with altered induction cocktails can also be a tool to identify possible molecular reasons for the observed 2-D/3-D differences, when the specific functions of the cocktail components within the adipogenic cascade are taken into account. For example, it is commonly acknowledged that indomethacin functions as a PPARγ ligand, similar to thiazolidinediones (TZDs) [41]. The addition of exogenous PPARγ ligands is not necessarily required for the *in vitro* differentiation of 3T3-L1 cultures, suggesting that preadipocytes have acquired the ability to produce an endogenous ligand for PPARγ. However, when preadipocytes were cultured without IBMX, adipogenic differentiation became dependent on the addition of exogenous PPARγ ligands [39]. IBMX is known to increase intracellular cAMP concentrations, which stimulates cAMP-dependent protein kinase pathways. These pathways not only involve the upregulation of C/EBPβ expression [9], but have also been suggested to produce one or more specific endogenous PPARγ ligands [42]. In 3T3-L1 cells, ligand activation of PPARγ is only required transiently during adipogenesis, but not in mature adipocytes [2,42]. Interestingly, although several synthetic PPARγ ligands are known, a natural, high-affinity agonist has not been identified up to now [42,43]. In contrast to preadipocytes, differentiation of ASC has been shown to always require the presence of an exogenous ligand, indicating that the endogenous synthesis of PPARγ ligand(s) is insufficient to trigger adipogenesis [44].

This corresponds to our results with ASC 2-D cultures, where adipogenesis was also strongly impaired when indomethacin was omitted from the induction cocktail. Furthermore, in our study, the addition of indomethacin without stimulating the endogenous ligand production via IBMX also proved to be insufficient to induce adipocyte conversion. In 3-D spheroid cultures, however, adipogenesis was still possible when either of these two factors was omitted, thus resembling the behavior previously associated with preadipocytes, as described above. These results suggest that in the 3-D environment, upregulation of PPARγ and, in turn, the start of the adipogenic program, requires less stimulation by either exogenous agonists (like indomethacin) or endogenous ligands produced via the IBMX-induced pathway involving

C/EBPβ. This implies that in the spheroid model, (a) endogenous PPARγ ligands are produced also through different pathways not involving IBMX, (b) lower concentrations of these ligands are required to effectively upregulate PPARγ expression, or (c) local concentrations of these factors are higher than in 2-D cultures as a result of the compact, tissue-like structure of the spheroids.

4.6 Conclusion

In summary, this study revealed that the requirements for the induction of adipogenic differentiation of hASC vary greatly depending on the culture dimensionality. Our human ASC spheroid model, which was established previously (chapter 3), was applied to characterize adipogenesis in a scaffold-free 3-D environment on a functional and molecular level, especially in comparison to conventional 2-D culture. The application of a short-term induction protocol limiting the exposure time of the cells to the complete hormonal cocktail, as well as the use of induction media without IBMX or indomethacin, were sufficient for the development of functional adipocytes in 3-D spheroids, but not in 2-D monolayers. In strong contrast to the latter, the spheroids induced with these protocols, which provide reduced exogenous stimulation, were comparable to those differentiated under standard conditions. Taken together, our results demonstrated that in 3-D ASC spheroids, adipogenesis proved to be less dependent on exogenous stimulation than in conventional 2-D culture.

Beyond its contribution to a better understanding of adipogenic differentiation, the outcome of this study also has some relevance for applications in regenerative medicine. For their use in tissue engineering, spheroid cultures can be embedded into hydrogels as carrier materials with the goal of a subsequent implantation or injection [45,46]. Moreover, they can also be transplanted directly [47], or used as building blocks for engineering larger tissues using the organ printing technique [48]. As several studies have demonstrated, for the generation of functional adipose tissue an *in vitro* precultivation period including adipogenic induction leads to better adipose tissue development *in vivo* after implantation [22,23]. Our results show that in ASC spheroids the treatment with a hormonal cocktail for only 2 days is sufficient for a sustainable induction of the adipogenic cascade. As in clinical practice a short precultivation time span is of advantage, spheroid-based culture of hASC in combination with a short-term induction protocol could serve as a fast, flexible and reproducible method for the generation of engineered adipose tissue.

Furthermore, this study may also have implications for the cocultivation of ASC with other cell types (chapters 5&6). As the generation of a functional vasculature is an important aspect in the engineering of almost all tissue types [49], especially for those as highly

vascularized as fat [50,51], the development of coculture models of adipocytes with endothelial cells (EC) is highly desirable. Such models could also contribute to shedding further light on the close interplay between adipogenesis and angiogenesis, particularly in a 3-D environment [52,53]. Direct cocultures of adipocyte precursor cells with EC, in which adipogenesis can be induced, are difficult to establish not only due to the different requirements for media and supplements in general, but also because of concerns that specific components of the hormonal adipogenic cocktail like IBMX could impair EC proliferation [54]. Our work has not only demonstrated that for 3-D spheroid cocultures the exposure time of the EC to the induction cocktail may be kept short without affecting adipogenesis, but also that certain components could be omitted from the cocktail at all.

In conclusion, these first results demonstrate that our spheroid model not only represents a powerful tool to investigate adipose tissue development and functions in a 3-D context, but can also serve as a starting point to establish a 3-D coculture model combining ASC with, for example, endothelial cells. Moreover, it has the potential to be used for applications in tissue engineering aiming at the regeneration of soft tissue defects.

4.7 References

1. Tong Q, Hotamisligil G S. Molecular mechanisms of adipocyte differentiation. *Rev Endocr Metab Disord* 2001; **2***, 4*, 349–355.
2. Rosen E D, MacDougald O A. Adipocyte differentiation from the inside out. *Nat Rev Mol Cell Biol* 2006; **7***, 12*, 885–896.
3. Fruhbeck G. Overview of adipose tissue and its role in obesity and metabolic disorders. *Methods Mol Biol* 2008, vol. 456, 1–22.
4. Maury E, Brichard S M. Adipokine dysregulation, adipose tissue inflammation and metabolic syndrome. *Mol Cell Endocrinol* 2010; **314***, 1*, 1–16.
5. Nawrocki A R, Scherer P E. Keynote review: The adipocyte as a drug discovery target. *Drug Discovery Today* 2005; **10***, 18*, 1219–1230.
6. Klein J, Perwitz N, Kraus D, Fasshauer M. Adipose tissue as source and target for novel therapies. *Trends in Endocrinology and Metabolism* 2006; **17***, 1*, 26–32.
7. Gregoire F M, Smas C M, Sul H S. Understanding adipocyte differentiation. *Physiol Rev* 1998; **78***, 3*, 783–809.
8. Rosen E D, Spiegelman B M. Molecular regulation of adipogenesis. *Annu Rev Cell Dev Biol (Annual review of cell and developmental biology)* 2000; **16**, 145–171.
9. Avram M M, Avram A S, James W D. Subcutaneous fat in normal and diseased states: 3. Adipogenesis: From stem cell to fat cell. *J Am Acad Dermatol* 2007; **56***, 3*, 472–492.
10. Darlington G J, Ross S E, MacDougald O A. The role of C/EBP genes in adipocyte differentiation. *J Biol Chem* 1998; **273***, 46*, 30057–30060.
11. Siersbaek R, Nielsen R, Mandrup S. PPARgamma in adipocyte differentiation and metabolism--novel insights from genome-wide studies. *FEBS Lett* 2010; **584***, 15*, 3242–3249.
12. Abbott A. Cell culture: biology's new dimension. *Nature* 2003; **424***, 6951*, 870–872.
13. Boudreau N, Weaver V. Forcing the third dimension. *Cell* 2006; **125***, 3*, 429–431.
14. Cukierman E, Pankov R, Stevens D R, Yamada K M. Taking cell-matrix adhesions to the third dimension. *Science* 2001; **294***, 5547*, 1708–1712.
15. Chun T H, Hotary K B, Sabeh F, Saltiel A R, Allen E D, Weiss S J. A pericellular collagenase directs the 3-dimensional development of white adipose tissue. *Cell* 2006; **125***, 3*, 577–591.
16. Pedersen J A, Swartz M A. Mechanobiology in the third dimension. *Ann Biomed Eng* 2005; **33***, 11*, 1469–1490.
17. Jing K, Heo J Y, Song K S, Seo K S, Park J H, Kim J S, Jung Y J, Jo D Y, Kweon G R, Yoon W H, Hwang B D, Lim K, Park J I. Expression regulation and function of Pref-1 during adipogenesis of human mesenchymal stem cells (MSCs). *Biochim Biophys Acta* 2009; **1791***, 8*, 816–826.
18. Kakudo N, Shimotsuma A, Kusumoto K. Fibroblast growth factor-2 stimulates adipogenic differentiation of human adipose-derived stem cells. *Biochem Biophys Res Commun* 2007; **359***, 2*, 239–244.
19. Janderova L, McNeil M, Murrell A N, Mynatt R L, Smith S R. Human mesenchymal stem cells as an in vitro model for human adipogenesis. *Obesity* 2003; **11***, 1*, 65–74.

20. Xiang Y, Zheng Q, Jia B B, Huang G P, Xu Y L, Wang J F, Pan Z J. Ex vivo expansion and pluripotential differentiation of cryopreserved human bone marrow mesenchymal stem cells. *J Zhejiang Univ Sci B* 2007; **8***, 2*, 136–146.

21. Li W, Vogel C F, Fujiyoshi P, Matsumura F. Development of a human adipocyte model derived from human mesenchymal stem cells (hMSC) as a tool for toxicological studies on the action of TCDD. *Biol Chem* 2008; **389***, 2*, 169–177.

22. Weiser B, Prantl L, Schubert T EO, Zellner J, Fischbach-Teschl C, Spruss T, Seitz A K, Tessmar J, Goepferich A, Blunk T. In vivo development and long-term survival of engineered adipose tissue depend on in vitro precultivation strategy. *Tissue Eng Part A* 2008; **14***, 2*, 275–284.

23. Bauer-Kreisel P, Goepferich A, Blunk T. Cell-delivery therapeutics for adipose tissue regeneration. *Adv Drug Deliv Rev* 2010; **62***, 7-8*, 798–813.

24. Gimeno R E, Klaman L D. Adipose tissue as an active endocrine organ: recent advances. Cardiovascular and renal. *Current Opinion in Pharmacology* 2005; **5***, 2*, 122–128.

25. Halberg N, Wernstedt-Asterholm I, Scherer P E. The adipocyte as an endocrine cell. *Endocrinol Metab Clin North Am* 2008; **37***, 3*, 753-68, x-xi.

26. Lago F, Gómez R, Gómez-Reino J J, Dieguez C, Gualillo O. Adipokines as novel modulators of lipid metabolism. *Trends Biochem Sci* 2009; **34***, 10*, 500–510.

27. Wang P, Mariman E, Renes J, Keijer J. The secretory function of adipocytes in the physiology of white adipose tissue. *J Cell Physiol* 2008; **216***, 1*, 3–13.

28. Yamada K M, Cukierman E. Modeling tissue morphogenesis and cancer in 3D. *Cell* 2007; **130***, 4*, 601–610.

29. Mazzoleni G, Di Lorenzo D, Steimberg N. Modelling tissues in 3D: the next future of pharmaco-toxicology and food research? *Genes Nutr* 2009; **4***, 1*, 13–22.

30. Lin R Z, Chang H Y. Recent advances in three-dimensional multicellular spheroid culture for biomedical research. *Biotechnol J* 2008; **3***, 9-10*, 1172–1184.

31. Potapova I A, Gaudette G R, Brink P R, Robinson R B, Rosen, Cohen I S, Doronin S V. Mesenchymal stem cells support migration, extracellular matrix invasion, proliferation, and survival of endothelial cells in vitro. *Stem Cells* 2007; **25***, 7*, 1761–1768.

32. Bartosh T J, Ylostalo J H, Mohammadipoor A, Bazhanov N, Coble K, Claypool K, Lee R H, Choi H, Prockop D J. Aggregation of human mesenchymal stromal cells (MSCs) into 3D spheroids enhances their antiinflammatory properties. *Proc Natl Acad Sci U S A* 2010; **107***, 31*, 13724–13729.

33. Bhang S H, Cho S W, La W G, Lee T J, Yang H S, Sun A Y, Baek S H, Rhie J W, Kim B S. Angiogenesis in ischemic tissue produced by spheroid grafting of human adipose-derived stromal cells. *Biomaterials* 2011; **32***, 11*, 2734–2747.

34. Feve B. Adipogenesis: cellular and molecular aspects. *Best Pract Res Clin Endocrinol Metab* 2005; **19***, 4*, 483–499.

35. Farmer S R. Transcriptional control of adipocyte formation. *Cell Metab* 2006; **4***, 4*, 263–273.

36. Kim J B, Spiegelman B M. ADD1/SREBP1 promotes adipocyte differentiation and gene expression linked to fatty acid metabolism. *Genes Dev* 1996; **10***, 9*, 1096–1107.

37. Kim J B, Sarraf P, Wright M, Yao K M, Mueller E, Solanes G, Lowell B B, Spiegelman B M. Nutritional and insulin regulation of fatty acid synthetase and leptin gene expression through ADD1/SREBP1. *J Clin Invest* 1998; **101***, 1*, 1–9.

38. Farmer S R. Regulation of PPAR[gamma] activity during adipogenesis. *Int J Obes Relat Metab Disord* 2005; **29***, S1*, S13-S16.

39. Hamm J K, Park B H, Farmer S R. A role for C/EBPbeta in regulating peroxisome proliferator-activated receptor gamma activity during adipogenesis in 3T3-L1 preadipocytes. *J Biol Chem* 2001; **276***, 21*, 18464–18471.

40. Temple K A, Basko X, Allison M B, Brady M J. Uncoupling of 3T3-L1 gene expression from lipid accumulation during adipogenesis. *FEBS Lett* 2007; **581***, 3*, 469–474.

41. Lehmann J M, Lenhard J M, Oliver B B, Ringold G M, Kliewer S A. Peroxisome proliferator-activated receptors alpha and gamma are activated by indomethacin and other non-steroidal anti-inflammatory drugs. *J Biol Chem* 1997; **272***, 6*, 3406–3410.

42. Tzameli I, Fang H, Ollero M, Shi H, Hamm J K, Kievit P, Hollenberg A N, Flier J S. Regulated production of a peroxisome proliferator-activated receptor-gamma ligand during an early phase of adipocyte differentiation in 3T3-L1 adipocytes. *J Biol Chem* 2004; **279***, 34*, 36093–36102.

43. Samarasinghe S P, Sutanto M M, Am Danos, Johnson D N, Brady M J, Cohen R N. Altering PPARgamma ligand selectivity impairs adipogenesis by thiazolidinediones but not hormonal inducers. *Obesity (Silver Spring)* 2009; **17***, 5*, 965–972.

44. Rodriguez A M, Elabd C, Delteil F, Astier J, Vernochet C, Saint-Marc P, Guesnet J, Guezennec A, Amri E Z, Dani C, Ailhaud G. Adipocyte differentiation of multipotent cells established from human adipose tissue. *Biochem Biophys Res Commun* 2004; **315***, 2*, 255–263.

45. Laib A M, Bartol A, Alajati A, Korff T, Weber H, Augustin H G. Spheroid-based human endothelial cell microvessel formation in vivo. *Nat Protoc* 2009; **4***, 8*, 1202–1215.

46. Verseijden F, Posthumus-van S SJ, Farrell E, van Neck J W, Hovius S E, Hofer S O, van Osch G J. Prevascular structures promote vascularization in engineered human adipose tissue constructs upon implantation. *Cell Transplant* 2010; **19***, 8*, 1007–1020.

47. Ota K, Saito S, Hamasaki K, Tanaka N, Orita K. Transplantation of xenogeneic hepatocytes: three-dimensionally cultured hepatocyte (spheroid) transplantation into the spleen. *Transplant Proc* 1996; **28***, 3*, 1430–1432.

48. Mironov V, Visconti R P, Kasyanov V, Forgacs G, Drake C J, Markwald R R. Organ printing: tissue spheroids as building blocks. *Biomaterials* 2009; **30***, 12*, 2164–2174.

49. Kaully T, Kaufman-Francis K, Lesman A, Levenberg S. Vascularization--the conduit to viable engineered tissues. *Tissue Eng Part B Rev* 2009; **15***, 2*, 159–169.

50. Christiaens V, Lijnen H R. Angiogenesis and development of adipose tissue. Molecular and cellular aspects of adipocyte development and function. *Mol Cell Endocrinol* 2010; **318***, 1-2*, 2–9.

51. Hausman G J, Richardson R L. Adipose tissue angiogenesis. *J Anim Sci* 2004; **82***, 3*, 925–934.

52. Nishimura S, Manabe I, Nagasaki M, Hosoya Y, Yamashita H, Fujita H, Ohsugi M, Tobe K, Kadowaki T, Nagai R, Sugiura S. Adipogenesis in obesity requires close interplay between differentiating adipocytes, stromal cells, and blood vessels. *Diabetes* 2007; **56***, 6*, 1517–1526.

53. Neels J G, Thinnes T, Loskutoff D J. Angiogenesis in an in vivo model of adipose tissue development. *FASEB J* 2004; **18***, 9*, 983–985.

54. Kang J H, Gimble J M, Kaplan D L. In vitro 3D model for human vascularized adipose tissue. *Tissue Eng Part A* 2009; **15***, 8*, 2227–2236.

CHAPTER 5

3-D Cocultures of hASC and hMVEC – Establishment of Culture Conditions

5.1 Abstract

Native adipose tissue is not only highly vascularized, but undergoes continuous expansion and regression. It is well known that adipogenesis and angiogenesis are closely associated *in vivo*, with their reciprocal regulation being based on an intensive cellular crosstalk between (pre-)adipocytes and endothelial cells. However, the molecular basis of adipose tissue angiogenesis is still poorly understood. Therefore, our goal was to adapt our previously established ASC monoculture spheroid model for its use as a sustainable *in vitro* coculture system.

As a main challenge, suitable culture conditions for the coculture spheroids had to be established. Since simple mixtures of PGM2 and EGM2 turned out to largely inhibit adipogenic differentiation, protocols including a pre-induction step of the ASC were applied, but could not solve the problem of low lipid accumulation. Subsequently, different media formulations were evaluated and EGF (which is usually included in EGM2) could be identified as the factor responsible for the reduced adipogenesis. Accordingly, elimination of EGF from the culture medium led to strongly improved adipocyte conversion without affecting MVEC proliferation. Components of the adipogenic induction cocktail, however, proved to have a negative effect on MVEC viability. Therefore, it was necessary to keep MVEC exposure to the hormonal cocktail short, which could be accomplished by using a short-term induction protocol. With the newly established conditions, including a PGM2/EGM2 mixture without EGF as a basic medium and a 2-day adipogenic induction period, ASC/MVEC cocultures could successfully be maintained and differentiated towards the adipogenic lineage.

This 3-D spheroid coculture model can serve as a valuable tool for characterizing the cellular interactions of developing adipocytes and endothelial cells in a 3-D system, which can help to gain further insight into the development of vascularized adipose tissue.

5.2 Introduction

Native adipose tissue is highly vascularized, with every adipocyte being associated with at least one capillary [1–3]. During adipose tissue development, adipogenesis and angiogenesis are spatially and temporally tightly associated. The close interaction between (pre-)adipocytes and endothelial cells (the central cell type in angiogenesis) is characterized by cellular crosstalk not only in the embryonic stage, but also in adult organisms, where adipose tissue undergoes continuous expansion and regression [3–5]. The reciprocal regulation of adipogenic differentiation and vascular development has been demonstrated *in vivo* after the implantation of murine preadipocytes [6,7]. In *in vitro* studies it could be shown that ASC and (pre-)adipocytes produce several angiogenic factors like VEGF, HGF or TGF-β or leptin [3,8–10].

However, the molecular basis of adipose tissue angiogenesis is still poorly understood. To gain further knowledge about the interactions between adipose tissue and its vasculature, the development of suitable *in vitro* models is desirable. The insights gathered from such *in vitro* systems can also provide valuable information for applications in tissue engineering, as the development of a functional vasculature is crucial for the generation of larger tissue equivalents and still remains one of the big challenges in regenerative medicine [11].

Up to now, only a few studies focused on the crosstalk between (pre-)adipocytes and endothelial cells in a controlled *in vitro* setting. Several of those have been performed using a 2-D approach, with both cell types cocultured either directly or indirectly via Transwell inserts [12]. Alternatively, conditioned media or culture plates coated with EC matrix were applied [12–14]. However, in these 2-D models many important aspects of the *in vivo* situation are poorly represented, including extensive direct cell-cell contacts and the influence of the extracellular matrix, which are both part of the 3-D microenvironment [15–17].

In some previous 3-D studies 3T3-L1 cells, human preadipocytes, hASC or mature human adipocytes were cocultured with endothelial cells after embedding them in collagen or fibrin gels [18–20] or after seeding them on silk scaffolds [21], all of which still could not provide immediate cell-cell contacts and contained exogenous matrix or scaffold materials with unknown effects. In contrast, a spheroid-based coculture system could serve as a powerful tool to study the interactions between developing adipocytes and endothelial cells in a 3-dimensional system without these drawbacks. Such coculture spheroid systems have already been described for the combination of EC with human osteoblasts or with MSC subsequently induced to undergo osteogenic differentiation [22,23].

The goal of this chapter was to modify our previously established ASC monoculture spheroid model (chapters 3&4) for its use in coculture applications. In this 3-D system, hASC would be combined with human microvascular endothelial cells (hMVEC) to form coculture spheroids

containing both cell types. Within these it should be possible to perform hormonal induction of adipogenesis to generate constructs which resemble native developing adipose tissue. These constructs could then be used to investigate the interdependence of adipogenic differentiation and angiogenesis in an *in vivo*-like system.

One of the main challenges for the development of such a direct coculture model was the establishment of suitable culture conditions. As the different cell types included in the coculture have different requirements, a compromise medium had to be found which provides acceptable conditions for both ASC and MVEC maintenance, a process for which no fixed formulae exist [24]. In our case, it was not only necessary to determine culture conditions suitable to maintain the cells, but also to develop a protocol for the induction of adipogenesis in the ASC without impairing MVEC viability and proliferation. The different steps taken towards the establishment of such a coculture protocol are described in this chapter.

5.3 Materials and Methods

5.3.1 Materials

Human adipose derived stem cells (ASC) were obtained from PromoCell (Heidelberg, Germany; lot 8073006.12); Adult Human Dermal Blood Microvascular Endothelial Cells (MVEC) were purchased from Lonza (Verviers, Belgium; lot 0000122821). Preadipocyte Growth Medium 2 (PGM2, consisting of PBM2, 10% FBS and 1% penicillin/streptomycin solution) and EGM2-MV BulletKit (containing Endothelial Basal Medium 2 [EBM2], 5% FBS, GA-1000 [Gentamicin, Amphotericin-B], hydrocortisone, ascorbic acid, EGF, VEGF, IGF and bFGF) were also from Lonza (Verviers, Belgium). Fetal bovine serum (FBS, lot 40A0044K), penicillin-streptomycin solution, 0.25% trypsin/EDTA solution and phosphate buffered saline (PBS) were from Invitrogen (Darmstadt, Germany). Agarose, indomethacin, dexamethasone, glycerol standard solution, dimethylsulfoxide (DMSO), calf thymus DNA, Oil Red O and osmium tetroxide were purchased from Sigma-Aldrich (Munich, Germany). 3-isobutyl-methylxanthine (IBMX) was bought from Serva (Heidelberg, Germany). Hoechst 33258 dye was obtained from Polysciences (Warrington, PA, USA). Bovine insulin was kindly provided by Sanofi-Aventis (Frankfurt a. M., Germany). All other chemicals were from Merck (Darmstadt, Germany). All cell culture plastics were from Corning (Bodenheim, Germany).

5.3.2 Methods

5.3.2.1 Cell culture

5.3.2.1.1 Expansion of ASC and MVEC

Human adipose-derived stem cells (ASC) were thawed after cryopreservation (passage 3) and seeded in culture flasks. They were expanded in Preadipocyte Growth Medium (PGM2), i.e. Preadipocyte Basal Medium (PBM2) containing 10% FBS, penicillin (100 U/ml) and streptomycin (100 µg/ml). P4 cells were used for all experiments. Microvascular endothelial cells (MVEC) were also thawed after cryopreservation (passage 2) and expanded in culture flasks with complete EGM2-MV medium (referred to as EGM2 in this chapter). All cells were passaged at 90% confluency. Passage 3 or 4 cells were used for all experiments.

5.3.2.1.2 ASC/MVEC cocultures – initial protocol

For 3-D spheroid cocultures, after expansion in culture flasks ASC and MVEC were trypsinized and equal cell numbers of both cell types (750 cells) were seeded into 96-well-plates coated with 1.5% agarose according to the liquid overlay technique. From this time point, the culture medium was composed of 50% PGM2 and 50% EGM2 (50:50 growth

medium). Culture plates were kept on an orbital shaker at 50 rpm during incubation. Adipogenic induction was performed after 2 days by exchanging half of the medium with induction medium (IM), consisting of 50:50 growth medium supplemented with a hormonal cocktail, resulting in final concentrations of 1.7 µM insulin, 1 µM dexamethasone, 200 µM indomethacin and 500 µM 3-isobutyl-1-methylxanthine (IBMX). The time point of induction was always referred to as day 0. Cells were kept in IM over the whole culture period. As spheroids would be lost with complete removal of medium from the wells, all medium changes were performed by replenishing only half of the medium volume. All cultures were incubated at 37°C, 5% CO_2. Medium was exchanged every 3-4 days.

ASC monocultures were performed accordingly, with the total cell numbers per spheroid being equal to the total cell numbers in the cocultures. Culture media were either the same as for the cocultures for comparability, or PGM2 alone when explicitly stated.

For 2-D cocultures, ASC and MVEC were trypsinized and equal numbers of both cell types were seeded into 24-well-plates at a total density of 30.000 cells/cm². Otherwise, culture protocols were identical to those used for the 3-D cultures.

5.3.2.1.3 ASC/MVEC cocultures with "pre-induction" protocols

Using "pre-induction" protocols, ASC were expanded in culture flasks as described above and induced to undergo adipogenesis before the start of the cocultures. For 2-D pre-induction, ASC were treated with induction medium (PGM2 containing the standard hormonal cocktail) for 7 days while still in the culture flasks. Subsequently, they were trypsinized and seeded into agarose-coated 96-well-plates together with an equal amount of MVEC to form spheroids of 3000 cells. From this time point, medium was 50:50 growth medium, and culture conditions for the spheroids were as described in the previous section. In parallel, pre-induced ASC and MVEC were cocultured in 24-well-plates as monolayers, applying the same culture conditions as for the spheroids. For pre-induction in 3-D, at first monoculture spheroids (1500 cells) were generated from ASC. After 2 days adipogenic differentiation was induced with the standard hormonal cocktail in PGM2. On day 6 after induction, an MVEC suspension of 1500 cells per well was added to the pre-induced ASC spheroids. Media and culture protocols were the same as described in the previous section from this time point.

5.3.2.1.4 Evaluation of culture media and EGF effects

To optimize culture media for adipogenic differentiation, at first different media containing varying proportions of EGM2 were applied for ASC monocultures in 2-D and 3-D. Cells were seeded as monolayers or as spheroids using either PGM2 alone, PGM2 with 20% EGM2 or

PGM2 with 50% EGM2. After 2 days, the hormonal induction cocktail was added to all groups up to day 14, when cultures were harvested for histological staining. Media were exchanged every 3-4 days.

In a different experiment, the influence of epidermal growth factor (EGF) on lipid accumulation was assessed. Normally, EGF is included in the complete EGM2. ASC were seeded in 2-D using 50:50 growth medium with or without EGF, PGM2 alone or EGM2 without EGF. Adipogenic induction with the hormonal cocktail was performed 2 days later (referred to as day 0). A Live/Dead assay was performed on day 5, histological staining for lipids on day 14.

5.3.2.1.5 Influence of the hormonal cocktail on the MVEC

The influence of the hormonal induction cocktail (HC) on MVEC viability and proliferation was investigated using 2-D MVEC cultures in 24-well-plates. All cells were cultured in a 50:50 mixture of PGM2 and EGM2 without the addition of EGF. Starting at day 0 (i.e. 2 days after seeding), cells in one group were treated with the HC for 5 days, in another group for 2 days and subsequently with insulin only, and in a third group cells were not exposed to the HC at all. On day 5, cell viability was determined with a Live/Dead assay, and the cell number per well was assessed by measuring the DNA content.

5.3.2.1.6 ASC/MVEC cocultures – final protocol

For 3-D spheroid cocultures, after expansion in culture flasks, ASC and MVEC were trypsinized and equal cell numbers of both cell types (2500 cells) were seeded into 96-well-plates coated with 1.5% agarose according to the liquid overlay technique. From this time point, the culture medium was composed of 50% PGM2 and 50% EGM2. Culture plates were kept on an orbital shaker at 50 rpm during incubation. As spheroids would be lost with complete removal of medium from the wells, all medium changes were performed by replenishing only half of the medium volume. Adipogenic induction was performed after 2 days by exchanging half of the medium with induction medium (IM), consisting of 50:50 growth medium (still without EGF) supplemented with a hormonal cocktail, resulting in final concentrations of 1.7 µM insulin, 1 µM dexamethasone, 200 µM indomethacin and 500 µM 3-isobutyl-1-methylxanthine (IBMX). The time point of induction was referred to as day 0. On day 2 after induction, IM was replaced by 50:50 growth medium (without EGF) containing 1.7 µM insulin only (final concentration). This was done by exchanging half of the medium for three times in order to reduce the concentration of the hormonal inducers. All cultures were incubated at 37°C, 5% CO_2. Medium was exchanged every 3-4 days.

ASC monocultures were performed accordingly, with the total cell numbers per spheroid being equal to the total cell numbers in the cocultures. Culture media were either the same as for the cocultures for comparability, or PGM2 alone when explicitly stated.

5.3.2.2 Lipid staining with Oil Red O or osmium tetroxide

To visualize triglyceride accumulation, cultures were harvested and staining with Oil Red O (ORO) or osmium tetroxide (OsO_4) was performed. For this purpose spheroids were pooled in PBS, transferred to microcentrifuge tubes, washed with PBS, fixed in 10% formalin (1h, 4°C), stained with ORO (3 mg/ml solution in 60% isopropanol) for 4h or with OsO_4 (1% aqueous solution) for 1 h on ice and washed three times with PBS. Stained spheroids were embedded in Tissue-Tek (Hartenstein Laborbedarf, Würzburg, Germany), snap frozen and cut into 10-µm-thick cryosections. After removal of Tissue-Tek by washing in water, the sections were mounted in glycerol. Serial sections were prepared from all spheroids and sections from the center region were used for histological evaluation. For 2-D cultures, staining was performed directly in the 24-well plates. Microscopical bright field images were acquired using a DS-5M camera (Nikon, Düsseldorf, Germany) attached to a Leica DM IRB microscope (Leica Microsystems, Wetzlar, Germany) or an Olympus BX51 microscope with a DP71 camera (Olympus, Hamburg, Germany).

5.3.2.3 Determination of the DNA content

2-D monolayers were washed twice with PBS, harvested in lysis buffer (2 mM EDTA, 2M NaCl, 50 mM Na_3PO_4, pH 7,4) and sonicated. 3-D spheroids were pooled, washed twice with PBS, resuspended in lysis buffer and sonicated as well. DNA content was determined using the intercalating Hoechst 33258 dye (0.1 µg/ml in 0.1 M NaCl, 1 mM EDTA, 10 mM Tris, pH 7.4). Fluorescence intensities were determined at an excitation wavelength of 365 nm and an emission wavelength of 458 nm with a LS 55 fluorescence spectrometer (PerkinElmer, Wiesbaden, Germany) and correlated to DNA contents using standard dilutions of double-stranded DNA (from calf thymus). All measurements were performed in three biological replicates; one replicate was derived from one well for 2-D cultures and an exact number of approximately 10 spheroids for 3-D cultures, respectively.

5.3.2.4 Live/Dead assay

Cell viability in 2-D cultures was assessed with the Live/Dead Cell Staining Kit II (PromoCell, Heidelberg, Germany). Cultures were washed three times with PBS and

incubated with the staining solution (4 µM EthD-III, 2 µM Calcein AM) for 45 min. Live cells showed green calcein fluorescence, dead cells were indicated by red fluorescence of DNA-intercalating EthD-III in the nuclei. The staining was evaluated by imaging with an Olympus IX51 inverted fluorescence microscope with an XC30 camera using CellSens Dimension software (all from Olympus, Hamburg, Germany). Different filters were used for the imaging of calcein and EthD-III fluorescence (ex./em. 460-490 nm/520 nm and ex./em. 510-550 nm/590 nm, respectively).

5.3.2.5 Statistics

Quantitative results are presented as mean value ± standard deviation. Differences between multiple groups were analyzed for significance using one-way analysis of variances (ANOVA) with subsequent multiple comparisons according to Tukey's post-hoc test. A value of $p<0.05$ was regarded statistically significant. Statistical analysis was performed using PASW Statistics 18 software (SPSS Inc., Chicago, IL, USA).

5.4 Results and Discussion*

5.4.1 ASC/MVEC cocultures: spheroid formation and culture medium

When coculturing two or more different cell types, the establishment of suitable culture conditions is a crucial, yet usually time-consuming step [24]. In our case, ASC and MVEC have different requirements with regard to the medium composition, inevitably leading to the utilization of a medium mixture. Endothelial cells usually require the presence of several growth factors, like VEGF, IGF, bFGF and EGF to remain viable and to proliferate, which are included in the commercially available Endothelial Growth Medium 2 (EGM2). As these factors logically also promote ASC proliferation, it cannot be excluded that adipogenic differentiation, which is accompanied by a growth arrest [25–27], may be impaired. On the other hand, the hormonal cocktail usually applied to induce adipogenic differentiation could have negative effects on MVEC viability [21]. However, the relevance of these influences for our specific application was difficult to predict. Therefore, in a first attempt of culturing ASC together with MVEC in the spheroid model, a protocol similar to the standard conditions for ASC monoculture spheroids was utilized, using a 50:50 mixture of PGM2 and EGM2 as culture medium. The components of the adipogenic cocktail were applied in the same concentrations as in ASC monoculture. At the same time, ASC alone were cultured as spheroids in the 50:50 mixture and in PGM2 to evaluate the influence of the medium mixture on adipogenesis in monocultures. Uninduced coculture spheroids were used as controls.

In all cases a single spheroid formed in each well one day after seeding. Volumes of coculture spheroids in an uninduced control group strongly increased over time, indicating a high proliferation rate which can be attributed to the growth factors present in the medium mixture (Fig. 5-1 a). However, in the cocultures treated with the hormonal cocktail a volume increase could not be observed (Fig. 5-1 b). Furthermore, spheroid sizes were smaller than in the corresponding monocultures at day 13 (Fig. 5-1 c). Interestingly, in both mono- and cocultures kept in 50:50 medium, cells contained barely any lipid droplets after 2 weeks of culture, as detected by microscopical observation. In contrast, ASC spheroids in PGM2 showed prominent lipid accumulation without a significant volume increase (Fig. 5-1 d), which was consistent with previous experiments. Also in 2-D cocultures of the two cell types extensive proliferation, but only minimal lipid inclusions could be observed when a 50:50 (PGM2:EGM2) medium mixture was used (data not shown). Obviously, under these conditions ASC in 2-D and 3-D culture kept proliferating despite the presence of the adipogenic cocktail. Since usually a growth arrest occurs after the induction of adipogenesis,

* *As the establishment of suitable culture conditions for the 3-D ASC/MVEC coculture model was a multi-step process, with each experiment being based on the results of the previous one, results and discussion are combined in one section.*

this could be an explanation for the strongly reduced lipid accumulation under the coculture conditions applied here. Most likely the extensive proliferation was caused by one or more of the growth factors included in EGM2, e.g. the epidermal growth factor (EGF) [28,29].

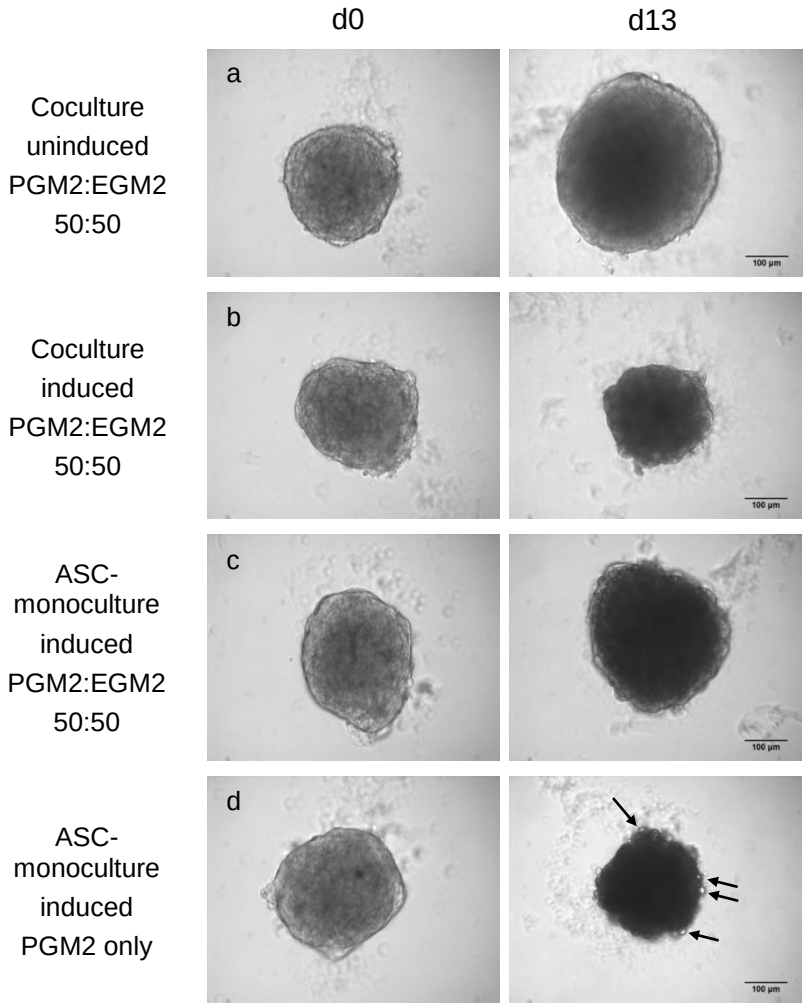

Figure 5-1: *Whole Spheroids (1500 cells) on day 0 (i.e. the day of induction) and day 13. Cocultures of ASC and MVEC, uninduced (a) and induced (b) to undergo adipogenesis. ASC monocultures, induced, in a PGM2/EGM2 mixture (c) and in PGM2 only (d). Lipid droplets are indicated by arrows. Please note that only lipid droplets in the periphery of the spheroids appear on the images, while they could be observed also in the center of the constructs during live microscopy. Scale bars are 100 µm.*

In conclusion, these first experiments suggested that the spheroid model is in principle suitable for the cocultivation of ASC and MVEC in a 3-dimensional environment. However, with the goal of a better understanding of the interdependence of adipogenesis and angiogenesis, the ability to perform adipogenic differentiation within such a coculture system is highly desirable. Therefore, in the next steps of this project the focus was set on optimizing culture protocols in order to make adipogenesis possible to a significant extent under coculture conditions.

5.4.2 Cocultivation using a pre-induction protocol

5.4.2.1 Pre-induction in 2-D

The growth factors contained in the EGM2 can not only stimulate proliferation of the endothelial cells, but also of the ASC [30]. Therefore, the growth arrest, which is required for the initiation of the adipogenic cascade, possibly did not occur in our first experiments, resulting in attenuated adipogenesis.

In an attempt to circumvent this problem without changing media compositions, alternative induction protocols involving an ASC pre-induction step were applied, similar to those described for cocultures on silk scaffolds [21]. Pre-induction means that prior to starting the coculture, ASC monolayers were cultured separately in PGM2 and adipogenesis was induced at confluence. After several days in monoculture, these pre-induced cells were trypsinized and seeded as 3-D spheroids (and additionally as 2-D cultures) together with endothelial cells. The trypsinization step had to be performed before the cells became too fragile as a result of the increasing lipid inclusions. At the start of the cocultures, the hormonal inducers were replaced by insulin only.

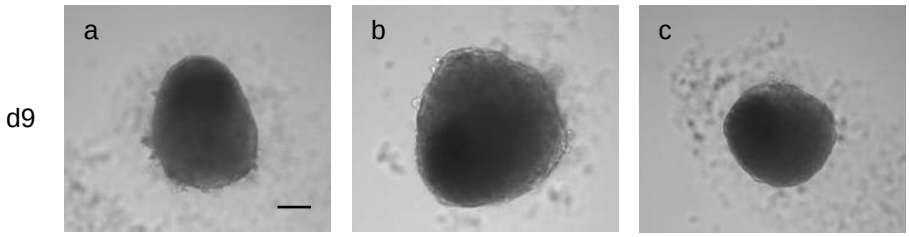

Figure 5-2: *3-D cocultures of ASC and MVEC (a) and ASC monocultures (b,c); 3000 cells per spheroid. Microscopical brightfield images on day 9 after the start of the 3-D culture (i.e. day 16 after induction). Culture media were as indicated. The culture protocol included a 7-day "pre-induction" step in 2-D. Scale bars are 100 µm.*

Microscopical observation revealed that neither the cocultures, nor the ASC monocultures developed significant amounts of lipid droplets 9 days after uniting both cell types (i.e. 16 days after adipogenic induction of the ASC). This was not only true for the spheroid cultures (Fig. 5-2), but also for the 2-D monolayers (not shown). Interestingly, also for the groups receiving PGM2 only, no significant lipid accumulation took place (Fig. 5-2 c). As adipogenesis usually can be readily induced under the latter conditions, we could conclude that the trypsination step necessarily performed after the 2-D pre-induction was the cause for the lack of adipogenic conversion. Thus, the application of a 2-D pre-induction step proved to be unsuitable for achieving a significant lipid accumulation within the cocultures.

5.4.2.2 Pre-induction in 3-D

In order to avoid the additional trypsinization after pre-induction, the culture protocol was again altered. In a new experiment, a pre-induction phase in 3-D was introduced, meaning that in a first step ASC were seeded as spheroids and adipogenesis was induced with the hormonal cocktail in PGM2 alone. After 6 days, an MVEC suspension was added to all pre-induced ASC spheroids in their respective wells, with the culture medium being a PGM2:EGM2 (50:50) mixture including insulin.

When cultures were harvested 14 days after adipogenic induction, i.e. 8 days after starting the coculture, OsO_4-stained cryosections revealed that overall very little fat was accumulated within the constructs (Fig. 5-3 B). Interestingly, only in the central areas of the spheroids a significant amount of lipid droplets could be detected, which can be explained by the fact that the endothelial cells formed a layer around the pre-formed ASC spheroids after their addition. This "two-layer structure" could also be observed by bright field microscopy (Fig. 5-3 A). Furthermore, a strong volume increase under coculture conditions occurred, which apparently could again be related to the presence of the different growth factors within the EGM2 medium.

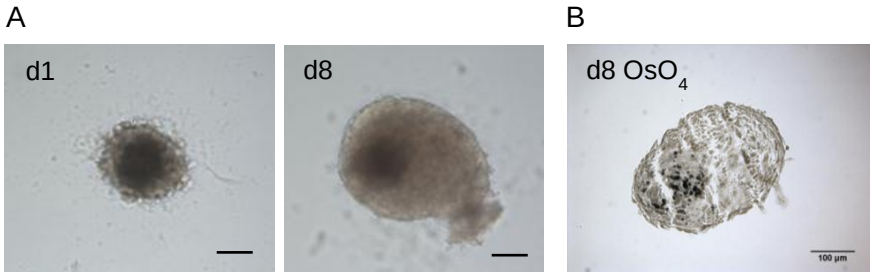

Figure 5-3: *ASC/MVEC coculture spheroids. ASC monocultures were pre-induced for 6 days, followed by the addition of MVEC.* ***A)*** *Bright field images of the spheroids on the days 1 and 8 after starting the coculture.* ***B)*** *Cryosection from day 8, stained for triglycerides with OsO_4. Scale bars are 100 µm each.*

In conclusion, the utilization of a culture protocol including a pre-induction phase was not successful with regard to an improved lipid accumulation in the coculture spheroids, regardless whether it was performed in 2-D with a subsequent trypsination, or directly in ASC spheroids. Therefore, it appeared to be inevitable to alter the media composition in order to find suitable culture conditions for the cocultures.

5.4.3 Optimization of the culture medium – the role of EGF

As the application of a pre-induction step did not lead to the desired results, in a different approach the focus was set on optimizing the medium composition in order to make direct

coculturing possible. As already mentioned, one or more of the growth factors present in EGM2, and therefore also in the coculture media used in the previous experiments, possibly have a negative effect on adipogenic differentiation in our system. As a consequence, reducing the proportion of EGM2 within the medium mixture might increase adipogenesis efficiency. To test this hypothesis, cocultures as well as ASC monocultures were kept in different medium mixtures in the form of either 2-D monolayers or 3-D spheroids. Representative images of the monocultures on day 14 after induction are depicted in Fig. 5-4. When a PGM2:EGM2 mixture with a 50:50-ratio was used, in mono- as well as cocultures (2-D and 3-D) strong proliferation and only minimal lipid accumulation could be detected, which was in accordance with the previous results. A reduction of the EGM2 proportion to 20% led to a comparably higher number of lipid droplets in both culture systems. However, especially in the 2-D cultures it could be observed that under these conditions proliferation was still very high, and cells did not exhibit the typical morphology of developing adipocytes, as they did with PGM2 only. Instead, single cells only contained very few lipid droplets, with the cell density being much higher than in PGM2. Also in 3-D spheroids lipid accumulation was still drastically reduced as compared to PGM2 only.

All in all, changing the EGM2 proportion within the coculture medium did not lead to the desired results regarding adipogenic differentiation. With all culture conditions involving complete EGM2 within the medium, adipogenesis was strongly impaired.

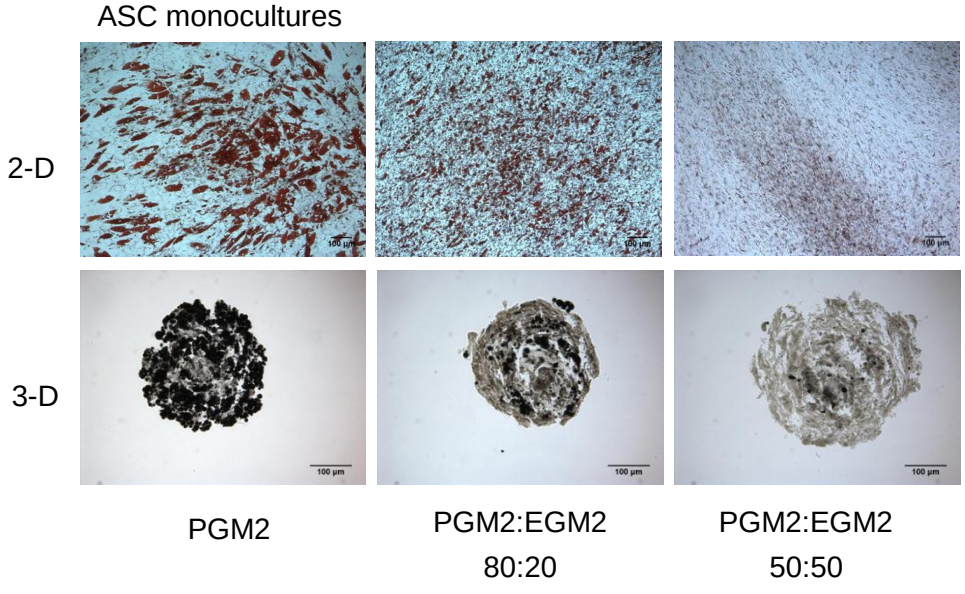

Figure 5-4: *ASC monocultures in 2-D and 3-D on day 14 after induction of adipogenesis. Triglycerides stained with ORO (in 2-D) or with OsO_4 (in 3-D, cryosections), respectively. The culture media were as indicated. Scale bars are 100 µm.*

Therefore, it was necessary to identify the specific component(s) within the EGM2 which were responsible for the inhibition of adipogenesis in order to adjust culture conditions accordingly. Most likely, the epidermal growth factor (EGF) included in the medium was the main cause for the reduced lipid accumulation, as it has been reported in literature that EGF can, dependent on its concentration, inhibit adipogenic differentiation in 3T3-L1 cells [29] and in primary preadipocytes [31] as well as *in vivo* [28].

To verify this hypothesis, in a 2-D experiment ASC were cultured and induced using different media, either with or without the addition of EGF. When a PGM2:EGM2 mixture including EGF was used, ORO staining revealed that the accumulation of triglycerides was again very low (Fig. 5-5 c). In contrast, the elimination of EGF from the medium led to extensive adipogenic conversion (Fig. 5-5 d), with the differentiation rate being similar to PGM2 only (Fig. 5-5 a). Interestingly, when EGM2 alone (not including PGM2) without EGF supplementation was used, adipogenic differentiation was again much lower, and the cells had developed an elongated morphology, which is untypical for maturing adipocytes (Fig. 5-5 b). These results not only indicated that the presence of PGM2 is necessary for adipogenesis, but also proved our hypothesis that EGF was a crucial factor for the inhibition of adipogenic differentiation in ASC. As a consequence, cultivation without EGF was a promising option also for adipogenesis in ASC/MVEC cocultures.

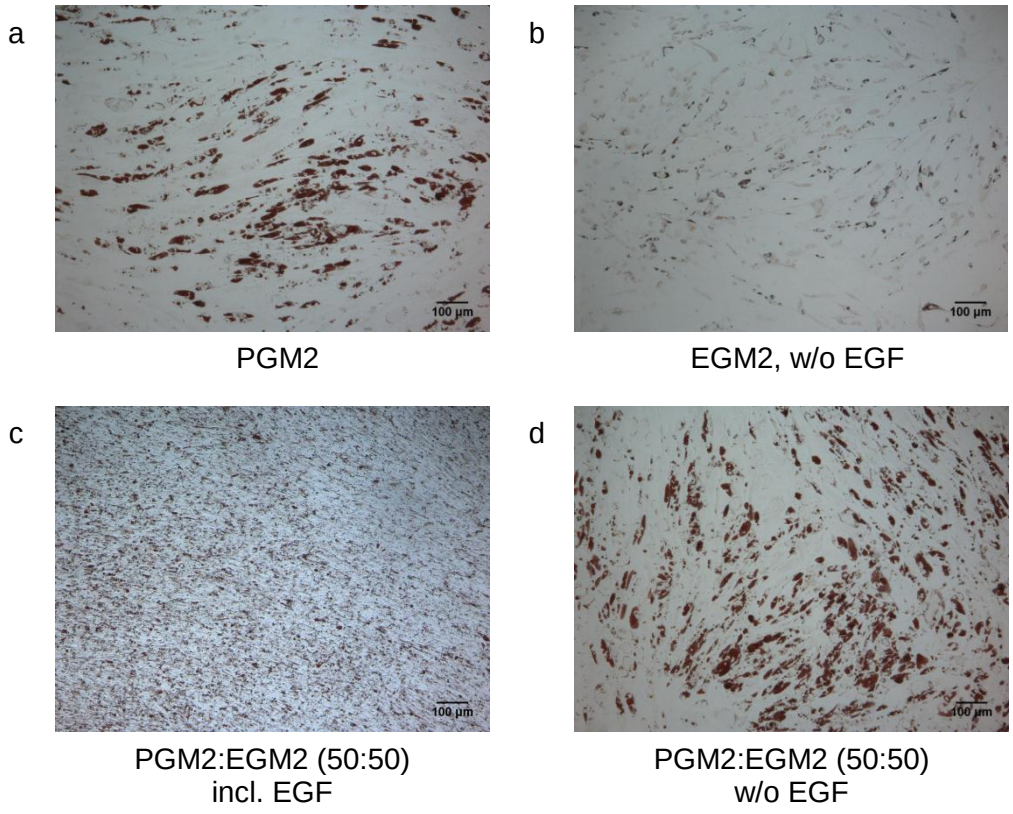

Figure 5-5: *ASC monocultures on day 14 after induction of adipogenesis. Culture media were as indicated. Bright field images after staining with Oil Red O (ORO). Scale bars are 100 µm.*

However, before EGF-free media were actually used for cocultures, we tested if endothelial cell viability and proliferation were impaired under these conditions. When EGM2 alone, yet without EGF, was used, no differences regarding MVEC morphology and viability could be detected in comparison to complete EGM2 (Fig. 5-6 A, a+b). Interestingly, DNA content on day 5 was even higher, indicating an increased proliferation rate (Fig. 5-6 B). With an EGF-free PGM2:EGM2 mixture, cells also remained viable (Fig. 5-6 A, c), and proliferation was comparable to EGM2 (Fig. 5-6 B). Thus, the elimination of EGF from the culture media, as well as the addition of the PGM2 fraction, appeared to have no negative effects on MVEC culture. In conclusion, a medium mixture of PGM2 and EGM2, but without EGF, was chosen as basic medium for the following coculture experiments, as it allowed for adipogenic differentiation of the ASC without damaging the MVEC.

5.4.4 Influence of the hormonal induction cocktail on the MVEC

In order to induce adipogenic differentiation of the ASC within the cocultures, it was necessary to expose the cells to the usual hormonal induction cocktail. However, the effect these inducers could have on the endothelial cells had to be considered, too. It has already been reported for human umbilical vein endothelial cells (HUVEC) that particularly IBMX and thiazolidinediones (which are, like indomethacin, PPARγ agonists) can significantly reduce endothelial cell proliferation and viability [21].

To evaluate the influence of the adipogenic cocktail on the MVEC, they were cultured in 2-D in PGM2/EGM2 medium mixture with or without the addition of hormonal inducers. Strikingly, the addition of the hormonal cocktail (HC) over the whole period of 5 days caused most of the MVEC to detach from the culture plate, with the remaining cells showing a low viability rate (Fig. 5-6 A, d). Accordingly, DNA content on day 5 was strongly reduced (Fig. 5-6 B). However, when the HC was only applied for 2 days, and then replaced by insulin only, no negative effect on the MVEC could be observed on day 5. Cell viability and DNA contents were comparable to the untreated group (Fig 5-6). These results indicated that a 2-day-period of HC supplementation did not significantly impair MVEC viability and proliferation, while irreversible cell damage appeared to result when the inducers stayed on the cultures for a longer time span.

In the first part of this project it had been demonstrated that for our 3-D ASC spheroids a short-term induction period of 2 days was sufficient to induce adipogenesis (Chapter 4). For the cocultivation with MVEC, this represents a great advantage, because exposure time to the HC can be kept short in order to induce ASC differentiation without significantly affecting MVEC viability and proliferation.

In summary, it was determined that optimal culture conditions for ASC/MVEC coculture spheroids include PGM2:EGM2 (50:50) – without the addition of EGF – as a basic medium, as well as the usage of a short-term induction protocol for adipogenic differentiation with an initial HC supplementation period of 2 days.

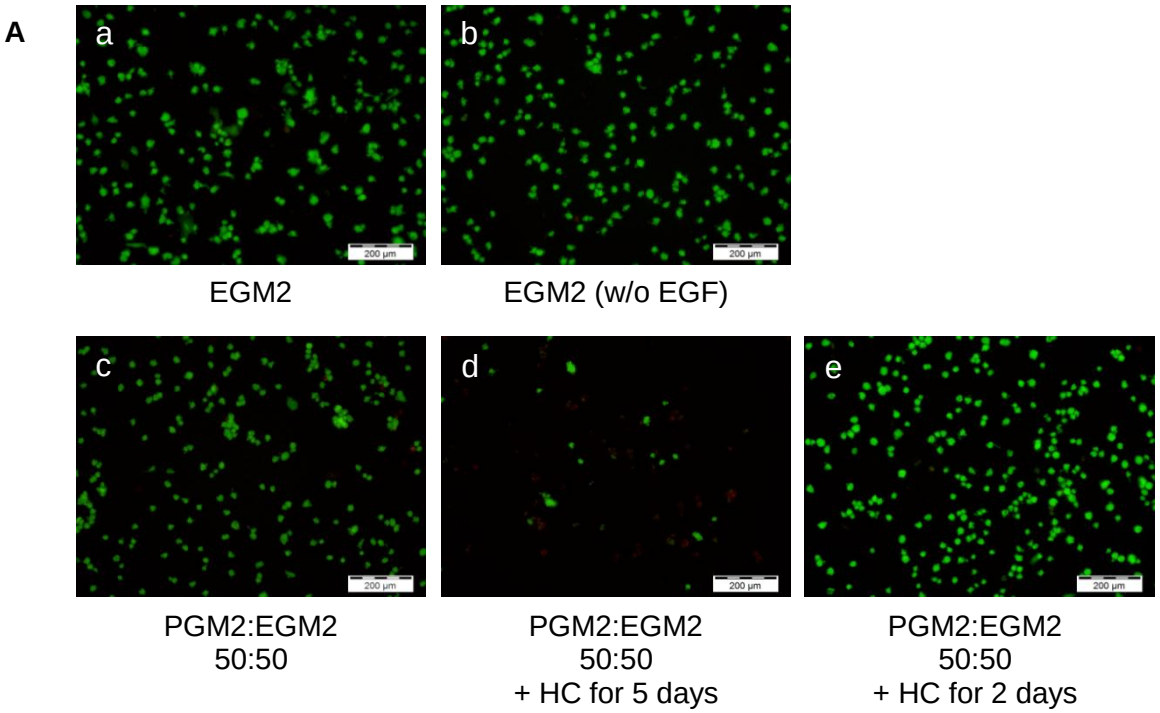

Figure 5-6: *MVEC were seeded in 2-D monolayers using different media as indicated. After 2 days (i.e. on day 0), the hormonal induction cocktail was added to some groups for 2 or 5 days, respectively.* ***A)*** *Live/Dead-staining on day 5. Green calcein fluorescence indicates live cells, red EthD-III fluorescence indicates dead cells. Scale bars are 200 µm.* ***B)*** *Quantification of the DNA content per well on day 5. * indicates statistically significant differences compared with all other groups ($p<0.05$).*

5.4.5 Coculture spheroids: Application of the new culture protocol

Based on the results from the previous sections, the newly established culture conditions were applied to 3-D ASC/MVEC cocultures: 50% ASC and 50% MVEC were seeded into agarose-coated 96-well-plates with PGM2:EGM2 (50:50) to form spheroids and induced with the standard hormonal cocktail for 2 days, followed by supplementation with insulin only. For comparison, ASC monocultures were kept under the same conditions or in PGM2 only.

After a single spheroid had formed in each well, cells in all induced groups began to accumulate lipids, which could be observed via bright field microscopy. After 15 days, histological staining for triglycerides on cryosections revealed that cocultures had developed lipid inclusions in a similar manner to ASC monocultures. For the monocultures lipid accumulation did not appear to be impaired when a PGM2:EGM2 medium mixture, and not PGM2 alone, was used (Fig. 5-7).

These results proved that the culture conditions established previously were indeed suitable for the 3-D cocultivation of ASC and MVEC, as adipogenesis could be successfully induced in the cocultures using the short-term induction protocol.

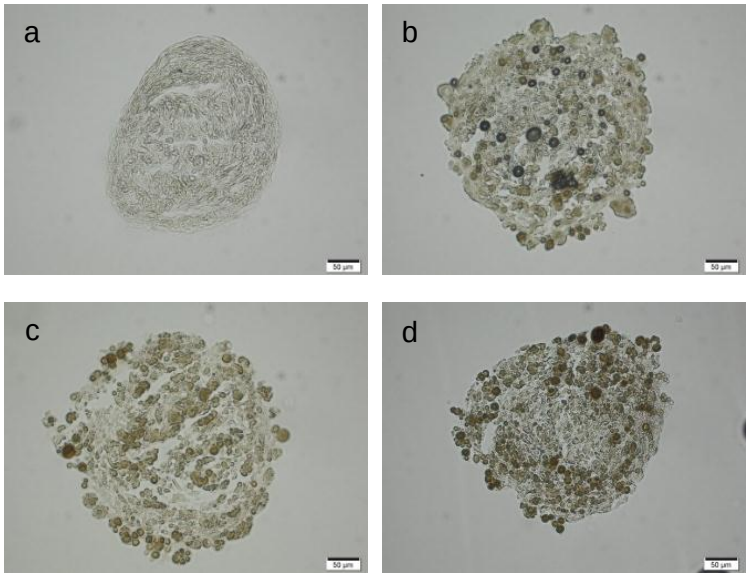

Figure 5-7: *Cryosections of OsO_4-stained spheroids (5000 cells) on day 15 after induction. a) Cocultures uninduced in 50:50 medium b) Cocultures induced in 50:50 medium c) ASC monocultures induced in 50:50 medium d) ASC monocultures induced in PGM2. Scale bars are 50 µm.*

5.5 Conclusion

In a multi-step process, it was possible to develop a culture protocol for the cocultivation of ASC and MVEC in a 3-D spheroid model. A suitable medium formulation was found after eliminating EGF from a 50:50 mixture of PGM2 and EGM2, which had attenuated adipogenic differentiation in the cocultures. As different culture methods involving a pre-induction step failed to produce satisfying results with regard to lipid accumulation, direct coculture using the improved media was determined as an optimal protocol. Furthermore, the application of a short-term induction protocol proved to be ideal, as the exposure time of the MVEC to potentially harmful components of the adipogenic cocktail could be kept short, yet ASC could still undergo adipogenesis.

With the newly developed coculture system, it is possible to investigate the interactions of ASC and MVEC in a more *in-vivo*-like context. Since the ASC can be differentiated towards the adipogenic lineage (and potentially also other lineages), our model system can be applied to further study the reciprocal regulation of adipogenesis and angiogenesis, as it occurs during adipose tissue development. Specifically, a critical point, which will be addressed in the following chapter, is how the presence of endothelial cells affects ASC/preadipocytes on a functional and molecular level in a 3-D microenvironment, for example with regard to lipid accumulation and gene expression. Moreover, our coculture system can potentially be used as the basis for the development of vascularized tissue grafts for applications in regenerative medicine.

5.6 References

1. Crandall D L, Hausman G J, Kral J G. A review of the microcirculation of adipose tissue: anatomic, metabolic, and angiogenic perspectives. *Microcirculation* 1997; **4***, 2*, 211–232.
2. Cao Y. Angiogenesis modulates adipogenesis and obesity. *J Clin Invest* 2007; **117***, 9*, 2362–2368.
3. Christiaens V, Lijnen H R. Angiogenesis and development of adipose tissue. Molecular and cellular aspects of adipocyte development and function. *Mol Cell Endocrinol* 2010; **318***, 1-2*, 2–9.
4. Hausman G J, Richardson R L. Adipose tissue angiogenesis. *J Anim Sci* 2004; **82***, 3*, 925–934.
5. Lijnen H R. Angiogenesis and obesity. *Cardiovasc Res* 2008; **78***, 2*, 286–293.
6. Fukumura D, Ushiyama A, Duda D G, Xu L, Tam J, Krishna V, Chatterjee K, Garkavtsev I, Jain R K. Paracrine regulation of angiogenesis and adipocyte differentiation during in vivo adipogenesis. *Circ Res* 2003; **93***, 9*, e88-97.
7. Neels J G, Thinnes T, Loskutoff D J. Angiogenesis in an in vivo model of adipose tissue development. *FASEB J* 2004; **18***, 9*, 983–985.
8. Lolmede K, Durand d SFV, Galitzky J, Lafontan M, Bouloumie A. Effects of hypoxia on the expression of proangiogenic factors in differentiated 3T3-F442A adipocytes. *Int J Obes Relat Metab Disord* 2003; **27***, 10*, 1187–1195.
9. Rehman J, Traktuev D, Li J, Merfeld-Clauss S, Temm-Grove C J, Bovenkerk J E, Pell C L, Johnstone B H, Considine R V, March K L. Secretion of angiogenic and antiapoptotic factors by human adipose stromal cells. *Circulation* 2004; **109***, 10*, 1292–1298.
10. Kilroy G E, Foster S J, Wu X, Ruiz J, Sherwood S, Heifetz A, Ludlow J W, Stricker D M, Potiny S, Green P, Halvorsen Y D, Cheatham B, Storms R W, Gimble J M. Cytokine profile of human adipose-derived stem cells: expression of angiogenic, hematopoietic, and pro-inflammatory factors. *J Cell Physiol* 2007; **212***, 3*, 702–709.
11. Bauer-Kreisel P, Goepferich A, Blunk T. Cell-delivery therapeutics for adipose tissue regeneration. *Adv Drug Deliv Rev* 2010; **62***, 7-8*, 798–813.
12. Lozito T P, Kuo C K, Taboas J M, Tuan R S. Human mesenchymal stem cells express vascular cell phenotypes upon interaction with endothelial cell matrix. *J Cell Biochem* 2009; **107***, 4*, 714–722.
13. Varzaneh F E, Shillabeer G, Wong K L, Lau D CW. Extracellular matrix components secreted by microvascular endothelial cells stimulate preadipocyte differentiation in vitro. *Metabolism* 1994; **43***, 7*, 906–912.
14. Hutley L J, Herington A C, Shurety W, Cheung C, Vesey D A, Cameron D P, Prins J B. Human adipose tissue endothelial cells promote preadipocyte proliferation. *Am J Physiol Endocrinol Metab* 2001; **281***, 5*, E1037-1044.
15. Griffith L G, Swartz M A. Capturing complex 3D tissue physiology in vitro. *Nat Rev Mol Cell Biol* 2006; **7***, 3*, 211–224.
16. Pampaloni F, Reynaud E G, Stelzer E HK. The third dimension bridges the gap between cell culture and live tissue. *Nat Rev Mol Cell Biol* 2007; **8***, 10*, 839–845.
17. Yamada K M, Cukierman E. Modeling tissue morphogenesis and cancer in 3D. *Cell* 2007; **130***, 4*, 601–610.

18. Aoki S, Toda S, Sakemi T, Sugihara H. Coculture of endothelial cells and mature adipocytes actively promotes immature preadipocyte development in vitro. *Cell Struct Funct* 2003; **28***, 1*, 55–60.

19. Borges J, Müller M C, Momeni A, Stark G B, Torio-Padron N. In vitro analysis of the interactions between preadipocytes and endothelial cells in a 3D fibrin matrix. *Minim Invasive Ther Allied Technol* 2007; **16***, 3*, 141–148.

20. Lai N, Jayaraman A, Lee K. Enhanced proliferation of human umbilical vein endothelial cells and differentiation of 3T3-L1 adipocytes in coculture. *Tissue Eng Part A* 2009; **15***, 5*, 1053–1061.

21. Kang J H, Gimble J M, Kaplan D L. In vitro 3D model for human vascularized adipose tissue. *Tissue Eng Part A* 2009; **15***, 8*, 2227–2236.

22. Stahl A, Wenger A, Weber H, Stark G B, Augustin H G, Finkenzeller G. Bi-directional cell contact-dependent regulation of gene expression between endothelial cells and osteoblasts in a three-dimensional spheroidal coculture model. Calcium Signaling and Disease. *Biochem Biophys Res Commun* 2004; **322***, 2*, 684–692.

23. Rouwkema J, Boer J de, Blitterswijk C A. Endothelial cells assemble into a 3-dimensional prevascular network in a bone tissue engineering construct. *Tissue Eng* 2006; **12***, 9*, 2685–2693.

24. Kirkpatrick C J, Fuchs S, Unger R E. Co-culture systems for vascularization--learning from nature. *Adv Drug Deliv Rev* 2011; **63***, 4-5*, 291–299.

25. Gregoire F M, Smas C M, Sul H S. Understanding adipocyte differentiation. *Physiol Rev* 1998; **78***, 3*, 783–809.

26. Feve B. Adipogenesis: cellular and molecular aspects. *Best Pract Res Clin Endocrinol Metab* 2005; **19***, 4*, 483–499.

27. Avram M M, Avram A S, James W D. Subcutaneous fat in normal and diseased states: 3. Adipogenesis: From stem cell to fat cell. *J Am Acad Dermatol* 2007; **56***, 3*, 472–492.

28. Serrero G, Mills D. Physiological role of epidermal growth factor on adipose tissue development in vivo. *Proc Natl Acad Sci U S A* 1991; **88***, 9*, 3912–3916.

29. Harrington M, Pond-Tor S, Boney C M. Role of epidermal growth factor and ErbB2 receptors in 3T3-L1 adipogenesis. *Obesity* 2007; **15***, 3*, 563–571.

30. Suga H, Shigeura T, Matsumoto D, Inoue K, Kato H, Aoi N, Murase S, Sato K, Gonda K, Koshima I, Yoshimura K. Rapid expansion of human adipose-derived stromal cells preserving multipotency. *Cytotherapy* 2007; **9***, 8*, 738–745.

31. Hauner H, Röhrig K, Petruschke T. Effects of epidermal growth factor (EGF), platelet-derived growth factor (PDGF) and fibroblast growth factor (FGF) on human adipocyte development and function. *Eur J Clin Invest* 1995; **25***, 2*, 90–96.

CHAPTER 6

Characterization of hASC/hMVEC Coculture Spheroids – Structure and Crosstalk

6.1 Abstract

Vascularization of engineered tissue transplants remains one on the biggest challenges in regenerative medicine. A possible strategy to generate prevascularized tissues *in vitro* involves the coculturing of tissue specific cells with endothelial cells in a 3-dimensional culture system. A coculture model of human adipose tissue using spheroids composed of adipose-derived stem cells (ASC) and microvascular endothelial cells (MVEC) was established previously in this project. In this chapter, our goal was to characterize this model system and to utilize it for gaining new insights into the cellular crosstalk between the two cell types.

Cellular self-organization and spheroid composition at different time points were evaluated via membrane staining, confocal microscopy and immunohistology. Although coculture spheroids were in general smaller than ASC monocultures, both cell types were included within the constructs, which remained stable and viable during prolonged culture. While MVEC were at first preferentially located on the surface of the spheroids, after a few days they gradually accumulated in specific regions of the constructs and began forming network-like structures. At the same time, the proportion of MVEC strongly decreased over time. An angiogenesis assay, in which the 3-D constructs were embedded in Matrigel, revealed that not only cocultures, but also ASC monocultures showed extensive sprouting, which was not significantly influenced by the presence of MVEC. When induced to undergo adipogenesis, ASC within coculture spheroids accumulated less triglycerides than in corresponding monocultures. A gene expression array after spheroid dissociation and magnetic bead-based separation supported these data, as most adipogenic marker genes were expressed less strongly in the cocultures on days 2 and 9 after induction. In contrast, some other genes associated with angiogenesis exhibited higher mRNA levels in cocultured ASC. Cryosections revealed an interesting regional separation, with lipid droplets developing only in those parts of the constructs not containing endothelial cells, while adipogenesis was inhibited in ASC close to the MVEC structures. These results suggest that the inhibitory effect on adipogenic differentiation is transmitted either via direct cell-cell contact or through short-range paracrine signaling.

In conclusion, the newly established 3-D coculture model was successfully applied to shed more light onto the complex cellular crosstalk and reciprocal regulation between developing adipocytes and endothelial cells within a 3-D microenvironment. Moreover, we gained further knowledge regarding cellular self-arrangement, which can help in the process of designing vascularized adipose tissue constructs.

6.2 Introduction

Blood vessel formation by angiogenesis is a complex multistep process. Under the influence of pro-angiogenic signals, which are for example released by a hypoxic, inflammatory or tumor cell, quiescent endothelial cells (EC) initiate angiogenic sprouting. As a first step, this process involves the loosening of EC-EC junctions, degradation of the ECM and the detachment of pericytes [1,2]. Subsequently, a small proportion of EC is selected to become “tip cells”, which lead vessel sprouting, and are followed by EC termed “stalk cells”, which form the trunk of the new capillary and eventually establish a vascular lumen. Finally, on contact with other EC, tip cells fuse with recipient vessels to from a continuous lumen allowing for blood flow [1].

In vivo, adipogenesis and angiogenesis are closely associated [3,4]. Angiogenic activity of adipose tissue has been known and clinically used for treating wounds and ischemic organs for more than 400 years [5]. In recent years, it was discovered that a number of angiogenic factors, such as VEGF, HGF, bFGF or TGFβ, are produced by growing adipocytes and also by adipose-derived stem cells (ASC) [6–8]. Of these, VEGF has been accepted to be responsible for most of the angiogenic activity in adipose tissue [8]. However, little is known about the temporal and spatial interplay between these factors necessary for angiogenesis and subsequent vessel remodeling during adipose tissue development [3,5].

Of course, the interaction between adipocytes and endothelial cells is not a one-way street. EC not only form passive conduits for delivering oxygen, but also establish organ-specific vascular niches, which stimulate organogenesis by the production of paracrine-tropic ‘angiocrine’ factors [2,9]. Thus, for a better understanding of adipose tissue development, it is not only necessary to further investigate how EC respond to signals derived from adipocytes, but also to explore the influence of EC on adipogenesis.

In general, cellular nutrient and oxygen supply within tissues can be provided by diffusion only up to a distance of 100-200 µm. For tissue engineering, this means that the survival of cells within larger transplants requires vascularization, which remains one of the main obstacles in regenerative medicine [10–12]. As spontaneous vessel ingrowth from the host is often too slow, additional strategies are needed to ensure sufficient supply of such tissue grafts. These strategies include scaffold design, the application of angiogenic factors, *in vivo* prevascularization, *in vitro* prevascularization and, of course, combinations of these. The first two approaches still rely on the ingrowth of host vessels. *In vivo* prevascularization can quickly provide perfusion, but has disadvantages regarding clinical practicality, as it requires two separate surgeries. *In vitro* prevascularization is based on 3-dimensional cocultures of EC with tissue specific cells under conditions suitable to induce the formation of a prevascular network. After implantation, this network can anastomose to the ingrowing host

vessels and therefore reduce the time needed for complete vascularization [10,13]. Studies dealing with the development of *in vitro* prevascularized tissues have been published for several tissues including skin, bone, skeletal and cardiac muscle, as reviewed by Rouwkema et al. [10].

In this project, initially a human ASC spheroid model suitable for the investigation of adipogenesis in a 3-dimensional context was developed (Chapter 3). Based on that, a coculture model using ASC and MVEC, which can be induced to undergo adipogenesis, could be established (Chapter 5). This model could represent a promising basis for the development of *in-vitro*-prevascularized adipose tissue grafts.

In this chapter, our primary goal was to characterize this newly developed 3-D coculture model and to utilize it for gaining new insights into the cellular crosstalk between ASC/adipocytes and endothelial cells. Therefore, we at first evaluated spheroid morphology, cell viability, triglyceride accumulation and its homogeneity, as well as cellular self-organization at different time points. Moreover, a Matrigel-based sprouting assay was applied to assess angiogenic function. Finally, the influence of the MVEC on adipogenic differentiation within the 3-D environment was examined on a molecular level by measuring gene expression of the ASC after dissociation of the spheroids and subsequent removal of the MVEC via magnetic bead-based sorting.

6.3 Materials and Methods

6.3.1 Materials

Human adipose derived stem cells (ASC) were obtained from PromoCell (Heidelberg, Germany; lot 8073006.12); Adult Human Dermal Blood Microvascular Endothelial Cells (MVEC) were purchased from Lonza (Verviers, Belgium; lot 0000122821). Preadipocyte Growth Medium 2 (PGM2, consisting of PBM2, 10% FBS and 1% penicillin/streptomycin solution) and EGM2-MV BulletKit (containing Endothelial Basal Medium 2 [EBM2], 5% FBS, GA-1000 [Gentamicin, Amphotericin-B], hydrocortisone, ascorbic acid, EGF, VEGF, IGF and bFGF) were also from Lonza (Verviers, Belgium). Fetal bovine serum (FBS, lot 40A0044K), penicillin-streptomycin solution, 0.25% trypsin/EDTA solution, phosphate buffered saline (PBS), Trizol reagent and Dynabeads CD31 were from Invitrogen (Darmstadt, Germany). Agarose, indomethacin, dexamethasone, bovine serum albumin (BSA), glycerol standard solution, dimethylsulfoxide (DMSO), calf thymus DNA, Oil Red O, Mayer´s hematoxylin solution and the membrane dyes PKH26 and PKH67 were purchased from Sigma-Aldrich (Munich, Germany). 3-isobutyl-methylxanthine (IBMX) was bought from Serva (Heidelberg, Germany), Thesit from Gepepharm (Siegburg, Germany). Hoechst 33258 dye was obtained from Polysciences (Warrington, PA, USA). Bovine insulin was kindly provided by Sanofi-Aventis (Frankfurt a. M., Germany). Matrigel (Growth Factor Reduced) was obtained from BD Biosciences (Heidelberg, Germany). Monoclonal mouse anti-human CD31 and polyclonal rabbit anti-mouse IgG/HRP antibodies as well as Glycergel mounting medium were purchased from Dako (Hamburg, Germany). Cy3-coupled donkey anti-mouse IgG antibody and IS mounting medium DAPI were bought from Dianova (Hamburg, Germany). All other chemicals were from Merck (Darmstadt, Germany).

6.3.2 Methods

6.3.2.1 Cell culture

6.3.2.1.1 Expansion of ASC and MVEC

Human adipose-derived stem cells (ASC) were thawed after cryopreservation (passage 3) and seeded in culture flasks. They were expanded in Preadipocyte Growth Medium (PGM2), i.e. Preadipocyte Basal Medium (PBM2) containing 10% FBS, penicillin (100 U/ml) and streptomycin (100 µg/ml). P4 cells were used for all experiments. Microvascular endothelial cells (MVEC) were also thawed after cryopreservation (passage 2) and expanded in culture flasks with complete EGM2-MV medium (referred to as EGM2 in this chapter). EGM2 contained 5% FBS, GA-1000 (Gentamicin, Amphotericin-B), hydrocortisone, ascorbic acid,

EGF, VEGF, bFGF and IGF. All cells were passaged at 90% confluence. Passage 3 or 4 cells were used for all experiments.

6.3.2.1.2 ASC/MVEC coculture spheroids

For 3-D spheroid cocultures, after expansion in culture flasks ASC and MVEC were trypsinized and equal cell numbers of both cell types (2500 cells) were seeded into 96-well-plates coated with 1.5% agarose according to the liquid overlay technique. From this time point, the culture medium was composed of 50% PGM2 and 50% EGM2 (without EGF). Culture plates were kept on an orbital shaker at 50 rpm during incubation. As spheroids would be lost with complete removal of medium from the wells, all medium changes were performed by replenishing only half of the medium volume. Adipogenic induction was performed after 2 days by exchanging half of the medium with induction medium (IM), consisting of 50:50 growth medium (without EGF) supplemented with a hormonal cocktail, resulting in final concentrations of 1.7 µM insulin, 1 µM dexamethasone, 200 µM indomethacin and 500 µM 3-isobutyl-1-methylxanthine (IBMX). The time point of induction was referred to as day 0. On day 2 after induction, IM was replaced by 50:50 growth medium (without EGF) containing 1.7 µM insulin only (final concentration). This was done by exchanging half of the medium for three times in order to reduce the concentration of the hormonal inducers. All cultures were incubated at 37°C, 5% CO_2. Medium was exchanged every 3-4 days.

ASC monocultures were performed accordingly, with the total cell numbers per spheroid being equal to the total cell numbers in the cocultures. Culture media were the same as for the cocultures for comparability.

6.3.2.2 Microscopical determination of spheroid size

At specific time points, microscopical bright field images of the co- and monoculture spheroids were acquired with a XC30 CCD camera attached to a IX51 inverted microscope using CellSens Dimension software (all from Olympus, Hamburg, Germany). Cross-sectional areas of at least 10 randomly selected spheroids were determined with ImageJ software (NIH, Bethesda, MD, USA). Equivalent diameters and spheroid volumes were calculated thereof.

6.3.2.3 Live/Dead Assay

Cell viability within the spheroids was assessed with the Live/Dead Cell Staining Kit II (PromoCell, Heidelberg, Germany). Spheroids were pooled, washed three times with PBS and incubated with the staining solution (4 µM EthD-III, 2 µM Calcein AM) for 45 min. The staining was evaluated by imaging with a confocal laser scanning microscope (Zeiss Axiovert 200M microscope coupled to a Zeiss LSM 510 scanning device, Carl Zeiss MicroImaging, Jena, Germany). Live cells showed green calcein fluorescence (ex. 488 nm, em. 505-550 BP), dead cells were indicated by red fluorescence of DNA-intercalating EthD-III in the nuclei (ex. 543 nm, em. LP 560). The z-stack mode was used to investigate viability inside the spheroids.

6.3.2.4 Determination of the intracellular triglyceride (TG) content

For analysis of the intracellular TG content 3-D spheroids were pooled, washed twice with PBS and resuspended in 0.5% aqueous Thesit solution. Subsequently, cells were sonicated and spectroscopic quantification of TG was performed using the enzymatic Serum Triglyceride Determination Kit from Sigma-Aldrich (Munich, Germany) according to the manufacturer's instructions, with assay conditions being adjusted to the 96-well plate format. For calibration, different glycerol standard dilutions were used. All TG data were acquired from three biological replicates; one replicate was derived from an exact number of approximately 20 spheroids for 3-D cultures. TG contents per spheroid were calculated and normalized to the DNA content, which was determined as described below.

6.3.2.5 Determination of the DNA content

3-D spheroids were pooled, washed twice with PBS, resuspended in lysis buffer (2 mM EDTA, 2M NaCl, 50 mM Na_3PO_4, pH 7,4) and sonicated as well. DNA content was determined using the intercalating Hoechst 33258 dye (0.1 µg/ml in 0.1 M NaCl, 1 mM EDTA, 10 mM Tris, pH 7.4). Fluorescence intensities were determined at an excitation wavelength of 365 nm and an emission wavelength of 458 nm with a TECAN Genios Pro plate reader (Männedorf, Switzerland) and correlated to DNA contents using standard dilutions of double-stranded DNA (from calf thymus). All measurements were performed in three biological replicates; one replicate was derived from an exact number of approximately 10 spheroids for 3-D cultures.

6.3.2.6 Lipid staining with Oil Red O

To visualize triglyceride accumulation, cultures were harvested and staining with Oil Red O (ORO) was performed. For this purpose, spheroids were pooled in PBS, transferred to microcentrifuge tubes, washed with PBS, fixed in 10% formalin (1h, 4°C), stained with ORO (3 mg/ml solution in 60% isopropanol) for 4h and washed three times with PBS. Stained spheroids were embedded in Tissue-Tek (Hartenstein Laborbedarf, Würzburg, Germany), snap frozen and cut into 10-µm-thick cryosections. After removal of Tissue-Tek by washing in water, the sections were mounted in glycerol. Serial sections were prepared from all spheroids and sections from the center region were used for histological evaluation. Microscopical bright field images were acquired with a DP71 camera attached to a BX51 microscope using CellSens Dimension software (all from Olympus, Hamburg, Germany).

6.3.2.7 Staining with PKH dyes and visualization of cellular distribution

To visualize the distribution of the two cell types in cocultures, ASC and MVEC were stained with different PKH membrane dyes according to the manufacturer´s protocol before starting the spheroid cultures. Both cell types were trypsinized, counted and washed with PBS. After centrifugation, cells were resuspended in Diluent C, and freshly mixed solutions of PKH26 or PKH67 were added, resulting of a dye concentration of 5 µM. After 3 min incubation at room temperature the reaction was stopped with FBS. Subsequently, cells were centrifuged and washed 3 times with full culture medium. After that, co- and monocultures were seeded as usual.

To evaluate cellular distribution, imaging was performed using a confocal laser scanning microscope (Zeiss Axiovert 200M microscope coupled to a Zeiss LSM 510 scanning device, Carl Zeiss MicroImaging, Jena, Germany). PKH26 was excited at 543 nm (He-Ne-Laser) and detected with a 560 nm longpass filter. PKH67 was excited at 488 nm (Ar-Laser) and detected with a 505-550 nm bandpass filter. Z-stacks were acquired to assess cell arrangement inside the constructs.

6.3.2.8 Sprouting in Matrigel

To investigate cellular sprouting, co- and monoculture spheroids were embedded in Matrigel 1 day after seeding. 8-well chamber slides (Ibidi, Martinsried, Germany) were at first coated with Matrigel on ice according to the manufacturer´s instructions and subsequently incubated for 15 min at 37 °C to induce gelation. After that, 5-10 spheroids (mono- or cocultures) were added to each well, and more Matrigel was pipetted into the wells to completely enclose the constructs. After gelation at 37 °C for 30 min, either EGM2 or a 50:50-mixture of PGM2 and

EGM2 was added to the wells and replaced with fresh medium after 3 days. Cultures were, as usual, incubated at 37 °C and 5% CO_2. Sprouting was visualized on day 5 after embedding into Matrigel using bright field microscopy as described in section 6.3.2.2.

6.3.2.9 Immunohistochemical staining for CD31

Cryosections of spheroids were histologically stained for CD31. Sections were fixed in acetone of -20 °C for 10 min, air dried for 10 min at room temperature (RT) and rehydrated with PBS for 5 min. Then, slides were incubated with blocking solution (1% BSA in PBS) for 20 min, followed by incubation with the primary antibody (mouse anti-human CD31, dilution 1:100) at RT overnight. After washing 3 times with PBS, they were incubated with the secondary antibody (rabbit anti-mouse HRP) for 30 min and again washed 3 times with PBS. Slides were developed with diaminobenzidine (Liquid DAB Substrate Pack, Biogenex, Fremont, CA, USA), counterstained with hematoxylin, mounted with Glycergel and imaged as described in section 6.3.2.6.

6.3.2.10 Immunofluorescence staining for CD31

For immunofluorescence, cryosections were fixed, air dried, rehydrated, treated with blocking solution and incubated with the primary antibody as described in the previous section. Subsequently, they were washed three times with PBS and incubated with the Cy3-coupled secondary antibody (donkey anti-mouse IgG) for 30 min in the dark. After washing 3 times with PBS, slides were mounted with DAPI mounting medium. All steps were performed at RT. Images were taken with an Olympus BX51 fluorescence microscope combined with a DP71 camera using CellSens Dimension software (all from Olympus, Hamburg, Germany). Different filters were used for the imaging of DAPI and Cy3 fluorescence (ex./em. 330-385 nm/420 nm and ex./em. 510-550 nm/590 nm, respectively).

6.3.2.11 Separation of MSC and MVEC using magnetic beads

To separate ASC and MVEC after 3-D coculture for subsequent analytics, spheroids had to dissociated at first. To do this, they were pooled, transferred to a microcentrifuge tube, washed 2 times with PBS and incubated with 0.25% trypsin/EDTA for 15 min while shaking. The reaction was stopped with FBS, and the resulting cell suspension was centrifuged (500g, 7 min). Cells were resuspended in PBS containing 1% BSA and incubated with 10 µl of anti-CD31 Dynabeads per sample at 4 °C for 30 min under vertical rotation. Subsequently, samples were placed in a magnet for 2 min to separate the cells and the supernatant

(containing CD31-negative cells) was transferred to another tube. The process was repeated several times to completely remove all CD31-positive cells. Then, each sample was centrifuged, and the pellet was used for further analysis.

6.3.2.12 Low Density Gene Expression Array

Gene expression of co- and monoculture spheroids was measured before adipogenic induction (i.e. on day 0) and on days 2 and 9 after induction. Uninduced constructs were used as control group. At each time point, 30 spheroids were harvested and pooled to result in one biological replicate. Samples were dissociated and MVEC were separated from the ASC using magnetic beads as described in the previous section. Monocultures were treated in the same way to ensure comparability. From the ASC fraction, total RNA was extracted using Trizol reagent according to the manufacturer´s instructions. RNA concentrations were determined spectrophotometrically with a NanoDrop 2000c analyzer (Thermo Fisher Scientific, Wilmington, DE, USA).

First strand cDNA was synthesized from total RNA using ImProm-II Reverse Transcription System (Promega, Mannheim, Germany) according to the manufacturer's protocol. qRT-PCR using custom-made TaqMan Low Density Arrays (Applied Biosystems, Darmstadt, Germany) containing primers and probes for several adipogenesis-related genes in 384-well micro fluidic cards was performed according to the manufacturer's instructions. cDNA samples were mixed with TaqMan Gene Expression Master Mix and filled into the ports of the micro fluidic cards. After centrifugation in order to distribute the cDNA samples to the reaction wells, the cards were sealed and RT-PCR was performed on a 7900HT Fast Real-Time System (Applied Biosystems, Darmstadt, Germany) over 40 cycles. Evaluation of expression data was carried out according to the ΔΔCt method. All Ct values were normalized to GAPDH. Expression values of ASC monocultures on day 0 were used as reference for all other groups. If a gene was not detectable in the reference group, a Ct value of 40 was assumed (corresponding to one cDNA replicate in the sample). Relative expression levels (RQ) were calculated as $2^{-\Delta\Delta Ct}$. All measurements were performed with three biological replicates. Genes specifically mentioned in the text or figures are listed in Table 6-1.

Table 6-1: *List of gene names, gene symbols, and TaqMan Assay ID's.*

Gene name	Gene symbol	Assay ID#
adiponectin	ADIPOQ	Hs00605917_m1
angiopoietin 1	ANGPT1	Hs00375822_m1

angiopoietin 2	ANGPT2	Hs00169867_m1
angiotensinogen	AGT	Hs00174854_m1
apelin	APLN	Hs00175572_m1
apolipoprotein E	APOE	Hs00171168_m1
CCAAT/enhancer binding protein (C/EBP), alpha	CEBPA	Hs00269972_s1
CCAAT/enhancer binding protein (C/EBP), beta	CEBPB	Hs00270923_s1
CCAAT/enhancer binding protein (C/EBP), delta	CEBPD	Hs00270931_s1
complement factor D (adipsin)	CFD	Hs00157263_m1
cytochrome P450, fam, 19, subf. A, polypept. 1 (aromatase)	CYP19A1	Hs00240671_m1
fatty acid binding protein 4 (aP2)	FABP4	Hs01086177_m1
fatty acid synthase	FASN	Hs00188012_m1
fatty acid transporter 1	FATP1	Hs01587917_m1
facilitated glucose transporter 4	GLUT4	Hs00168966_m1
glyceraldehyde-3-phosphate dehydrogenase	GAPDH	Hs99999905_m1
insulin-like growth factor 1	IGF1	Hs01547657_m1
interleukin 1, beta	IL1B	Hs00174097_m1
interleukin 6	IL6	Hs00985639_m1
leukemia inhibitory factor	LIF	Hs00171455_m1
lipoprotein lipase	LPL	Hs00173425_m1
nicotinamide phosphoribosyltransferase (visfatin)	NAMPT	Hs00237184_m1
peroxisome proliferator-activated receptor gamma	PPARG	Hs00234592_m1
sterol regulatory element binding transcription factor 1	SREBF1	Hs01088691_m1
transforming growth factor, beta	TGFB	Hs00234244_m1
vascular endothelial growth factor A	VEGFA	Hs00173626_m1

6.3.2.13 Statistics

All quantitative results are presented as mean value ± standard deviation. Differences between multiple groups were analyzed for significance using one-way analysis of variances (ANOVA) with subsequent multiple comparisons according to Tukey's post-hoc test. In the LDA differences between mono- and coculture at each time point were analyzed for significance using unpaired Students t-test. Differences within each culture system between time points were analyzed for significance using ANOVA with subsequent multiple comparisons according to Tukey's post-hoc test.

For all comparisons, a value of $p<0.05$ was regarded statistically significant. Statistical analysis was performed using PASW Statistics 18 software (SPSS Inc., Chicago, IL, USA).

6.4 Results

6.4.1 Cell viability, spheroid sizes and triglyceride accumulation in cocultures

ASC/MVEC coculture spheroids were produced and kept under the conditions determined in the previous chapter (chapter 5), i.e. using a PGM2/EGM2 mixture without EGF and applying a short-term induction protocol. Live/Dead staining was performed on day 7 after adipogenic induction in both uninduced and adipogenically induced cocultures and revealed that in both cases the vast majority of cells exhibited green fluorescence indicating viability (Fig. 6.1). Single dead cells were present primarily on the surface of the spheroids and often did not appear to be properly integrated into the 3-D constructs. This was in general comparable to the results from ASC monoculture spheroids (Fig. 3-10, chapter 3).

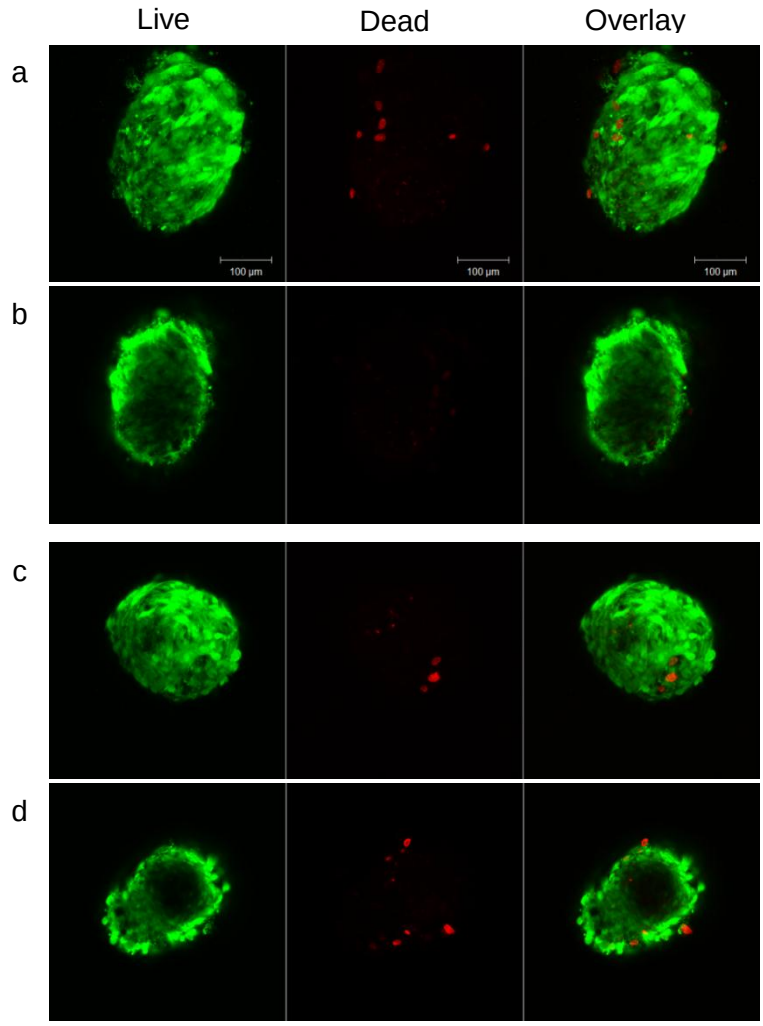

Figure 6-1: *Live/Dead-staining of uninduced (a/b) and adpogenically induced (c/d) coculture spheroids (d7). Optical sections acquired by confocal microscopy are depicted. In each row, green calcein fluorescence indicating live cells is shown on the left, red EthD-III fluorescence indicating dead cells in the middle and the overlay image on the right. a and c show 3-dimensional projections obtained from z-stacks, b and d show single optical sections from central regions of the spheroids. Scale bar is 100 µm.*

Cells were seeded as cocultures and ASC monocultures with a total number of 5000 cells per construct, which had previously been determined to be an optimal spheroid size for ASC monocultures (chapter 3), and the progression of spheroid sizes over culture time was monitored by the determination of construct volumes at different time points (Fig. 6-2 A). When 3-D spheroids had formed in each well after 1 day (i.e. on day -1), it became obvious that cocultures were of smaller size than ASC monocultures, with cocultures reaching about 72% of the monoculture volumes.

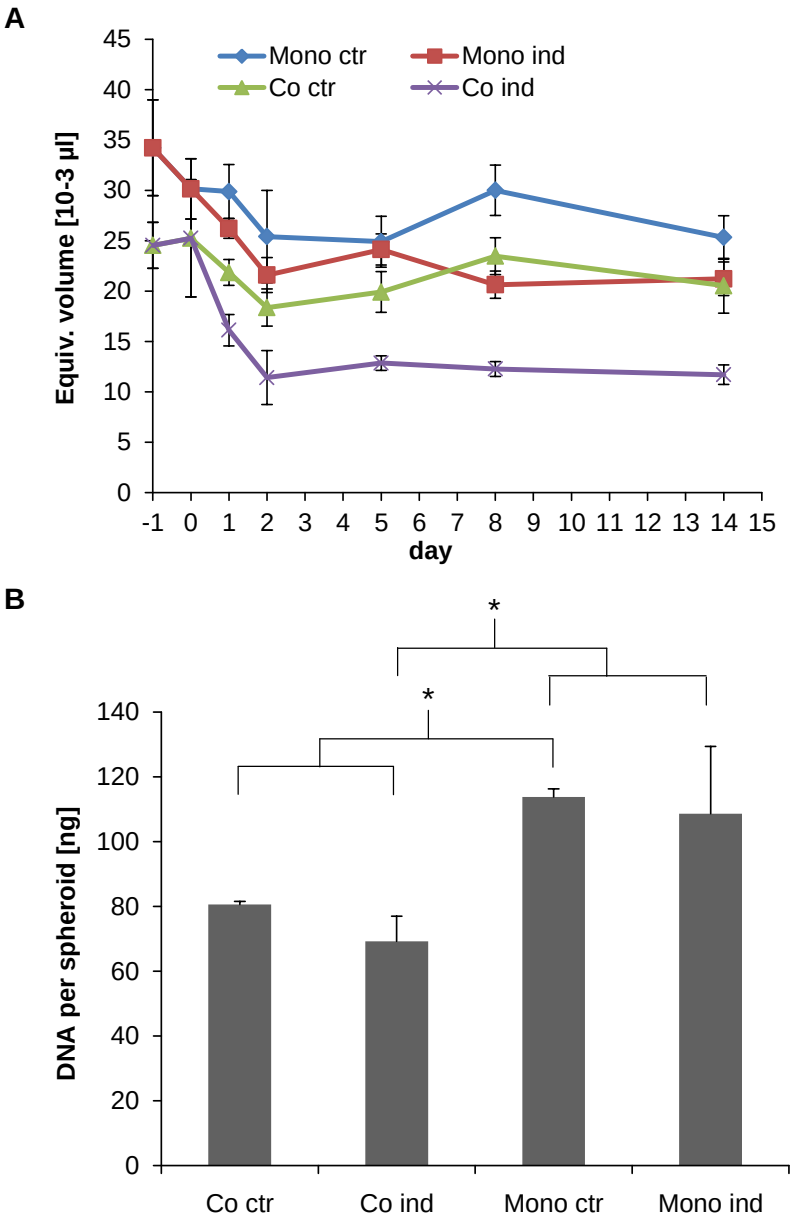

Figure 6-2: A) *Growth kinetics of coculture and ASC monoculture spheroids (induced on day 0 or uninduced) up to day 14. Spheroids were seeded with a total number of 5000 cells per construct.* ***B)*** *DNA content per spheroid of co- and monocultures on day 14.*

During the first days of culture, all spheroids decreased in size at least up to day 2. For both mono- and cocultures, the volume reduction was even more pronounced when cultures were induced to undergo adipogenesis. At later time points, volumes stabilized and remained within a certain range up to day 14 for each group. After two weeks of culture, volumes of the cocultures were approx. 81% of the corresponding monocultures for uninduced control groups and approx. 55% for induced groups.

In addition, DNA contents of the spheroids were determined after harvesting all groups on day 14 (Fig. 6-2 B). These data also revealed significant differences between the culture types, with DNA levels in cocultures reaching 71% and 63% of the corresponding ASC monocultures for control and induced groups, respectively. It is also worth mentioning that control and induced groups within one culture system were not significantly different.

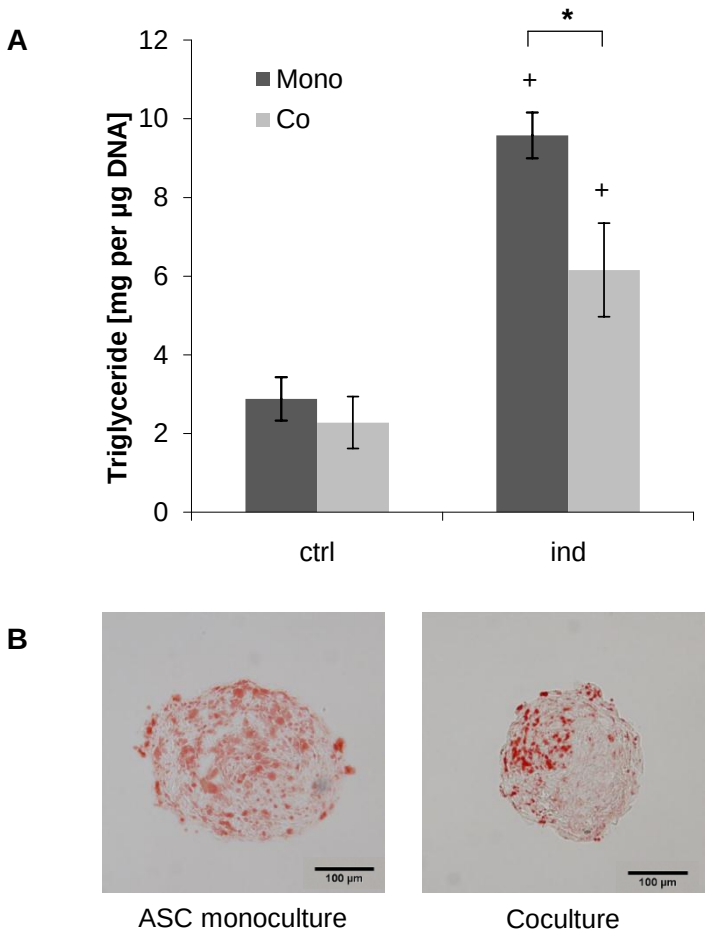

Figure 6-3: A) *Quantification of the intracellular TG content in co- and monoculture spheroids on day 9. TG contents were normalized to DNA contents (in cocultures corrected for the percentage of ASC). Statistically significant differences between co- and monocultures are indicated by * ($p<0.05$). + denotes significant differences compared to control groups ($p<0.05$).* ***B)*** *Histological analysis of the TG accumulation on day 14 after staining of cryosections with ORO. Scale bars are 100 µm.*

In a different experiment, triglyceride accumulation of the 3-D cocultures was investigated and compared to monocultures. After performing a TG assay on day 9, lipid contents were

normalized to corresponding DNA contents, which were (in case of the cocultures) corrected for the percentage of ASC present at that time point, as determined by immunostaining for CD31 after dissociating the spheroids. In both culture types ASC had accumulated significant amounts of TG as compared to uninduced controls, but strikingly the total TG level after adipogenic induction was significantly lower in cocultures than in ASC monoculture spheroids (Fig. 6-3 A). Oil Red O staining of cryosections supported these data; while ASC monoculture spheroids exhibited lipid droplets homogeneously distributed throughout the constructs on day 9, in the cocultures triglycerides appeared to have been accumulated predominantly in specific areas of the spheroids, leading to an inhomogeneous distribution and overall to a smaller number of lipid inclusions (Fig. 6-3 B).

6.4.2 Cell distribution in coculture spheroids

In order to distinguish ASC and MVEC and to evaluate cellular distribution *in situ* within the spheroids, it was necessary to label both cell types before mixing them to form the cocultures. For this purpose, the non-toxic fluorescent membrane dyes PKH26 and PKH67 were used to stain the ASC and MVEC, respectively. Imaging via confocal laser scanning microscopy (CLSM) could efficiently depict cell type arrangement up to optical sections lying about 70 to 80 µm below the surface of the constructs.

2 days after seeding the labeled cells as cocultures in a 50/50 ratio (ASC/MVEC), CLSM images revealed that both cell types had been integrated into the spheroids and were present in what appeared to be almost equal quantity, with the ASC seeming to be in a slight majority (Fig. 6-4 A). Interestingly, the surface region of the spheroids was apparently mainly constituted of endothelial cells, which arranged in a layer-like fashion. Nevertheless, MVEC could also be found in central areas of the constructs (Fig. 6-4 A,B). Cultures were induced with the adipogenic hormonal cocktail on day 0 and CLSM imaging was again performed on several time points later in culture. On day 3 after induction, the internal structure of the spheroids had changed as compared to day 0. By then, MVEC had started to accumulate in distinct regions within the constructs and to form cellular clusters. Moreover, the surface layer of MVEC could no longer be detected, and the overall proportion of endothelial cells appeared to be lower than on day 0. Images from days 5 and 7 indicated a further decrease of the MVEC proportion, accompanied by prominent cluster formation. Apart from the clusters, few MVEC could be found throughout the constructs at all by day 7, resulting in rather large EC-free regions (Fig. 6-5).

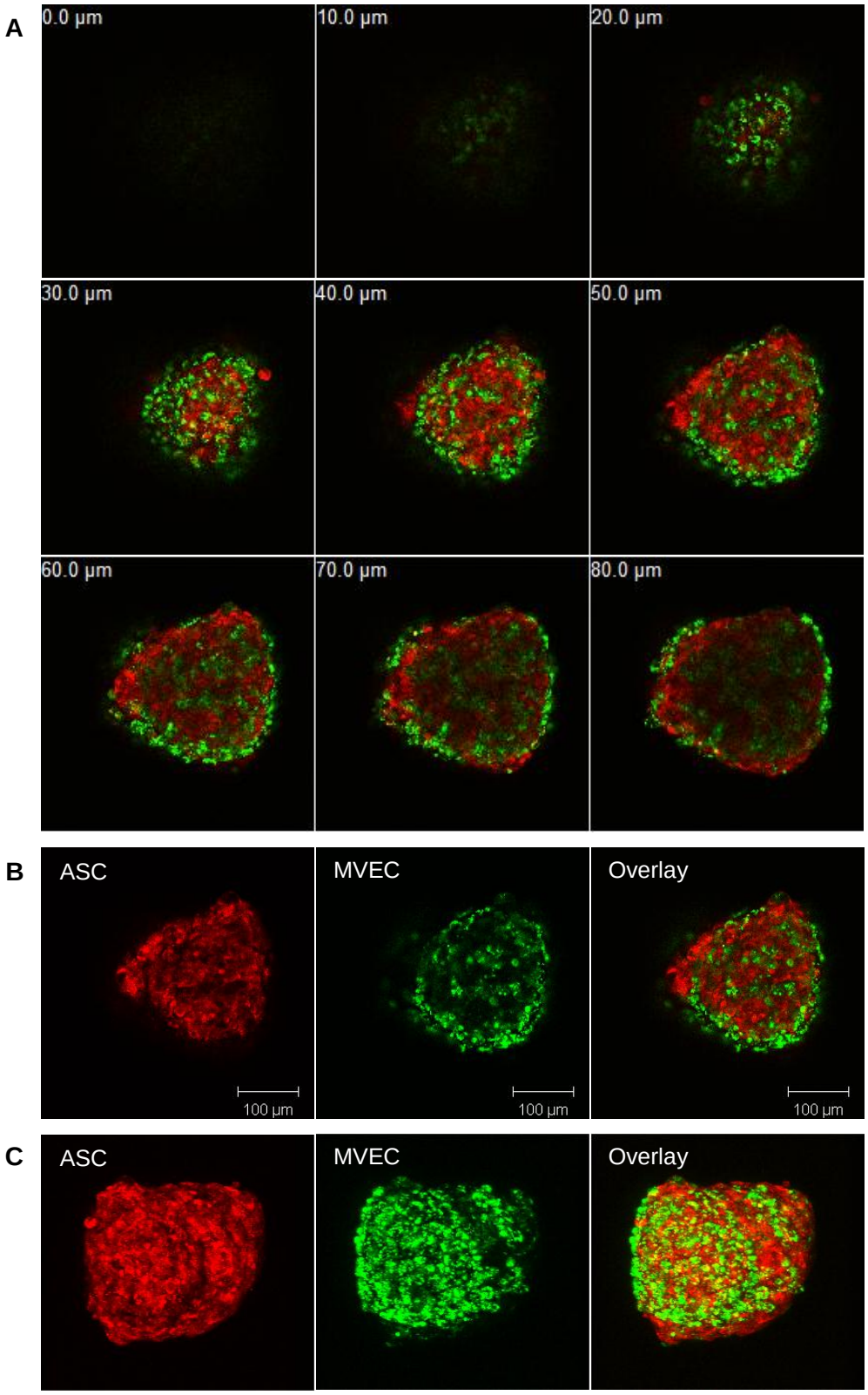

Figure 6-4: *Visualization of cellular assembly within ASC/MVEC (50/50) coculture spheroids on day 0 (i.e. 2 days after seeding) via confocal microscopy (CLSM). ASC were stained with PKH26 before seeding and exhibit red fluorescence, while MVEC were stained with PKH67 and show green fluorescence.* ***A)*** *Z-stack images of the cocultures, displaying optical sections of the spheroids with 10 µm intervals as indicated.* ***B)*** *Both fluorescence channels are shown separately and as an overlay for the optical section at 50 µm.* ***C)*** *3-dimensional projections of the spheroids calculated from the z-stacks. Scale bars are 100 µm.*

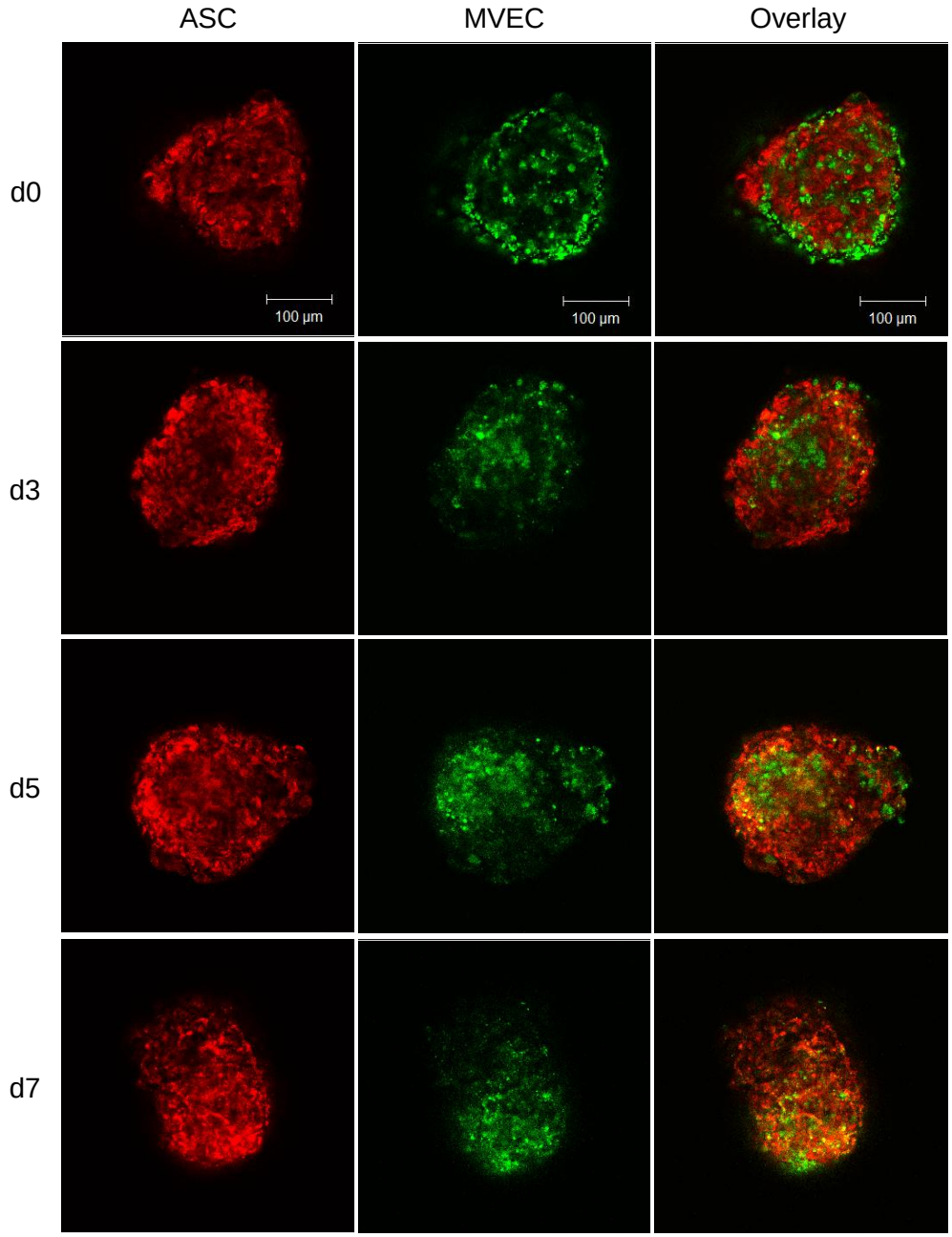

Figure 6-5: *Confocal images of the ASC/MVEC (50/50) coculture spheroids on days 0, 3, 5 and 7 after adipogenic induction. Cell staining was performed as described in Fig. 6-4 (ASC red, MVEC green). For each time point, both fluorescence channels are shown separately and as an overlay for the optical section at 50 µm. Scale bars are 100 µm.*

In a different experiment, coculture spheroids were produced with an ASC/MVEC ratio different from the usual 50/50. Here, only 20% ASC and 80% MVEC were used. Cells were again stained with the membrane dyes before seeding, but in contrast to the previous experiment the green PKH67 dye was used for the ASC, while MVEC were stained with the red PKH26. One day after seeding, i.e. on day -1, spheroids of smaller size than in the case of 50/50 cocultures had formed in each well.

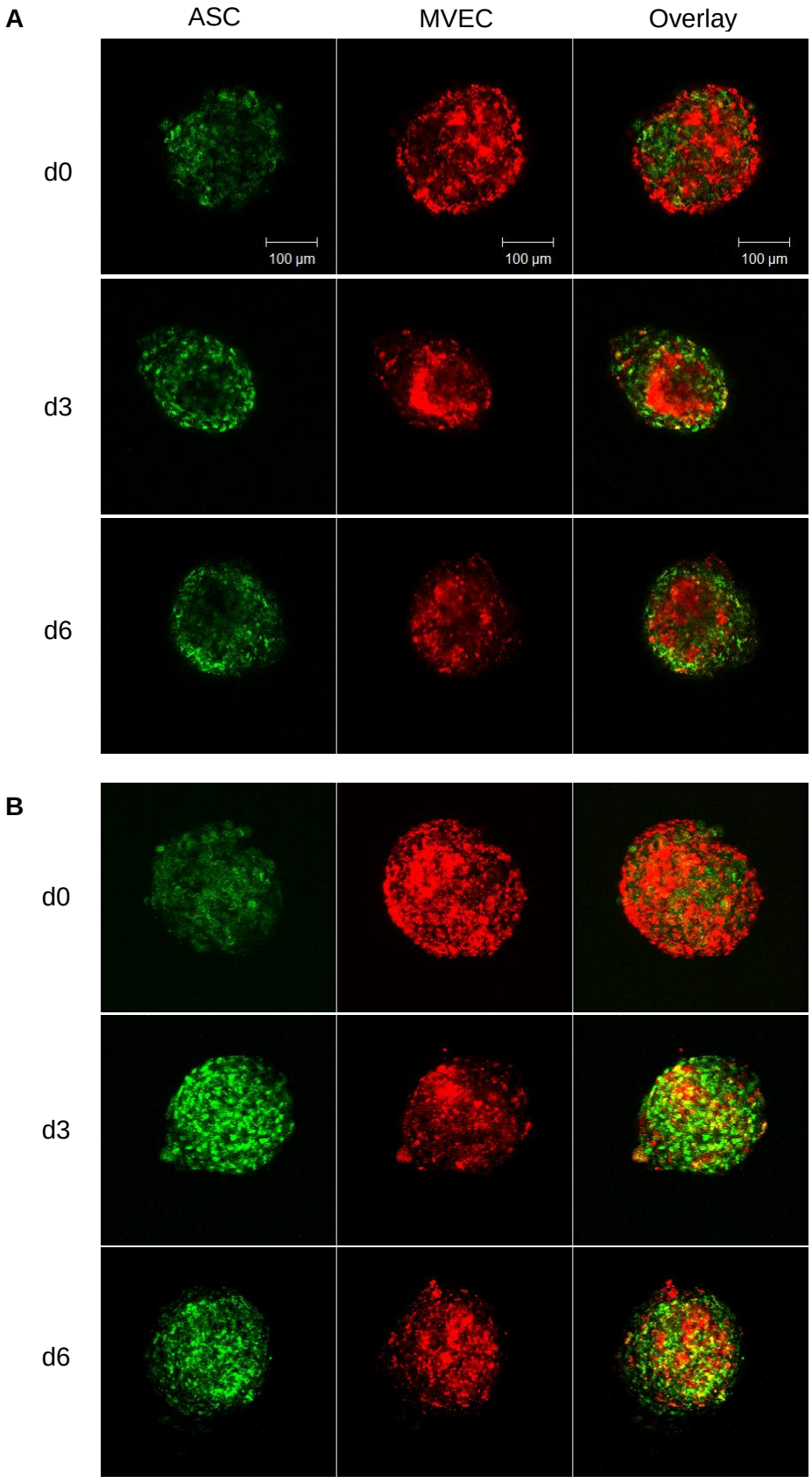

Figure 6-6: *Confocal images of ASC/MVEC (20/80) coculture spheroids on days 0, 3 and 6 after adipogenic induction. In contrast to Fig. 6-4 and 6-5, ASC were labeled with green PHK67 and MVEC with red PKH26.* ***A)*** *Optical sections at 50 µm (single channels and overlay) acquired with the z-stack function* ***B)*** *3-dimensional projections of the spheroids calculated from z-stacks. Scale bars are 100 µm.*

At this early time point, it could again be observed that the EC had accumulated in the periphery of the constructs, forming a surface layer (Fig. 6-6 A,B). As expected, the overall percentage of MVEC present in the spheroids was higher than in 50/50 cultures, yet cells were still randomly distributed over the central regions (Fig. 6-6 A). However, similar to the 50/50 cocultures, endothelial cells began to aggregate and form clusters during prolonged culture. The surface layer of MVEC could no longer be observed by day 3. The proportion of EC also decreased between days -1 and 6, but was still higher after 1 week than in the 50/50 spheroids (Fig. 6-6 A,B).

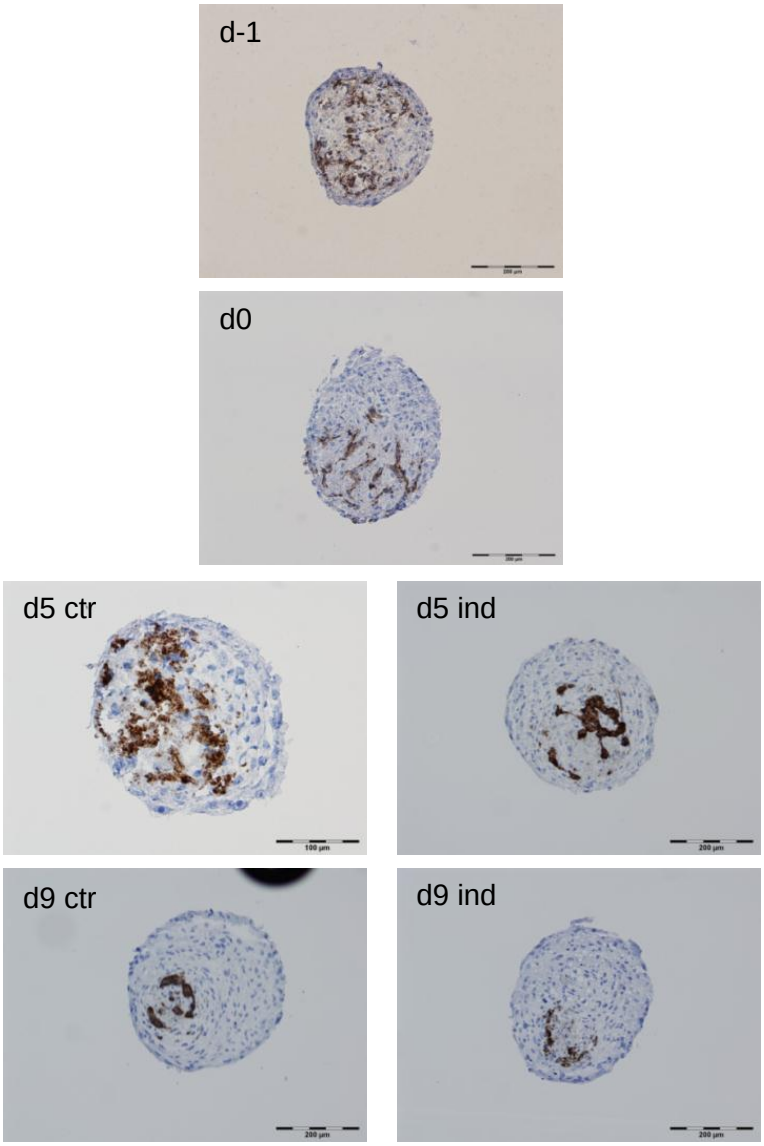

Figure 6-7: *Visualization of endothelial cell distribution and arrangement in 50/50 coculture spheroids. EC in cryoesctions were detected by immunohistochemical staining for CD31 (brown). Nuclei were counterstained with hematoxylin (blue). Scale bars are 200 µm.*

To investigate the cellular distribution in more detail, immunostaining was performed on cryosections of the spheroids, which were either induced to undergo adipogenesis on day 0

or not. On day -1 MVEC were distributed all over the sections, yet not randomly, but with a tendency to associate with other endothelial cells (Fig. 6-7). This behavior was even more obvious on day 0, when coherent MVEC networks could be detected, which appeared preferentially in certain regions of the spheroids, leaving the rest of the constructs virtually MVEC-free. The presence of endothelial cell structures could persistently be observed for the duration of the experiment (Fig. 6-7). The total amount of endothelial cells, however, decreased during ongoing culture, as it had been shown with the CLSM images. When immunofluorescence instead of immunohistochemical staining was applied, the process of EC structuring was also clearly detectable. In addition, some of the MVEC structures even appeared to contain lumen-like areas on day 2 and later (Fig. 6-8).

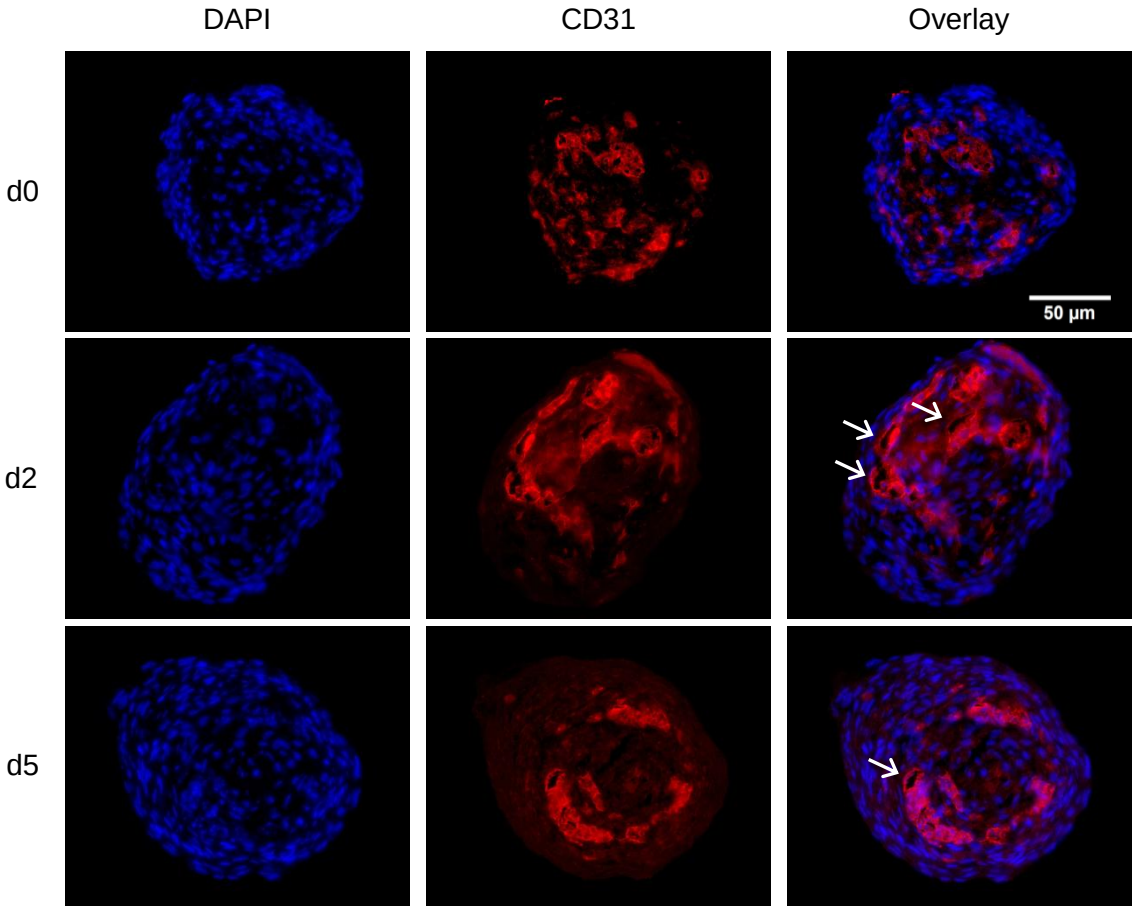

Figure 6-8: *Immunofluorescence staining of cryosections from ASC/MVEC (50/50) coculture spheroids. Endothelial cells were labeled with CD31 antibody and detected via Cy3 fluorescence (red). Nuclei were counterstained with DAPI (blue). Lumen-like areas are indicated by arrows. Scale bar is 50 µm.*

Based on these results, the question arose in which way the observed regional structuring of the MVEC within the spheroids was linked to the previously detected inhomogeneous triglyceride accumulation (cf. section 6.4.1). This was of particular interest, as on CD31/hematoxylin-stained sections of day 9, cocultures often appeared to contain lipid

droplets (appearing as circular cavities) predominantly in those parts of the constructs that were free of endothelial cells (Fig. 6-9 A).

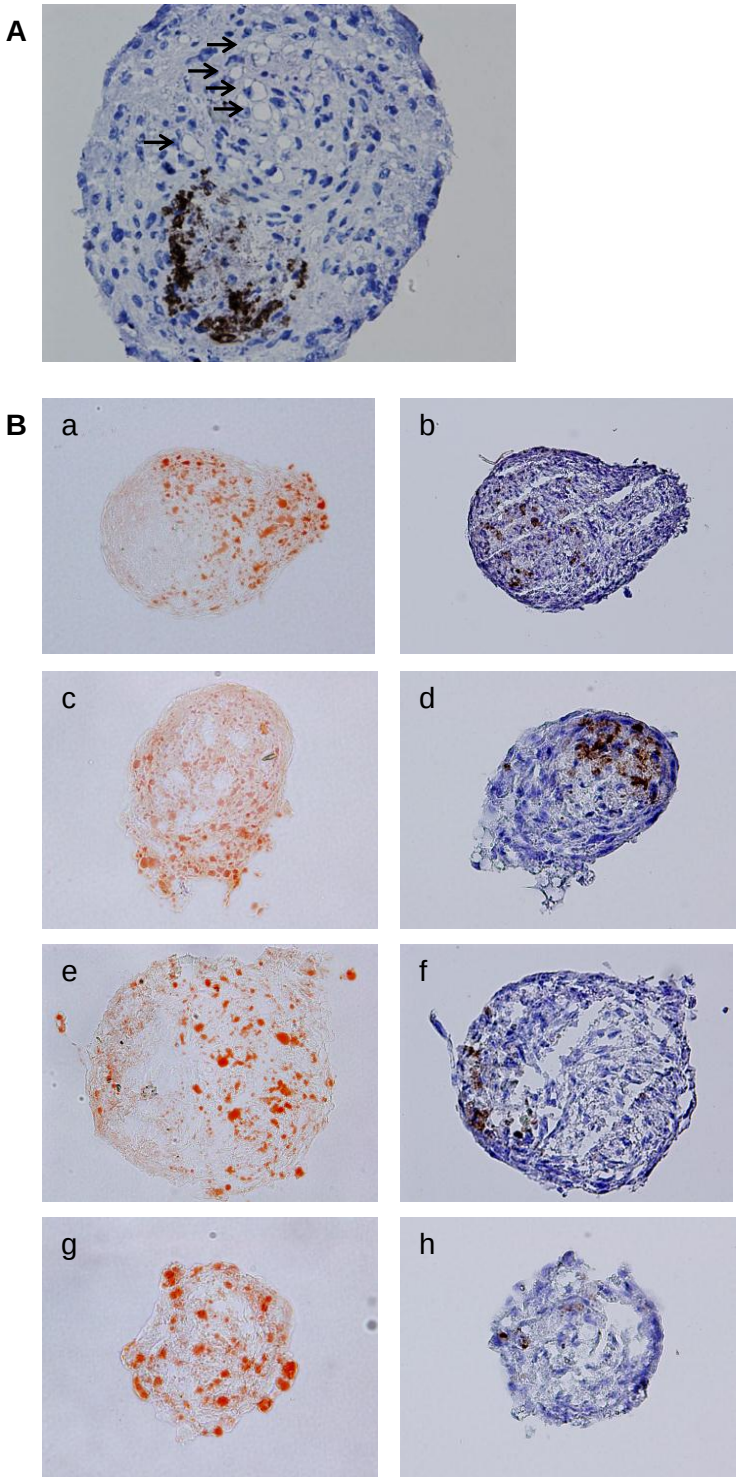

Figure 6-9: A) *Cryosection of cocultures stained for CD31 and counterstained with hematoxylin on day 9 after adipogenic induction (image identical to Fig 6-7, yet in higher magnification). Arrows denote some of the lipid droplets (appearing as cavities).* ***B)*** *Cryosections of cocultures on day 12 after induction. Sections were alternatingly attached to 2 different slides and stained with either ORO (left) or CD31/hematoxylin (right). In each row, both images represent two consecutive sections from the central region of the constructs.*

To address these observations in more detail, in a new experiment coculture spheroids (50/50 cell type ratio) were generated, induced with the adipogenic cocktail on day 0 and harvested on day 12. As ORO staining would get lost when staining for CD31 was performed on the same sections, cryosections were alternatingly attached to two different glass slides. Subsequently, these slides were either used for evaluating the ORO distribution or for immunohistochemical CD31 staining. In this way, it was possible to assess both lipid accumulation and MVEC structuring on consecutive sections (Fig. 6-9 B). Results from these experiments supported the previous observations: Again, lipid droplets could be detected almost exclusively in those areas of the constructs which did not contain any endothelial cells. On the other hand, in regions of the spheroids where MVEC were present, the surrounding ASC obviously had not accumulated any lipids (Fig 6-9 B, images a-f). Consequently, on sections which included no MVEC at all, triglycerides were distributed more or less homogeneously (Fig 6-9 B, images g, h).

6.4.3 Cellular sprouting in Matrigel-embedded coculture spheroids

Sprouting assays after embedding of cells or tissues into hydrogels can be used as *in vitro* angiogenesis models and have already been applied for coculture spheroid systems, e.g. of EC and fibroblasts or osteoblasts [14,15]. Our goal was to utilize a Matrigel sprouting method to evaluate EC functionality within the coculture spheroids. After optimizing the embedding method to make sure that the spheroids were surrounded with gel and did not sink to the bottom of the wells, reproducible sprouting could be observed. Co- and ASC monoculture spheroids were embedded into Matrigel one day after seeding and further cultured within the gel for 5 days.

At this time point, radially outgrowing sprouts originating from the spheroids had developed, with their length and number being dependent on the culture medium used. In case of the cocultures, these sprouts had reached a medium length of 330 µm when gel-embedded spheroids were supplemented with complete EGM2, but only few outgrowing structures of about 50 µm length had developed under culture with a PGM2/EGM2 mixture (50:50, w/o EGF; Fig 6-10 A, images a, b).

Surprisingly, when EGM2 was used as culture medium, extensive sprouting occurred not only with the cocultures, but also for the ASC monoculture spheroids. Length and density of the outgrowing structures were comparable between these two groups (Fig. 6-10 A, images a, c).

To investigate the sprouting process and the composition of the outgrowing structures more closely, ASC and MVEC were labeled with membrane dyes before seeding as coculture spheroids and embedding into Matrigel. After 5 days in the gel, confocal images of the

spheroids, including the sprouts, were acquired. The evaluation of z-stacks revealed that both cell types contributed to the sprout formation. However, the sprouts were mainly composed of ASC, whereas MVEC could be found within the sprouts only sporadically (Fig. 6-10 B).

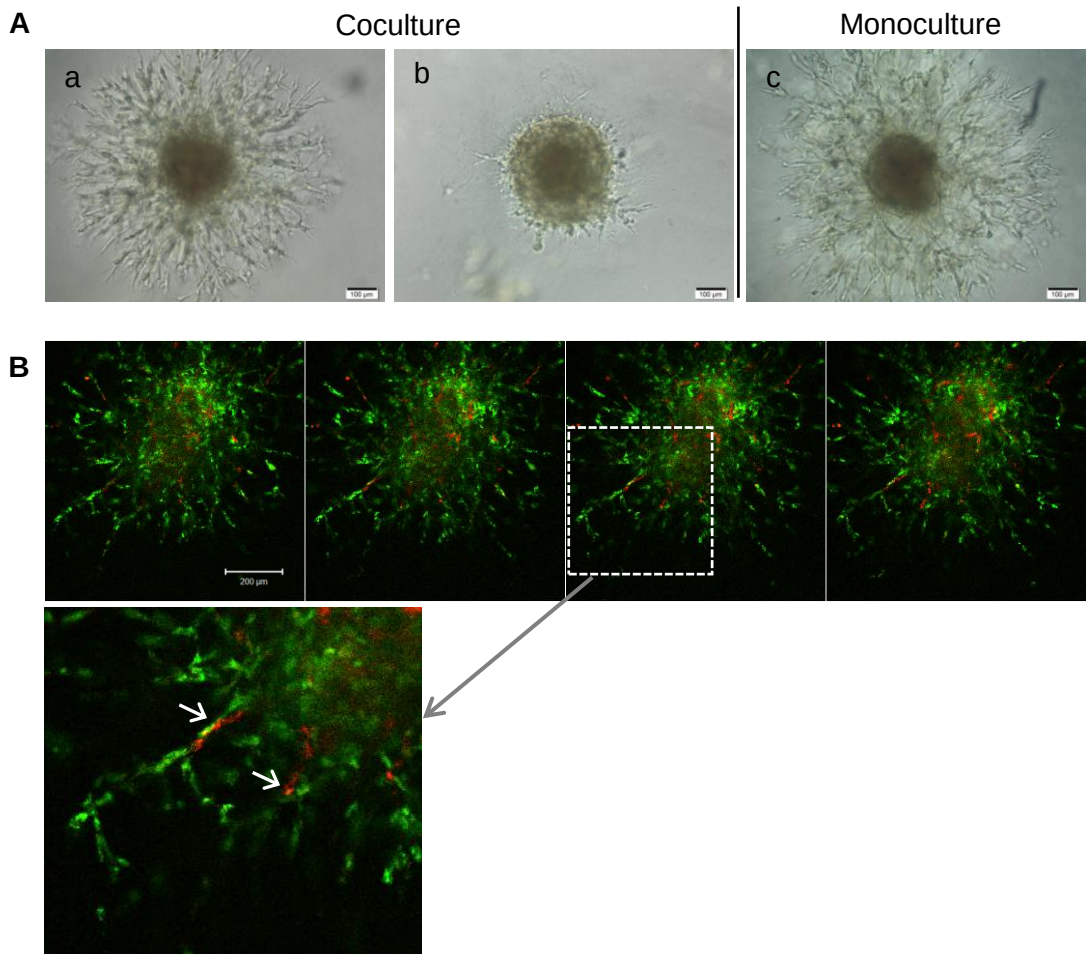

Figure 6-10: *Cellular sprouting after embedding of coculture (50/50) and ASC monoculture spheroids in Matrigel.* ***A)*** *Spheroids were embedded into Matrigel 1 day after seeding and cultured with EGM2 w/o EGF (a;c) or with PGM2:EGM2 (50:50) w/o EGF(b). Bright field images were acquired five days later. Scale bars are 100 µm.* ***B)*** *Cells were stained with green PKH67 (ASC) and red PKH26 (MVEC) before seeding as coculture spheroids, which were embedded into Matrigel 1 day later and cultured for 5 days with PGM2:EGM2 (50:50) w/o EGF. Confocal z-stack images of the gel-embedded spheroids were acquired via CLSM. The upper row shows a series of optical sections from the central region of the spheroids. Scale bar is 200 µm. A larger version of the area marked by the white box is depicted below. Arrows denote MVEC contributing to the sprouts.*

6.4.4 Gene expression of ASC in co- and monocultures during adipogenesis

To investigate how the presence of endothelial cells influenced ASC gene expression in our 3-D model system, a TaqMan Low Density Array was performed. The custom-made array contained several genes associated with adipogenesis and adipocyte functions as well as some angiogenesis-related genes. Co- and monoculture spheroids were either induced to undergo adipogenesis on day 0 (IND) or not (CTRL). On three time points, samples of the co- and monocultures were taken: on day 0 (before hormonal induction was performed) to obtain a reference value, on day 2, an early time point during adipogenesis, and finally on day 9 to represent a later stage of differentiation.

However, to be able to compare mRNA expression of the ASC between the two culture systems an isolation step had to be introduced after harvesting the cultures, in which MVEC had to be removed from the cultures. Therefore a cell separation protocol using anti-CD31-conjugated magnetic beads was established. It could be demonstrated that an ASC/MVEC mixture was successfully separated into a bead-free fraction that contained only CD31-negative cells and a bead-bound fraction including only CD31-positive cells (Fig. 6-11, a-c). When ASC and MVEC were labeled with 2 different PKH dyes prior to mixing, subsequent magnetic separation led to pure ASC and MVEC fractions, respectively, which proved that all EC, but no ASC were actually coupled to the beads (Fig. 6-11, d&e). To utilize this method for the 3-D cocultures, spheroids had to be dissociated by treating them with trypsin before magnetic separation. For comparability, this was also done for the ASC monocultures. Magnetic bead separation was also successful after the dissociation step (data not shown).

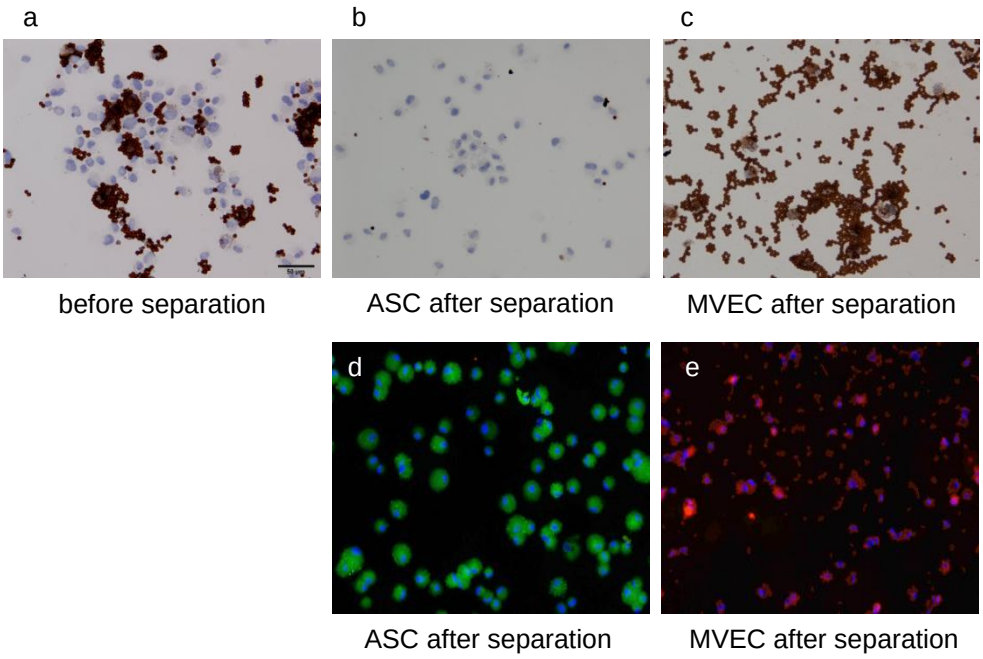

Figure 6-11: *Cell separation with magnetic beads: proof of principle. Anti-CD31-conjugated Dynabeads were added to an ASC/MVEC suspension and allowed to bind (a). The CD31-positive (c,e) and -negative (b,d) fractions were separated with a magnet. Immunostaining for CD31 (brown in images a-c) proved that the beads specifically bound to cells exhibiting the CD31 antigen (a), which could be completely removed from the ASC fraction (b) and were accumulated in the MVEC fraction (c). When cells were stained with PKH membrane dyes before mixing them (ASC: green; MVEC: red), it could be shown by immunofluorescence that indeed no MVEC remained in the non-binding fraction (d) and no ASC ended up in the bead-binding fraction (e). Please note that the beads (bound to cells or free) appear as brown dots in the IHC images (a-c) and as weakly red fluorescing dots in the IF images (d,e). Red MVEC fluorescence in (e) is strongly attenuated as cells are covered by the beads.*

For the LDA analysis, spheroids were harvested and dissociated at the specific time points mentioned above. ASC were depleted of MVEC by the newly established magnetic separation step, and total RNA was isolated from these samples, followed by reverse transcription and gene expression measurement with the 384-well arrays.

Data analysis revealed that the central adipogenic transcription factors PPARγ and C/EBPα were, as expected, strongly upregulated in all induced groups by day 2 and even more by day 9. The expression pattern was comparable for mono- and cocultures, and as a consequence no significant differences between the two culture types could be detected at any time point (Fig. 6-12 A,B). This was in general also true for other transcription factors like C/EBPβ and C/EBPδ (Fig. 6-12 C,D), which are usually upregulated during early adipogenesis, as well as SREBF1 (coding for SREBP1-c). Yet, the latter exhibited a significantly decreased expression in cocultures on day 9 when induced, but an increase when not induced (Fig. 6-12 E).

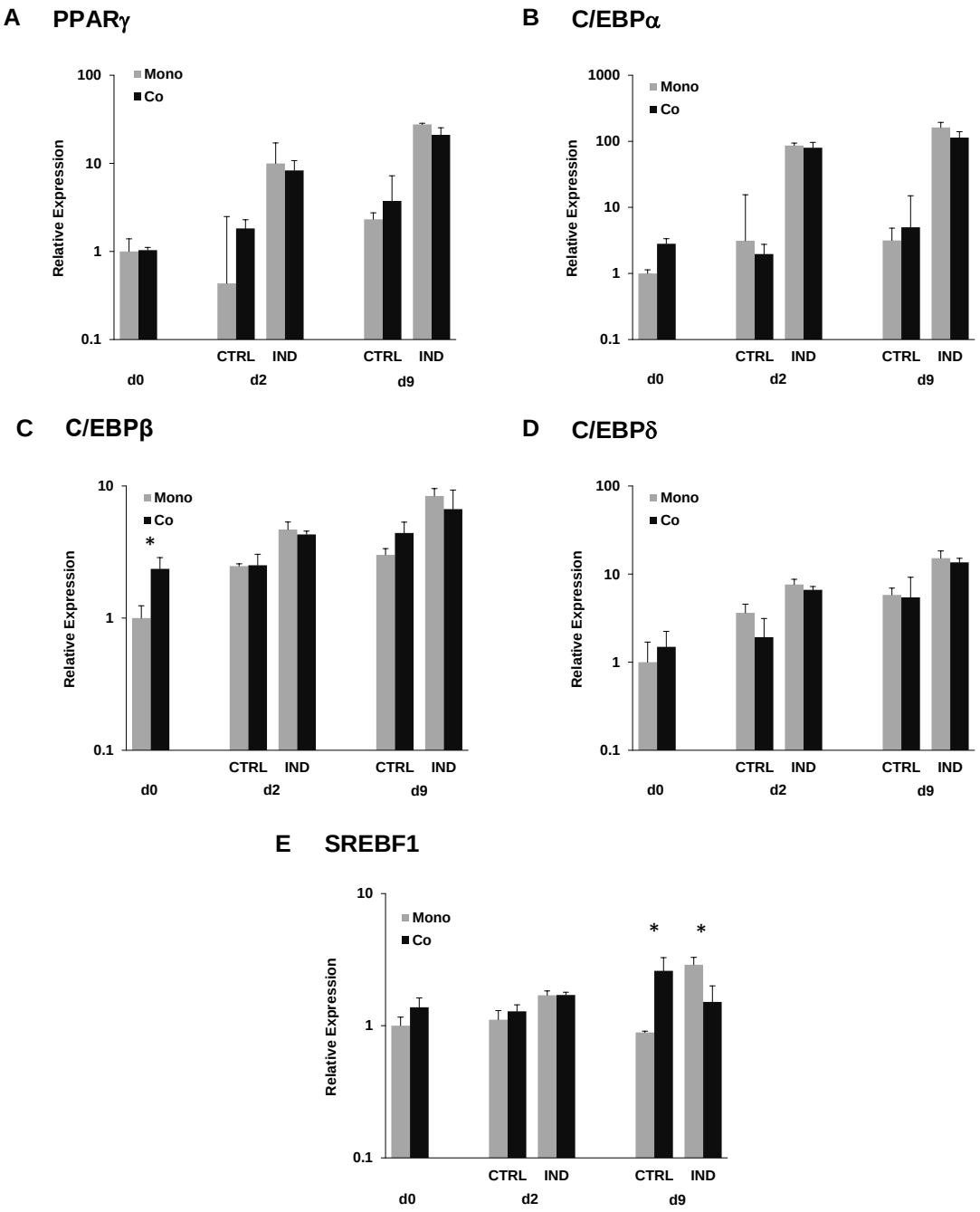

Figure 6-12: *Relative gene expression data (n=3) of the adipogenesis-related transcription factors PPARγ, C/EBPα, C/EBPβ, C/EBPδ and SREBF1 as determined by qRT-PCR using TaqMan Low Density Arrays. All mRNA levels are expressed relative to the value at d0 in monoculture. Statistically significant differences between co- and monocultures are indicated by * (p<0.05).*

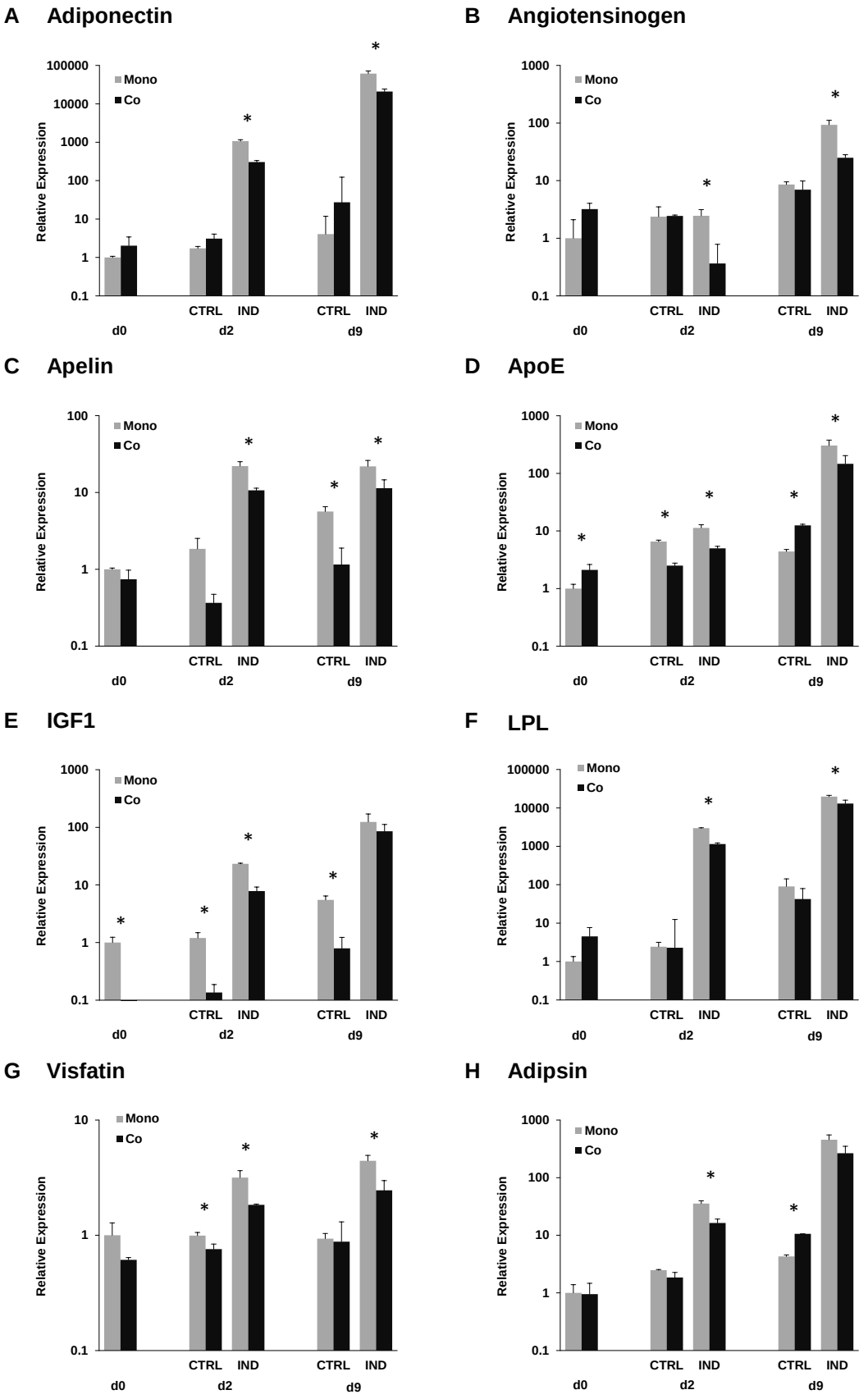

Figure 6-13: *Relative gene expression data (n=3) of several adipocyte marker genes as determined by qRT-PCR using TaqMan Low Density Arrays. All mRNA levels are expressed relative to the value at d0 in monoculture. Statistically significant differences between co- and monocultures are indicated by * (p<0.05).*

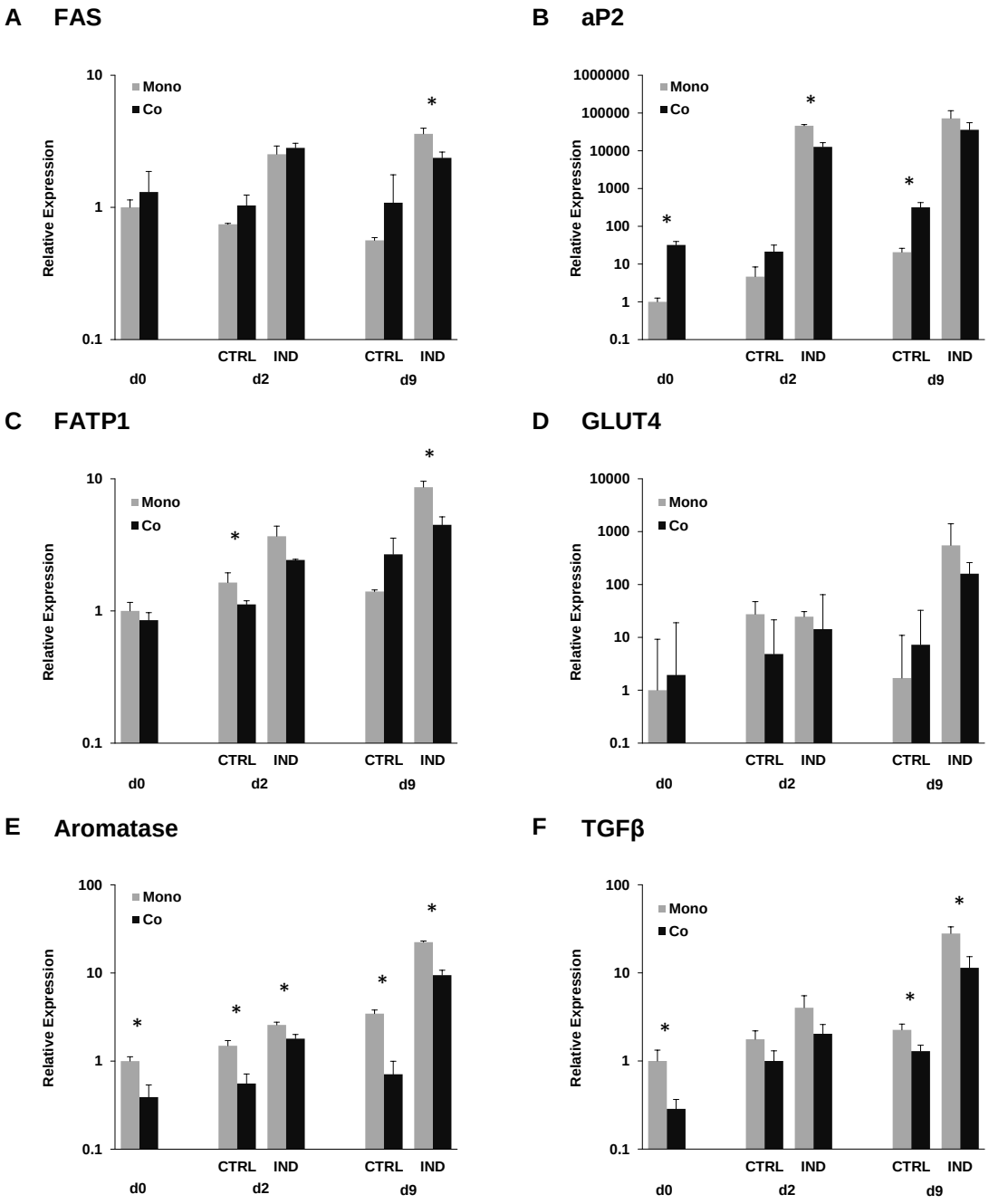

Figure 6-14: *Relative gene expression data (n=3) of several genes associated with lipid synthesis and transport (A-D) as well as other genes with reduced expression in cocultures (E,F) as determined by qRT-PCR using TaqMan Low Density Arrays: All mRNA levels are expressed relative to the value at d0 in monoculture. Statistically significant differences between co- and monocultures are indicated by * ($p<0.05$).*

In contrast to the transcription factors, many adipokines and other adipocyte marker genes exhibited a distinct difference in gene expression between cocultures and ASC monocultures, as shown in figures 6-13 and 6-14. Strikingly, in the vast majority of these genes the upregulation of mRNA levels after adipogenic induction was significantly reduced in cocultures as compared to monocultures. In most cases, e.g. for adiponectin, angiotensinogen, apelin, ApoE or LPL, this difference was detectable on day 2 as well as on

day 9. In other cases (e.g. for adipsin, FAS or aP2), at least a tendency, albeit not significant, could be observed at both post-induction time points. By contrast, none of these genes were expressed significantly higher in the induced cocultures at any time point. Apart from the mentioned differences, the general gene expression pattern of the ASC in the cocultures was comparable to monocultures.

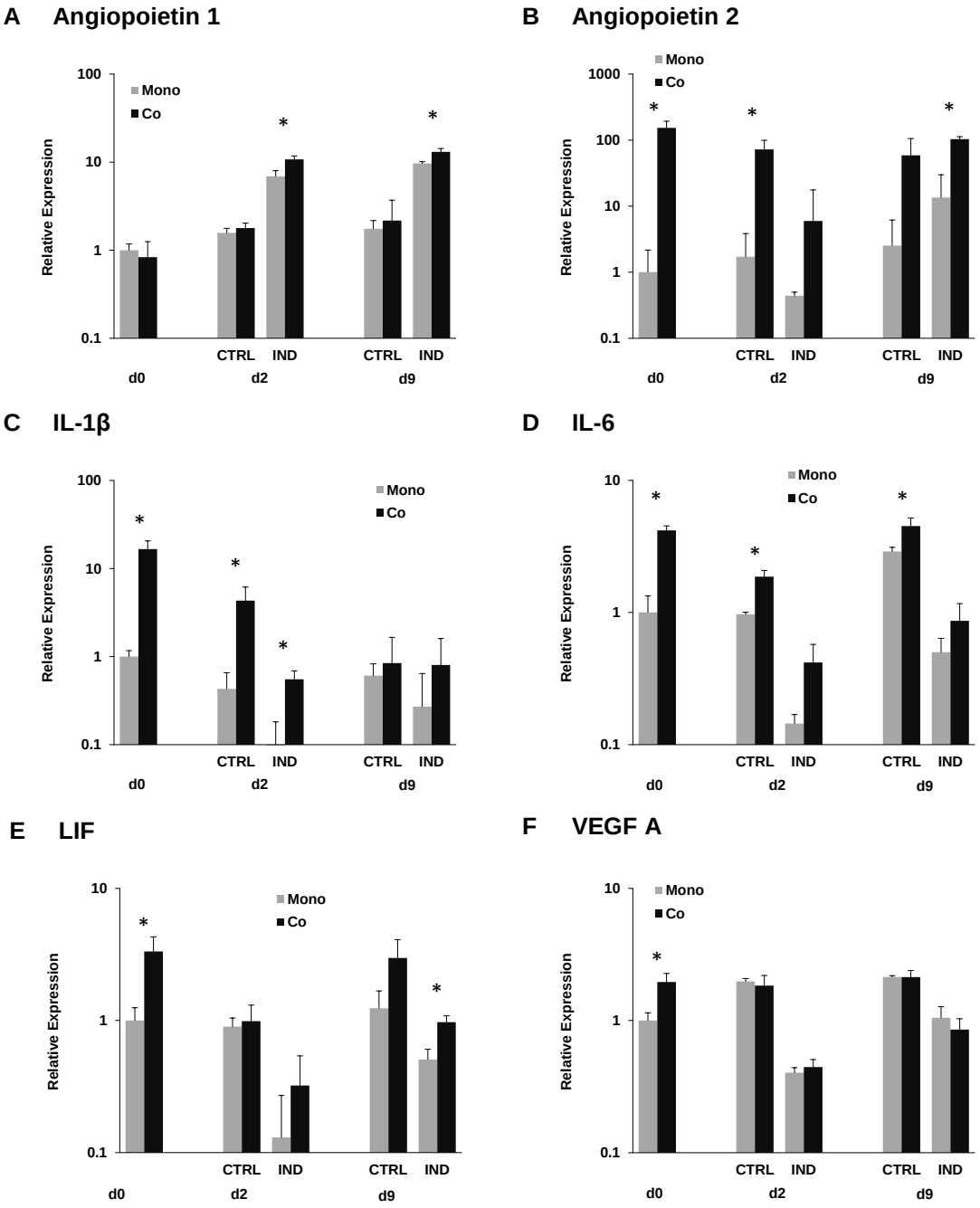

Figure 6-15: *Relative gene expression data (n=3) of several genes associated with angiogenesis as well as other genes with increased expression in cocultures as determined by qRT-PCR using TaqMan Low Density Arrays: All mRNA levels are expressed relative to the value at d0 in monoculture. Statistically significant differences between co- and monocultures are indicated by * (p<0.05).*

In addition to the adipogenesis-related genes mentioned above, also several other genes were included in our LDA. Interestingly, some of these genes were expressed on a higher level in cocultures as compared to ASC monocultures. For angiopoietin 2, IL-1β, IL-6, LIF and VEGF A, mRNA data revealed a significant difference between the two culture systems already on day 0, and in most of these also at later time points at least a tendency towards a higher expression could be observed, mostly independent of adipogenic induction (Fig. 6-15). This was in strong contrast to almost all of the genes associated with adipogenesis, for which a decreased expression had been detected in cocultures as described above.

6.5 Discussion

6.5.1 Structure of coculture spheroids: Cellular self-assembly, cell type distribution and EC networks

When ASC were cocultured with MVEC in our 3-D spheroid model using the optimized culture conditions established previously (Chapter 5), long-term stable constructs could be generated successfully. Over the whole culture time, these coculture spheroids were of smaller size than corresponding monocultures. This difference may partly be attributed to the fact that some of the MVEC seeded into the agarose-coated wells did not contribute to the formation of the spheroids. Indeed, a small number of single cells not included into the constructs could be observed within the wells after coculture spheroid formation (data not shown). However, confocal images of PKH-stained cocultures as well as cryosections stained for CD31 revealed that on early time points a large proportion of endothelial cells were present within the 3-D constructs, implying that the majority of the MVEC *was* included in the constructs. Instead, the main cause for the smaller volumes of the coculture spheroids can possibly be found in the different properties of the two cell types regarding cell size, cellular aggregation and tissue self-assembly. For fibroblast/HUVEC cocultures, Kunz-Schughart et al. hypothesized that the majority of EC were located in the extracellular space of the 3-D fibroblast structure and thus did not contribute to an overall increase in spheroid size [16]. As the ASC possess a morphology which is very similar to fibroblasts, this hypothesis may also play a role for our model.

It can be assumed that the distinct functional and morphological properties of the ASC and MVEC also account for the development of specific 3-dimensional patterns. In the first phase after spheroid formation, the surface layer of our constructs was predominantly composed of MVEC. Similar observations have been made for coculture spheroids of HUVEC with smooth

muscle cells (SMC) by Korff et al. [17]. For human osteoblasts (hOB) cocultured with HUVEC, it was also demonstrated that EC accumulated predominantly in the peripheral regions of spheroids, albeit this pattern developed only after several days of culture [14,18]. In contrast, when cocultured with fibroblasts, EC were located preferentially in the center of the constructs [15]. However, while in these studies an almost completely segregated distribution of the cell types was observed, in our coculture system EC were not only located in the surface layer, but also in central regions of the constructs shortly after spheroid self-assembly. This is in accordance with a recent study in which spheroids from BMSC and HUVEC were generated using a medium containing methylcellulose [19]. Herein, the authors suggest that the relative positioning of the different cell types may, among other factors, be determined by differences in cell-cell-adhesion and surface tension, as first proposed in the differential adhesion hypothesis in 1962 [20]. According to this hypothesis, the cells with the highest cohesion form the inner core of a spheroid, while those with a lower cohesion accumulate at the periphery [19–21]. The lower cellular cohesion of the MVEC as compared to the ASC also becomes obvious through the fact that the generation and maintenance of MVEC monoculture spheroids was, in strong contrast to ASC monocultures, not possible in our liquid overlay culture system due to a much lower tendency to self-aggregate and, as a consequence, a low mechanical stability of the resulting constructs.

For the cocultures, it became obvious that with increasing culture time the proportion of MVEC within the spheroids gradually decreased, both with and without adipogenic induction. Nevertheless, a small, but significant population of MVEC remained in the spheroids up to day 14, as confirmed by immunostaining and confocal microscopy. This observation was supported by total DNA measurement, which indicated that cell numbers in cocultures were significantly lower than in ASC monocultures at this time point, yet remained above 50% of those values. As only small numbers of dead cells were detected in the cocultures, which were not higher than in ASC monocultures, we can assume that the EC loss was mainly based on MVEC migrating out of and/or losing contact to the 3-D construct rather than apoptosis within the spheroid. This hypothesis is supported by the observation that the surface layer of endothelial cells was no longer present on day 3, which could indicate that the majority of EC forming this outer layer had detached from the spheroid, strongly reducing the overall number of MVEC.

A loss of endothelial cells during culture was also reported in other studies involving coculture spheroids. Interestingly, with fibroblast/HUVEC spheroids it was found that independent of the initial seeding ratio, eventually a constant proportion of 10% EC was detected after prolonged culture [16], suggesting that in the 3-D environment cells migrate and self-assemble in a certain way, so that an optimal cell-type-ratio is achieved. A similar behavior of EC loss after high seeding ratios was also observed with large BMSC/HUVEC

spheroids, however with the final EC proportion not being constant and reaching a minimum of 5% [22]. In this project, the dependence on initial seeding ratio was not extensively studied, but our data suggest that the use of 80% MVEC instead of 50% resulted in a higher proportion of endothelial cells after 7 days of culture.

While the overall MVEC proportion decreased in our spheroids over time, the remaining endothelial cells began to organize themselves, forming a network of vascular-like structures. At the same time, they started to accumulate in specific regions of the constructs, leaving other parts almost free of EC. Interestingly, the cells aligned in a similar way, regardless of whether the cultures were adipogenically induced or not. In immunofluorescence images, some of the MVEC clusters even appeared to contain lumina as early as 4 days after seeding, which suggests that indeed capillary-like structures had developed at least in parts of the MVEC network. The formation of an extensive endothelial cell network has also been described for EC grown on fibroblast sheets or in fibroblast/HUVEC spheroids, and in both cases some of the structures contained lumina [16,23]. For BMSC/EC spheroid cultures, Rouwkema et al. reported the development of organized EC structures when only 2% of the seeded cells were HUVEC, with lumina developing after implantation of the constructs into nude mice [22]. For ASC/HUVEC spheroids, an EC proportion of 80% was reported to be necessary for the formation of prevascular structures [24]. Kang et al. cocultured hASC and HUVEC on silk fibroin scaffolds and observed extensive lumen formation after 2 weeks of culture [25]. In general, the formation of EC structures was observed in all of these studies. However, the experimental setup applied in them was different from ours, regarding either the cell types used (HUVEC vs. MVEC), the method of 3-D culture, the spheroid sizes, the culture media or combinations of these, which may account for the observed differences. HUVEC are embryonic and may not only differ from organ-specific EC, but with respect to clinical applications, the use of HUVEC is problematic due to incompatibility with the host's immune system, whereas MVEC could be isolated from autologous adipose tissue together with ASC [26,27].

6.5.2 Cellular sprouting of co- and monocultures: Angiogenesis assays

Several *in vitro* angiogenesis assays have been described in literature for the evaluation of endothelial cell functionality and its dependence on exogenous factors [28–30]. In most of these, the outgrowth of cellular strands from cultures embedded into a gel-based matrix is evaluated. In this project, we utilized a sprouting assay in which our co- and monoculture spheroids were embedded into Matrigel. The outgrowth of cellular strands from the spheroids was more prominent when EGM2 alone was applied instead of EGM2/PGM2 mixture, which can be explained by the higher concentrations of growth factors present [31–33]. However, it

was remarkable that under EGM2 treatment extensive sprouting not only took place for the cocultures, but also for ASC monoculture spheroids, with strand length and density being comparable between the two groups. As ASC are pluripotent, they can be differentiated towards the endothelial lineage by providing appropriate culture conditions. In principle, this might be an explanation for the observed sprouting of ASC monocultures [34,35], although it is highly unlikely to have occurred to such a large extent in a rather short time period. Outgrowth of cellular strands from BMSC and ASC spheroids in fibrin gels has already been described by Verseijden et al., however possible reasons for this behavior were not discussed [36]. Wenger et al. observed sprouting after embedding hOB/HUVEC coculture and hOB monoculture spheroids into collagen gel. They suggested that hOB outgrowth was of a different type that HUVEC sprouting: While the latter would involve a linear alignment of migrating endothelial cells, sprouts from hOB monocultures did not contain nuclei and therefore could represent cell filopodia invading the surrounding matrix [14]. However, in our coculture model, PKH-staining revealed that the sprouts of co- and monocultures were indeed composed of multiple cells. In the case of cocultures both ASC and MVEC could be detected within the outgrowing strands (with ASC being in a vast majority), and branching occurred frequently. All in all, cellular sprouting did not appear to be influenced by the presence of endothelial cells within the spheroids. In general, with respect to the observed outgrowth also from ASC monocultures, the significance of this type of *in vitro* assays for the evaluation of angiogenesis should be carefully considered in future applications.

6.5.3 Adipogenic differentiation of coculture spheroids: Influence of the endothelial cells

Concerning the cellular crosstalk between (developing) adipocytes and endothelial cells, one of the major questions we intended to address was the influence of the EC on the adipogenic differentiation of the ASC. Although there have been several studies describing the cocultivation of (pre)adipocytes and EC as described above, only a small number of reports dealing with the specific effects of the coculture environment on ASC functions in more detail can be found in the literature. Some of these have described an increase in preadipocyte proliferation, e.g. after exposing human preadipocytes to hMVEC-conditioned medium [37], after combining these two cell types in a fibrin matrix [38], or when 3T3-L1 cells were cocultured with HUVEC in 2-D [39].

With respect to adipogenesis, results from previous studies were rather conflicting, and appeared to be strongly influenced by culture conditions. For example, an earlier study reported that exposure to EC-conditioned medium stimulated adipogenic differentiation of human preadipocytes, however the effect was completely masked by the application of an

exogenous induction cocktail [40]. In contrast, Hutley et al. observed an increased differentiation after direct coculture with EC [41], while in another report, direct coculture of ASC with HUVEC significantly reduced adipogenesis [42]. When evaluating these reports, one has to consider that these studies were conducted using 2-D culture. Taking into account our results from Chapter 4, the process of adipogenesis may however differ significantly in a 2-D culture system as compared to a 3-D environment.

There are also some studies in which hydrogel-based 3-D culture techniques were utilized. Coculturing rat lung EC and mature adipocytes in a collagen gel led to a dedifferentiation of the adipocytes, but not treatment with conditioned medium [43]. Lai et al. combined 3T3-L1 preadipocytes with HUVEC, also in collagen gels, and observed an elevated triglyceride accumulation, but only with a very high seeding density and using a preadipocyte/HUVEC ratio of 90:10, whereas in most other cases adipogenesis was rather reduced as compared to monocultures [39]. Whereas the culture systems applied in these studies either lacked direct cell-cell-contact or a 3-dimensional environment, our spheroid model was able to provide both of these prerequisites and therefore more closely mimicked conditions that can be found *in vivo*. We could demonstrate that the cocultivation with MVEC significantly reduced the triglyceride accumulation within ASC in comparison to monoculture spheroids when they were induced to undergo adipogenesis. Furthermore, cryosections revealed a distinct spatial distribution of lipid accumulation, which occurred preferentially in regions of the constructs that were free of endothelial cells – a phenomenon which will be discussed later in more detail. The observed decrease in adipogenic differentiation was in accordance with a recent study, which utilized coculture spheroids of BMSC and HUVEC. Interestingly, therein the authors report that at the same time osteogenic differentiation was elevated under coculture conditions [19], an observation supported also by several studies using 2-D culture models [44–46]. Thus, it is possible that EC signaling plays a role in the determination of mesenchymal cell fate.

While many of the above studies were primarily based on qualitative data, in this project our goal was to investigate the effects of a direct 3-D coculture of ASC with MVEC for the first time also on gene expression level, with our focus being on adipogenic differentiation. In order to assess mRNA levels of the ASC only, it was necessary to remove the MVEC from our cocultures after harvesting the samples. Therefore, the two cell types were separated using CD31-coupled magnetic beads after enzymatic dissociation of the spheroids. Beforehand, the efficiency of this magnetic sorting method, which has already been demonstrated for cocultures of HUVEC and human osteoprogenitor cells [45], was verified in our culture system.

Gene expression analysis was performed using TaqMan Low Density Arrays, which included, among others, many adipogenesis-related genes. mRNA levels of the central

transcription factors that regulate adipogenesis, PPARγ and C/EBPα, were comparable between mono- and cocultures. However, gene expression levels of various adipogenic markers and adipokines, such as adiponectin, angiotensinogen, apelin, ApoE, LPL or visfatin were significantly lower in the ASC when cocultured with endothelial cells than in monoculture spheroids after adipogenic induction. For the genes mentioned, the difference between the two culture systems was not only evident on day 9, but already on day 2 after application of the adipogenic cocktail. For other genes, e.g. adipsin, FAS, aP2 and FATP1, such a significant difference was detected at least for one of the time points. For virtually all of the adipogenic markers, there was at least a trend towards a lower expression in the cocultures. Thus, we could show that the significantly reduced ASC lipid accumulation detected within the cocultures was reflected also on gene expression level. The fact that the relevant genes were only reduced to a certain degree is supported by the results from histological staining, which had shown that lipid accumulation in the cocultures was more or less limited to MVEC-free areas. These data may indicate that in the coculture spheroids, adipogenesis is strongly inhibited in the ASC which are close to the MVEC, while normal differentiation takes place within the more distant ASC, resulting in the partially reduced expression of marker genes that has been observed in the LDA.

Interestingly, genes not directly associated with adipogenesis did not exhibit a decrease in expression in the cocultures. On the contrary, for some of these genes even higher mRNA levels could be detected in the presence of endothelial cells. For example, expression of angiopoietin 1 (Ang-1), which is known as a potent angiogenic factor [2,8,37], was significantly elevated on days 2 and 9 after induction. Furthermore, expression of VEGF A as well as angiopoietin 2 (Ang-2), IL-1β, IL-6 and LIF was increased in coculture already on day 0, i.e. 2 days after seeding. Ang-2 plays an important role in angiogenesis, as in the presence of VEGF it may stimulate vessel growth by loosening endothelial-periendothelial cell interactions, degrading the ECM and enabling EC migration and proliferation [2,8,37]. The interleukins IL-1β [47,48] and IL-6 [49,50] have also been described to be involved in stimulating angiogenesis. Upregulation of Ang-1 and IL-1β was also observed by Aguirre et al., who cocultured BMSC and bone marrow-derived endothelial progenitor cells (BM-EPCs) in 2-D, yet without adipogenic differentiation and without separating the two cell types before PCR analysis [51]. Although our data require further confirmation through additional experiments and/or analytical methods, the observed gene expression patterns suggest an upregulation of pro-angiogenic factors in ASC within coculture spheroids in response to the presence of MVEC.

Apart from these findings, the regional selectivity of TG accumulation in the coculture spheroids was of special interest. As described above, about 2 days after seeding the EC began organizing in a network-like fashion, while at the same time accumulating in certain

regions of the spheroids. Strikingly, the evaluation of consecutive cryosections stained for triglycerides and CD31, respectively, revealed that after adipogenic induction lipid droplets developed mainly in those areas of the constructs not containing endothelial cells anymore. While the reduction of adipogenesis was obviously caused by the MVEC included in the spheroids, the observed spatial selectivity can also help to understand the nature of the interplay between the two cell types. In general, it is possible that the EC communicate with the ASC through paracrine signaling pathways, ECM components or direct cell-cell-interactions [7]. However, paracrine regulation via the secretion of growth factors and cytokines from the EC should have affected all of the ASC within the spheroid. While it cannot be ruled out that adipogenic differentiation was also somewhat reduced in ASC distant from the MVEC, a complete absence in TG accumulation only occurred for ASC in close proximity to the endothelial cell structures and clusters. These findings suggest that the signaling events involved in the inhibition of adipogenic differentiation are only effective over a short distance around the endothelial cells. The effective range of the responsible factors may, for example, be limited due to their fast degradation, as a result of their almost complete uptake by the surrounding cells, or because their transport is hindered by the dense ECM present in the 3-D spheroids. Another explanation would be that direct cell-cell contact is necessary for EC to influence adipogenic differentiation.

Other studies have also shown that spatial proximity can be necessary for certain MVEC influences to come into effect. For example, using 2-D cultures, it was demonstrated in two independent studies that MVEC only enhanced osteogenic differentiation of BMSC in direct coculture, but not when conditioned media were applied, or when EC were cultured on transwell inserts in the same medium [44,52]. In another report, these findings could be attributed to the formation of gap junctions between the two cell types being necessary for signal transduction [53]. Similarly, conditioned media from HUVEC were shown to have no effect also on MSC adipogenesis [46].

Further investigations are needed to elucidate the specific signaling pathways involved in the cellular crosstalk between ASC and EC during adipose tissue development. In this context, in previous work, the Wnt pathway has been suggested to play a role [19,42]. Recent research has established Wnt/β-catenin signaling as a potent inhibitor of adipogenesis [54,55]. Moreover, it has also been suggested that this pathway is an important regulator of mesenchymal cell fate, e.g. by stimulating osteogenesis and inhibiting adipogenesis [56,57]. An enhanced osteogenesis has, as already mentioned, also been detected using coculture models more or less similar to ours [19]. In a similar way, the Wnt pathway could be responsible for the reduction of adipogenic differentiation observed in our spheroid system. On the other hand, we also have to consider previous findings demonstrating that an increase of Wnt signaling also occurred after exposing ASC to EC-conditioned medium,

albeit with a different expression pattern of the single Wnt genes as compared to direct coculture, meaning that at least part of the EC-mediated reduction of adipogenesis can be attributed to effects not requiring direct cell-cell contact [42]. However, these results, which are based on 2-D cultures, are not in disagreement with our data, because as mentioned above, it is possible that in our 3-D spheroid model secreted factors were trapped within the ECM or quickly taken up by the surrounding ASC, which could explain that the inhibiting paracrine effect on adipogenesis was limited to ASC close to the EC.

Nevertheless, we could not detect a downregulation of PPARγ or C/EBPα in our cocultures, whereas in other reports the Wnt effector β-catenin was found to suppress expression of these transcription factors [57,58]. Consequently, further studies have to be performed to clarify the role of the Wnt/β-catenin signaling pathway in the regionally selective reduction of adipogenic differentiation within the ASC/MVEC coculture spheroids.

6.6 Conclusion

In this chapter, the 3-D ASC/MVEC coculture model established previously (Chapter 5) was characterized with regard to spheroid properties, cellular self-organization within the constructs and especially the regulatory interplay between the two cell types. The main focus was set on the influence of the endothelial cells on adipogenic differentiation.

While coculture spheroids were in general smaller than equivalent ASC monocultures, they remained mechanically stable and viable during prolonged culture. As described for other EC coculture systems, the proportion of endothelial cells within the constructs decreased over time, but at the same time the ASC supported the formation of endothelial cell networks in parts of the spheroids.

The spheroid coculture model was also successfully applied to investigate the regulatory influence of the EC on ASC differentiation. On a functional and also on a molecular level, we showed that adipogenesis in cocultures was significantly impaired as compared to ASC monocultures. Lipid accumulation was completely absent in close proximity to the EC structures, but not in more distant areas, meaning that the inhibitory effect on ASC adipogenesis was limited to a region within a short distance from the MVEC. While the specific mechanisms involved in this spatially selective inhibition remain to be clarified, our results indicate that the Wnt/β-catenin signaling pathway may play a role. Furthermore, expression of some pro-angiogenic factors by the ASC was elevated under coculture, which in turn could influence EC performance and functions. Thus, our coculture spheroids proved to be useful for shedding light onto the complex cellular crosstalk and reciprocal regulation between developing adipocytes and endothelial cells within a 3-D microenvironment.

Apart from that, the spheroids could serve as a tool to generate prevascularized adipose tissue for applications in regenerative medicine. Adipose tissue transplants based on our 3-D cocultures could help to improve nutrient and oxygen supply within the implanted grafts, as the preformed vascular structures within the constructs can connect with the host vasculature after implantation. This could prevent necrosis in the center of larger constructs and help to overcome limitations regarding transplant size.

6.7 References

1. Herbert S P, Stainier D YR. Molecular control of endothelial cell behaviour during blood vessel morphogenesis. *Nat Rev Mol Cell Biol* 2011; **12***, 9*, 551–564.
2. Carmeliet P, Jain R K. Molecular mechanisms and clinical applications of angiogenesis. *Nature* 2011; **473***, 7347*, 298–307.
3. Nishimura S, Manabe I, Nagasaki M, Hosoya Y, Yamashita H, Fujita H, Ohsugi M, Tobe K, Kadowaki T, Nagai R, Sugiura S. Adipogenesis in obesity requires close interplay between differentiating adipocytes, stromal cells, and blood vessels. *Diabetes* 2007; **56***, 6*, 1517–1526.
4. Christiaens V, Lijnen H R. Angiogenesis and development of adipose tissue. Molecular and cellular aspects of adipocyte development and function. *Mol Cell Endocrinol* 2010; **318***, 1-2*, 2–9.
5. Fukumura D, Ushiyama A, Duda D G, Xu L, Tam J, Krishna V, Chatterjee K, Garkavtsev I, Jain R K. Paracrine regulation of angiogenesis and adipocyte differentiation during in vivo adipogenesis. *Circ Res* 2003; **93***, 9*, e88-97.
6. Rehman J, Traktuev D, Li J, Merfeld-Clauss S, Temm-Grove C J, Bovenkerk J E, Pell C L, Johnstone B H, Considine R V, March K L. Secretion of angiogenic and antiapoptotic factors by human adipose stromal cells. *Circulation* 2004; **109***, 10*, 1292–1298.
7. Cao Y. Angiogenesis modulates adipogenesis and obesity. *J Clin Invest* 2007; **117***, 9*, 2362–2368.
8. Lijnen H R. Angiogenesis and obesity. *Cardiovasc Res* 2008; **78***, 2*, 286–293.
9. Butler J M, Kobayashi H, Rafii S. Instructive role of the vascular niche in promoting tumour growth and tissue repair by angiocrine factors. *Nat Rev Cancer (Nature reviews. Cancer)* 2010; **10***, 2*, 138–146.
10. Rouwkema J, Rivron N C, van Blitterswijk C A. Vascularization in tissue engineering. *Trends Biotechnol* 2008; **26***, 8*, 434–441.
11. Grellier M, Bordenave L, Amédée J. Cell-to-cell communication between osteogenic and endothelial lineages: implications for tissue engineering. *Trends Biotechnol* 2009; **27***, 10*, 562–571.
12. Kaully T, Kaufman-Francis K, Lesman A, Levenberg S. Vascularization--the conduit to viable engineered tissues. *Tissue Eng Part B Rev* 2009; **15***, 2*, 159–169.
13. Laschke M W, Harder Y, Amon M, Martin I, Farhadi J, Ring A, Torio-Padron N, Schramm R, Rucker M, Junker D, Haufel J M, Carvalho C, Heberer M, Germann G, Vollmar B, Menger M D. Angiogenesis in tissue engineering: breathing life into constructed tissue substitutes. *Tissue Eng* 2006; **12***, 8*, 2093–2104.
14. Wenger A, Stahl A, Weber H, Finkenzeller G, Augustin H G, Stark G B, Kneser U. Modulation of in vitro angiogenesis in a three-dimensional spheroidal coculture model for bone tissue engineering. *Tissue Eng* 2004; **10***, 9-10*, 1536–1547.
15. Wenger A, Kowalewski N, Stahl A, Mehlhorn A T, Schmal H, Stark G B, Finkenzeller G. Development and characterization of a spheroidal coculture model of endothelial cells and fibroblasts for improving angiogenesis in tissue engineering. *Cells Tissues Organs* 2005; **181***, 2*, 80–88.
16. Kunz-Schughart L A, Schroeder J A, Wondrak M, van Rey F, Lehle K, Hofstaedter F, Wheatley D N. Potential of fibroblasts to regulate the formation of three-dimensional

vessel-like structures from endothelial cells in vitro. *Am J Physiol Cell Physiol* 2006; **290***, 5*, 1385–1398.

17. Korff T, Kimmina S, Martiny-Baron G, Augustin H. Blood vessel maturation in a 3-dimensional spheroidal coculture model: direct contact with smooth muscle cells regulates endothelial cell quiescence and abrogates VEGF responsiveness. *FASEB J* 2001; **15***, 2*, 447–457.
18. Stahl A, Wenger A, Weber H, Stark G B, Augustin H G, Finkenzeller G. Bi-directional cell contact-dependent regulation of gene expression between endothelial cells and osteoblasts in a three-dimensional spheroidal coculture model. Calcium Signaling and Disease. *Biochem Biophys Res Commun* 2004; **322***, 2*, 684–692.
19. Saleh F A, Whyte M, Genever P G. Effects of endothelial cells on human mesenchymal stem cell activity in a three-dimensional in vitro model. *Eur Cell Mater* 2011; **22**, 242–257.
20. Steinberg M S. On the mechanism of tissue reconstruction by dissociated cells. I. Population kinetics, differential adhesiveness. and the absence of directed migration. *Proc Natl Acad Sci USA* 1962; **48**, 1577–1582.
21. Foty R A, Steinberg M S. The differential adhesion hypothesis: a direct evaluation. *Dev Biol (Developmental biology)* 2005; **278***, 1*, 255–263.
22. Rouwkema J, Boer J de, Blitterswijk C A. Endothelial cells assemble into a 3-dimensional prevascular network in a bone tissue engineering construct. *Tissue Eng* 2006; **12***, 9*, 2685–2693.
23. Sorrell J M, Baber M A, Caplan A I. A self-assembled fibroblast-endothelial cell co-culture system that supports in vitro vasculogenesis by both human umbilical vein endothelial cells and human dermal microvascular endothelial cells. *Cells Tissues Organs* 2007; **186***, 3*, 157–168.
24. Verseijden F, Posthumus-van S SJ, Farrell E, van Neck J W, Hovius S E, Hofer S O, van Osch G J. Prevascular structures promote vascularization in engineered human adipose tissue constructs upon implantation. *Cell Transplant* 2010; **19***, 8*, 1007–1020.
25. Kang J H, Gimble J M, Kaplan D L. In vitro 3D model for human vascularized adipose tissue. *Tissue Eng Part A* 2009; **15***, 8*, 2227–2236.
26. Hewett P W, Murray J C, Price E A, Watts M E, Woodcock M. Isolation and characterization of microvessel endothelial cells from human mammary adipose tissue. *In Vitro Cell Dev Biol Anim (In vitro cellular & developmental biology. Animal)* 1993; **29***, 4*, 325–331.
27. Springhorn J P. Isolation of human capillary endothelial cells from abdominal adipose tissue. *Cold Spring Harb Protoc* 2011; **2011***, 5*.
28. Auerbach R, Lewis R, Shinners B, Kubai L, Akhtar N. Angiogenesis assays: a critical overview. *Clin Chem* 2003; **49***, 1*, 32–40.
29. Ucuzian A A, Greisler H P. In vitro models of angiogenesis. *World J Surg* 2007; **31***, 4*, 654–663.
30. Goodwin A M. In vitro assays of angiogenesis for assessment of angiogenic and anti-angiogenic agents. *Microvasc Res* 2007; **74***, 2-3*, 172–183.
31. Liekens S, Clercq E de, Neyts J. Angiogenesis: regulators and clinical applications. *Biochem Pharmacol* 2001; **61***, 3*, 253–270.
32. Papetti M, Herman I M. Mechanisms of normal and tumor-derived angiogenesis. *Am J Physiol Cell Physiol* 2002; **282***, 5*, C947-970.

33. Ribatti D, Conconi M T, Nussdorfer G G. Nonclassic endogenous novel regulators of angiogenesis. *Pharmacol Rev* 2007; **59***, 2*, 185–205.

34. Planat-Benard V, Silvestre J-S, Cousin B, Andre M, Nibbelink M, Tamarat R, Clergue M, Manneville C, Saillan-Barreau C, Duriez M, Tedgui A, Levy B, Penicaud L, Casteilla L. Plasticity of human adipose lineage cells toward endothelial cells: physiological and therapeutic perspectives. *Circulation* 2004; **109***, 5*, 656–663.

35. Madonna R, Caterina R de. In vitro neovasculogenic potential of resident adipose tissue precursors. *Am J Physiol Cell Physiol* 2008; **295***, 5*, C1271-1280.

36. Verseijden F, Posthumus-van Sluijs S J, Pavljasevic P, Hofer S O, van Osch G J, Farrell E. Adult human bone marrow- and adipose tissue-derived stromal cells support the formation of prevascular-like structures from endothelial cells in vitro. *Tissue Eng Part A* 2010; **16***, 1*, 101–114.

37. Augustin H G, Koh G Y, Thurston G, Alitalo K. Control of vascular morphogenesis and homeostasis through the angiopoietin-Tie system. *Nat Rev Mol Cell Biol* 2009; **10***, 3*, 165–177.

38. Borges J, Müller M C, Momeni A, Stark G B, Torio-Padron N. In vitro analysis of the interactions between preadipocytes and endothelial cells in a 3D fibrin matrix. *Minim Invasive Ther Allied Technol* 2007; **16***, 3*, 141–148.

39. Lai N, Jayaraman A, Lee K. Enhanced proliferation of human umbilical vein endothelial cells and differentiation of 3T3-L1 adipocytes in coculture. *Tissue Eng Part A* 2009; **15***, 5*, 1053–1061.

40. Varzaneh F E, Shillabeer G, Wong K L, Lau D CW. Extracellular matrix components secreted by microvascular endothelial cells stimulate preadipocyte differentiation in vitro. *Metabolism* 1994; **43***, 7*, 906–912.

41. Hutley L, Shurety W, Newell F, McGeary R, Pelton N, Grant J, Herington A, Cameron D, Whitehead J, Prins J. Fibroblast growth factor 1: a key regulator of human adipogenesis. *Diabetes* 2004; **53***, 12*, 3097–3106.

42. Rajashekhar G, Traktuev D O, Roell W C, Johnstone B H, Merfeld-Clauss S, van Natta B, Rosen E D, March K L, Clauss M. IFATS collection: Adipose stromal cell differentiation is reduced by endothelial cell contact and paracrine communication: role of canonical Wnt signaling. *Stem Cells* 2008; **26***, 10*, 2674–2681.

43. Aoki S, Toda S, Sakemi T, Sugihara H. Coculture of endothelial cells and mature adipocytes actively promotes immature preadipocyte development in vitro. *Cell Struct Funct* 2003; **28***, 1*, 55–60.

44. Kaigler D, Krebsbach P H, West E R, Horger K, Huang Y-C, Mooney D J. Endothelial cell modulation of bone marrow stromal cell osteogenic potential. *FASEB J* 2005, 04-2529fje.

45. Guillotin B, Bareille R, Bourget C, Bordenave L, Amédée J. Interaction between human umbilical vein endothelial cells and human osteoprogenitors triggers pleiotropic effect that may support osteoblastic function. *Bone* 2008; **42***, 6*, 1080–1091.

46. Saleh F A, Whyte M, Ashton P, Genever P G. Regulation of mesenchymal stem cell activity by endothelial cells. *Stem Cells Dev* 2011; **20***, 3*, 391–403.

47. Voronov E, Shouval D S, Krelin Y, Cagnano E, Benharroch D, Iwakura Y, Dinarello C A, Apte R N. IL-1 is required for tumor invasiveness and angiogenesis. *Proc Natl Acad Sci USA* 2003; **100***, 5*, 2645–2650.

48. Nakao S, Kuwano T, Tsutsumi-Miyahara C, Ueda S, Kimura Y N, Hamano S, Sonoda K, Saijo Y, Nukiwa T, Strieter R M, Ishibashi T, Kuwano M, Ono M. Infiltration of COX-

2-expressing macrophages is a prerequisite for IL-1 beta-induced neovascularization and tumor growth. *J Clin Invest* 2005; **115***, 11*, 2979–2991.

49. Hernández-Rodríguez J, Segarra M, Vilardell C, Sánchez M, García-Martínez A, Esteban M-J, Grau J M, Urbano-Márquez A, Colomer D, Kleinman H K, Cid M C. Elevated production of interleukin-6 is associated with a lower incidence of disease-related ischemic events in patients with giant-cell arteritis: angiogenic activity of interleukin-6 as a potential protective mechanism. *Circulation* 2003; **107***, 19*, 2428–2434.
50. Kim J Y, Bae Y H, Bae M K, Kim S R, Park H J, Wee H J, Bae S K. Visfatin through STAT3 activation enhances IL-6 expression that promotes endothelial angiogenesis. *Biochim Biophys Acta* 2009; **1793***, 11*, 1759–1767.
51. Aguirre A, Planell J A, Engel E. Dynamics of bone marrow-derived endothelial progenitor cell/mesenchymal stem cell interaction in co-culture and its implications in angiogenesis. *Biochem Biophys Res Commun* 2010; **400***, 2*, 284–291.
52. Villars F, Bordenave L, Bareille R, Amédée J. Effect of human endothelial cells on human bone marrow stromal cell phenotype: role of VEGF? *J Cell Biochem* 2000; **79***, 4*, 672–685.
53. Villars F, Guillotin B, Amédée T, Dutoya S, Bordenave L, Bareille R, Amédée J. Effect of HUVEC on human osteoprogenitor cell differentiation needs heterotypic gap junction communication. *Am J Physiol, Cell Physiol* 2002; **282***, 4*, C775-85.
54. Rosen E D, MacDougald O A. Adipocyte differentiation from the inside out. *Nat Rev Mol Cell Biol* 2006; **7***, 12*, 885–896.
55. Prestwich T C, MacDougald O A. Wnt/beta-catenin signaling in adipogenesis and metabolism. *Curr Opin Cell Biol* 2007; **19***, 6*, 612–617.
56. Bennett C N, Longo K A, Wright W S, Suva L J, Lane T F, Hankenson K D, MacDougald O A. Regulation of osteoblastogenesis and bone mass by Wnt10b. *Proc Natl Acad Sci U S A* 2005; **102***, 9*, 3324–3329.
57. Kang S, Bennett C N, Gerin I, Rapp L A, Hankenson K D, MacDougald O A. Wnt signaling stimulates osteoblastogenesis of mesenchymal precursors by suppressing CCAAT/enhancer-binding protein alpha and peroxisome proliferator-activated receptor gamma. *J Biol Chem* 2007; **282***, 19*, 14515–14524.
58. Liu J, Wang H, Zuo Y, Farmer S R. Functional interaction between peroxisome proliferator-activated receptor gamma and beta-catenin. *Mol Cell Biol* 2006; **26***, 15*, 5827–5837.

CHAPTER 7

Summary and Conclusion

7.1 Summary

For many years, the role of fat tissue in humans was considered to be limited to energy storage and metabolism. Today, it is well recognized that white adipose tissue also represents an important endocrine organ, which is part of a complex signaling network involved in the regulation of many physiological and pathophysiological processes. Furthermore, an excessive increase in adipose tissue mass, often caused by a shifted balance of energy expenditure and intake, leads to obesity, which has been demonstrated to be closely associated with common medical conditions such as type 2 diabetes, dyslipidemia and hypertension, summarized under the term “metabolic syndrome”. Hence, adipose tissue possesses great pharmacological and therapeutic potential and is increasingly considered as a promising drug discovery target. To make use of this potential, a thorough understanding of adipose tissue development and adipocyte functions is a prerequisite. However, current research in this field is largely based on conventional 2-dimensional (2-D) *in vitro* models, which cannot fully capture the complex microenvironment present *in vivo*, including the extensive cell-cell and cell-matrix interactions **(Chapter 1)**. Therefore, this thesis was focused on the establishment and characterization of a 3-dimensional (3-D) human adipose tissue model. Such a model system would not only be useful for basic research, but could ideally also be applied in tissue engineering and regenerative medicine, as well as in drug screening assays.

The generation of multicellular spheroids as a 3-D culture system for 3T3-L1 preadipocytes was previously developed by our group. Based on the experiences with this mouse cell line, in this work a spheroid model using human adipose-derived stem cells (ASC) was successfully established **(Chapter 3)**. With this 3-D culture system, it was possible to produce mechanically stable spheroids of defined size, in which ASC could be induced to undergo adipogenic differentiation. Culture conditions and protocols were optimized regarding basic media, FBS supplementation and hormonal induction cocktail in order to facilitate practical handling and subsequent analytics, to enhance flexibility, and to improve cost effectiveness for routine culture. Cryoconservation and multiple passaging at least up to P4 did not impair cell performance and adipogenic differentiation. By varying seeding density, it could be demonstrated that spheroids made from up to 5000 cells still exhibited a homogeneous lipid accumulation throughout the constructs after induction with an adipogenic hormonal cocktail.

Whereas it is well established that adipogenic differentiation involves a complex, highly regulated cascade of gene expression events, which has been extensively investigated in many studies using conventional 2-D culture, the role and influence of a tissue-like 3-D environment with respect to this process is still largely unknown. The newly developed hASC

spheroid model was therefore applied to characterize the process of adipogenesis in a scaffold-free 3-D culture system on a functional and molecular level, with a special focus on the comparison to conventional 2-D culture **(Chapter 4)**. It was found that the application of a short-term induction protocol was sufficient to induce a strong adipogenic response in the 3-D spheroids, while lipid accumulation was only minimal under the same conditions in 2-D. A gene expression array revealed that these differences were also reflected on the molecular level, with many fat cell markers and adipokines, as well as important transcription factors, being expressed at much higher levels in 3-D than in 2-D. Similarly, both histology and gene expression data indicated that hormonal induction without either 3-isobutyl-methylxanthine (IBMX) or indomethacin was sufficient for the development of functional adipocytes in 3-D spheroids, but not in 2-D monolayers. These findings demonstrated that adipogenesis within the 3-D environment provided by the spheroids was less dependent on exogenous stimulation than in conventional 2-D monolayers.

In vivo, adipogenesis is closely associated with angiogenesis. The reciprocal regulation and the intensive cellular crosstalk between (pre-)adipocytes and endothelial cells is of great importance for adipose tissue development as well as for the continuous expansion and regression that WAT can undergo *in vivo*. Up to now, however, almost all of our knowledge regarding the interdependence of adipogenesis and vascular growth is based on studies using various 2-D coculture systems. Therefore, it was the aim of the second part of this thesis to establish and characterize a 3-D coculture model of human ASC and human microvascular endothelial cells (MVEC) based on the monoculture spheroids developed in the first part of this work. In a first step, suitable culture conditions had to be found, which would provide suitable conditions to guarantee viability and proliferation of both cell types, without inhibiting the process of adipogenic differentiation after hormonal induction **(Chapter 5)**. To achieve this goal, in a series of experiments various media mixtures and culture protocols were tested in 2-D and 3-D cocultures. After first attempts resulted in a strongly impaired lipid accumulation, EGF (which was part of the endothelial cell basal medium) could be identified as the factor responsible for the reduced adipogenesis. Furthermore, it could be demonstrated that components of the adipogenic induction cocktail compromised MVEC viability. Consequently, the elimination of EGF from the culture medium as well as the application of a short-term adipogenic induction protocol, which had been demonstrated to be sufficient within the 3-D spheroid system in Chapter 4, led to a strongly improved adipocyte conversion without affecting MVEC viability and proliferation. Using these newly established conditions, it was possible to successfully maintain ASC/MVEC coculture spheroids and differentiate them towards the adipogenic lineage.

This spheroid model was subsequently not only characterized with regard to cellular self-organization, but was also applied to investigate the cross-talk between the two cell types in

a 3-D environment (**Chapter 6**). The coculture spheroids, while being smaller in size than the equivalent ASC monocultures, remained viable and mechanically stable during prolonged culture. The endothelial cells, which at first could be found preferentially on the surface of the constructs, began to accumulate in specific regions of the spheroids after several days. While the overall proportion of MVEC decreased over time, the formation of network-like structures could be detected in those parts of the spheroids via immunohistochemistry and confocal microscopy. Importantly, with the focus being on the regulatory interplay between ASC and MVEC, our data demonstrated that in the coculture spheroids adipogenesis was significantly impaired as compared to ASC monocultures. This was not only shown by a reduced triglyceride accumulation, but also on the molecular level by performing a gene expression array after spheroid dissociation and magnetic bead-based separation of the cell types, with many adipogenic marker genes being less strongly expressed in the cocultures than in the monocultures after hormonal induction. Finally, immunostaining of cryosections revealed that lipid accumulation was completely absent only in close proximity to the MVEC structures, but not in more distant regions, which suggests a local inhibitory effect of the endothelial cells on adipogenic differentiation.

7.2 Conclusion

In this work, a 3-D spheroid model of human adipose tissue could be successfully established. This hASC-based model can serve as a valuable tool to investigate the development of adipose tissue in a 3-D microenvironment, as specific tissue-inherent factors such as cell-cell and cell-ECM interactions are much more closely resembled in the spheroids than in conventional 2-D monolayers. Our results could already demonstrate on a functional and molecular level that adipogenic differentiation appeared to be less dependent on exogenous hormonal stimulation in the 3-D spheroids than in 2-D culture. Furthermore, after adjusting culture conditions, the spheroid model proved to be suitable for coculturing ASC with endothelial cells as well, which opens up the possibility to study the cellular cross-talk between these two cell types during adipose tissue development, which is closely associated with angiogenesis and vascularization, in a more *in vivo*-like system. In this context, endothelial cells could be shown to form network-like structures within the 3-D constructs, while at the same time locally inhibiting the process of adipogenesis.

The spheroid system has the advantage of being flexible and easy to handle, while the small size guarantees sufficient nutrient and oxygen supply and allows for a homogeneous differentiation. Moreover, the absence of scaffold materials eliminates the often unknown influence of these substances on cellular performance.

The mono- and coculture spheroids not only represent a versatile tool for basic research, but could also be used for applications in drug screening. It is well known that in the commonly employed 2-D assays cellular response to specific agents may vary considerably from the corresponding *in vivo* effects. Therefore, our spheroid model could serve as a basis for the development and improvement of 3-D screening systems for drug discovery.

Apart from basic research and drug screening, the 3-D adipose tissue model developed in this thesis could also be useful for applications in tissue engineering and regenerative medicine. Specifically, the spheroids could function as building blocks for the regeneration of soft tissue defects, e.g. after incorporation into hydrogels, which would subsequently be implanted or injected into the host tissue. Here, the ASC/MVEC coculture spheroids appear to be especially promising, as their application in an *in vitro* prevascularization approach might help to overcome the problem of insufficient nutrient and oxygen supply in engineered tissue constructs after transplantation.

Appendix

List of Abbreviations

2-D	two-dimensional
3-D	three-dimensional
ANOVA	analysis of variance
ASC	adipose-derived stem cell(s)
AT	adipose tissue
BAT	brown adipose tissue
bFGF	basic fibroblast growth factor
BMSC	bone-marrow derived stem cell(s)
BSA	bovine serum albumin
BP	bandpass
cAMP	cyclic adenosine monophosphate
CCD	charge-coupled device
cDNA	complementary deoxyribonucleic acid
CLSM	confocal laser scanning microscopy
Ct	cycle threshold
CTRL	control
d…	day
DAB	3,3'-Diaminobenzidine
DAPI	4',6-diamidino-2-phenylindole
DEPC	diethylpyrocarbonate
DMEM	Dulbecco’s Modified Eagle’s Medium
DMSO	dimethyl sulfoxide
DNA	deoxyribonucleic acid
DNase	deoxyribonuclease
EC	endothelial cell(s)
ECM	extracellular matrix
EDTA	ethylenediaminetetraacetic acid
EGF	Epidermal growth factor
EBM2	Endothelial Cell Basal Medium 2
EGM2	Endothelial Cell Growth Medium 2
EthD-III	ethidium homodimer III
FBS	fetal bovine serum
FFA	free fatty acids
GM	growth medium

h…	human *(cell types)*
HC	hormonal cocktail
HGF	hepatocyte growth factor
hOB	human osteoblasts
HRP	horseradish peroxidase
HTS	high-throughput screening
HUVEC	human umbilical vein endothelial cell(s)
IFATS	International Fat Applied Technology Society
IBMX	3-isobutyl-1-methylxanthine
IGF	insulin-like growth factor
IM	induction medium
IND-P	permanent induction protocol
IND-S	short-term induction protocol
LDA	low density array
LP	longpass
MEM alpha	Minimum Essential Medium alpha modification
MMP	matrix metalloproteinase
MOPS	3-(N-morpholino)propanesulfonic acid
mRNA	messenger ribonucleic acid
MSC	mesenchymal stem cell(s)
MVEC	microvascular endothelial cells
NIH	National Institutes of Health
ORO	Oil Red O
P…	passage
PBS	phosphate buffered saline
PEG	polyethylene glycol
PBM2	Preadipocyte Basal Medium 2
PGM2	Preadipocyte Growth Medium 2
PLGA	poly(lactic-*co*-glycolic acid)
qRT-PCR	quantitative real time polymerase chain reaction
RNA	ribonucleic acid
rpm	revolutions per minute
RQ	relative expression level
RT	room temperature
SQ	SingleQuots
SVF	stromal-vascular fraction
TE	tissue engineering

TG	triglyceride
TGFβ	transforming growth factor beta
Tris	tris(hydroxymethyl)aminomethane
TZD	thiazolidinedione
U	units
VEGF	vascular endothelial growth factor
WAT	white adipose tissue
w/o	without

Curriculum Vitae

Personal Data

Name:	Christian Muhr
Date of birth:	29/03/1981
Place of birth:	Roding
Nationality:	German

Professional Experience

Since 02/2012	Haupt Pharma Amareg GmbH, Regensburg Project manager pharmaceutical development
11/2007 – 02/2012	PhD program in Pharmaceutical Technology
05/2012 – 02/2012	Department of Trauma, Hand, Plastic and Reconstructive Surgery, University of Würzburg (Prof. Dr. Torsten Blunk)
11/2007 – 04/2012	Department of Pharmaceutical Technology, University of Regensburg (Prof. Dr. Achim Göpferich)
08/2007 – 09/2007	Stadt Apotheke, Furth im Wald Pharmacist
07/2007	Approbation zum Apotheker (Acquisition of the license to practice as a pharmacist)
11/2006 – 04/2007	Bayer Health Care AG, Leverkusen Internship in the pharmaceutical industry (quality control)
05/2006 – 10/2006	Forum Apotheke, Regensburg Internship in a public pharmacy
09/2000 – 07/2001	Kreiskrankenhaus Roding Civilian Service

Education

10/2001 – 04/2006	University of Regensburg Study of Pharmacy
09/1991 – 06/2000	Joseph-von-Fraunhofer-Gymnasium, Cham Grammar school, graduation with Abitur
09/1987 – 07/1991	Grundschule Roding Primary school

List of Publications

Publications

1. **Muhr C**, Winnefeld M, Seitz AK, Göpferich A, Bauer-Kreisel P, Blunk T. Adipogenesis in 3-D spheroids of is less dependent on exogenous stimulation than in conventional 2-D culture. *To be submitted to Tissue Engineering, Part A.*

2. **Muhr C**, Winnefeld M, Seitz AK, Göpferich A, Bauer-Kreisel P, Blunk T. Cocultures of human adipose-derived stem cells and endothelial cells in a 3-D spheroid model: Establishment and characterization. *To be submitted to Experimental Cell Research.*

3. Seitz AK., **Muhr C**, Ratzinger S, Bauer-Kreisel P, Goepferich A, Blunk T. Effect of a prolyl hydroxylase inhibitor on adipogenesis in 2-D and 3-D culture. *To be submitted to BBRC Journal.*

4. Seitz AK, Ratzinger S, **Muhr C**, Bauer-Kreisel P, Grässel S, Goepferich A, Blunk T. Collagen XVI is downregulated during adipogenesis in vitro. *To be submitted to Matrix Biology.*

Conference contributions:

Oral Presentations:

1. **Muhr C**, Winnefeld M, Pielmeier C, Seitz AK, Göpferich A, Bauer-Kreisel P, Blunk T. Adipogenesis in 3-D spheroids of adipose-derived stem cells is less dependent on exogenous stimulation than in conventional 2-D culture. *TERMIS-EU 2011 Meeting*. Granada, Spain (2011).

2. Blunk T, **Muhr C**, Dietl S, Seitz AK, Goepferich A, Winnefeld M, Bauer-Kreisel P. 3D spheroids of adipose-derived stem cells as building blocks for adipose tissue regeneration. *World Conference on Regenerative Medicine*, Leipzig, Germany (2011).

3. **Muhr C**, Winnefeld M, Nestmeyer M, Göpferich A, Bauer-Kreisel P, Blunk T. 3D Coculture Spheroids of Adipose-derived Stem Cells and Microvascular Endothelial Cells – Local Inhibition of Adipogenesis. *3rd International Conference "Strategies in Tissue Engineering",* Würzburg, Germany (2012)

Poster Presentations:

1. Seitz A, Ratzinger S, **Muhr C,** Weiser B, Goepferich A, Bauer-Kreisel P, Grässel S, Blunk T. Collagen XVI expression is downregulated during adipogenesis in 2-D and 3-D culture. *Keystone symposium "Molecular Control of Adipogenesis and Obesity", Keystone*, Colorado, USA (2010).

2. Werner K, **Muhr C**, Jakubietz M, Jakubietz R, Schmidt K, Bauer-Kreisel P, Blunk T. Towards the reconstruction of the subcutaneous fat layer. *World Conference on Regenerative Medicine*, Leipzig, Germany (2011).

3. Wittmann K, **Muhr C**, Storck K, Staudenmaier R, Wiese H, Maier G, Bauer-Kreisel P, Blunk T. Combination of long-term stable fibrin gels and porous scaffolds for engineering of volume-stable adipose tissue. *World Conference on Regenerative Medicine*, Leipzig, Germany (2011).

4. Blunk T, **Muhr C**, Dietl S, Goepferich A, Winnefeld M, Bauer-Kreisel P. Local inhibition of adipogenesis in 3D coculture of adipose-derived stem cells and microvascular endothelial cells. *3rd TERMIS World Congress 2012*, Vienna, Austria (2012).

5. Wittmann K, **Muhr C**, Storck K, Staudenmaier R, Wiese H, Maier G, Bauer-Kreisel P, Blunk T. Development of volume-stable adipose tissue constructs by combining fibrin gels and porous support structures. *3rd TERMIS World Congress 2012*, Vienna, Austria (2012).

6. Wittmann K, Storck K, Staudenmaier R, Wiese H, Maier G, **Muhr C**, Bauer-Kreisel P, Blunk T. Development of volume-stable adipose tissue constructs. *3rd International Conference "Strategies in Tissue Engineering",* Würzburg, Germany (2012)

7. Dietl S, Wittmann K, **Muhr C**, Blunk T, Bauer-Kreisel P. Engineering adipose tissue constructs using different fibrin gel modifications. *3rd International Conference "Strategies in Tissue Engineering",* Würzburg, Germany (2012)

Acknowledgements

An dieser Stelle möchte ich mich bei all jenen bedanken, die einen großen oder kleineren Beitrag zum Gelingen dieser Arbeit geleistet haben.

Mein besonderer Dank gilt Herrn Prof. Dr. Torsten Blunk für die intensive und kompetente Betreuung dieser Arbeit, sowohl in Regensburg als auch in Würzburg. Die vielen ausführlichen und fruchtbaren Diskussionen in freundschaftlicher Atmosphäre, sein großes Interesse am Fortgang der Arbeit, seine motivierende Art und seine Fähigkeit, in allem etwas Positives zu sehen haben entscheidend zum Gelingen dieser Arbeit beigetragen. Seine Gewissenhaftigkeit und seine Auffassung von Wissenschaft haben mich sicherlich geprägt. Ich bedanke mich außerdem für sein Vertrauen und seine Unterstützung in vielerlei Hinsicht, besonders auch für die Möglichkeit zur Teilnahme an nationalen und internationalen Kongressen.

Ebenso danke ich Herrn Prof. Dr. Achim Göpferich für die Möglichkeit zur Promotion an seinem Lehrstuhl, die Überlassung des Themas, die stets wohlwollende Begleitung der Arbeit, die wertvollen Anregungen sowie die Übernahme des Erstgutachtens. Auch ihm danke ich für die Möglichkeit zur Teilnahme an Kongressen.

Bei der Beiersdorf AG bedanke ich mich für die finanzielle Unterstützung dieses Projektes. Insbesondere danke ich Herrn Dr. Marc Winnefeld für die Möglichkeit zur Durchführung der LDA-Messungen in seinem Labor. Ihm und dem gesamten Team vom Labor Spezielle Hautpflege gilt mein Dank für die gute Zusammenarbeit sowie für die freundliche Aufnahme und die angenehme Zeit als Gast in Hamburg.

Frau Dr. Petra Bauer-Kreisel danke ich für die Einführung in die Zellkultur, ihre wertvollen Ratschläge und Hinweise sowie ihre vielfältige Unterstützung „im Hintergrund“, in Regensburg wie in Würzburg.

Bei allen aktuellen und ehemaligen Kollegen am Lehrstuhl für Pharmazeutische Technologie in Regensburg bedanke ich mich für ihre Hilfsbereitschaft sowie das angenehme Arbeitsklima. Insbesondere gilt mein Dank:

- Dr. Annina Seitz für die gute Zusammenarbeit im Zelllabor und die vielen Diskussionen rund ums Thema Fett.
- Anne Heller für die angenehme gemeinsame Laborzeit.
- Dr. Jörg Teßmar für seine pragmatische Art und für die Einladungen zu diversen sportlichen und kulinarischen Großveranstaltungen.

- Den TA´s und den Sekretärinnen für ihre technische und organisatorische Unterstützung.
- Carolin Pielmeier und Viktoria Meßmann für die Unterstützung im Labor.
- Allen, die bei der Betreuung der Studentenpraktika mit mir zusammengearbeitet haben.

Mein Dank gilt auch der stetig wachsenden Zahl an Kollegen im Forschungsbereich der Klinik für Unfallchirurgie am Uniklinikum Würzburg. Hier bedanke ich mich besonders bei:

- Prof. Dr. Rainer Meffert für die Schaffung der Voraussetzungen für gute Forschungsarbeit und die freundliche Aufnahme an seiner Klinik.
- Katharina Werner, Katharina Wittmann, Susanne Dietl, Andrea Lenertz und Markus Nestmeier für die konstruktive und unkomplizierte Zusammenarbeit, die entspannte gemeinsame Zeit in Labor und Büro sowie die zahlreichen Unternehmungen außerhalb der Arbeitszeit. Dank ihnen habe ich mich in Würzburg schnell zuhause gefühlt.
- Den technischen Mitarbeiterinnen im Labor sowie den Sekretärinnen für ihre Unterstützung.

Schließlich gilt mein ganz besonderer Dank meinen Eltern, die mich auf meinem Weg stets unterstützt haben wo sie nur konnten, und die immer hinter mir stehen.